



Nauris Zdanovskis

**Brain Qualitative and Quantitative
Radiological Biomarker Association
with Cognitive Impairment
and Dementia**

Summary of the Doctoral Thesis for obtaining
the scientific degree “Doctor of Science (*PhD*)”

Sector Group – Medical and Health Sciences
Sector – Clinical Medicine
Sub-Sector – Roentgenology and Radiology

Rīga, 2023



Nauris Zdanovskis

ORCID 0000-0002-8255-7392

**Brain Qualitative and Quantitative
Radiological Biomarker Association
with Cognitive Impairment
and Dementia**

Summary of the Doctoral Thesis for obtaining
the scientific degree “Doctor of Science (*PhD*)”

Sector Group – Medical and Health Sciences

Sector – Clinical Medicine

Sub-Sector – Roentgenology and Radiology

Riga, 2023

The Doctoral Thesis was developed at Rīga Stradiņš University, Department of Radiology; Riga East University Hospital “Gaiļezers”, Latvia

Supervisor of the Doctoral Thesis:

Dr. med., Professor **Ardis Platkājis**
Rīga Stradiņš University, Latvia

Official Reviewers:

Dr. med., Associate Professor **Maija Radziņa**,
Rīga Stradiņš University, Latvia

Dr. phil., Professor **Jurģis Šķilters**,
University of Latvia

PhD Associate Professor **Isabel Fragata**,
NOVA University of Lisbon, Portugal

Defence of the Doctoral Thesis will take place at the public session of the Promotion Council of Clinical Medicine on 13 December 2023 at 13.00 in the Hippocrates Lecture Theatre, Dzirciema Street 16, Rīga Stradiņš University and remotely via online platform *Zoom*

The Doctoral Thesis is available in RSU Library and on RSU website:
<https://www.rsu.lv/en/dissertations>



This research has been developed with financing from the European Social Fund and the Latvian state budget within the project No. 8.2.2.0/20/I/004 “Support for involving doctoral students in scientific research and studies” at Rīga Stradiņš University.

Secretary of the Promotion Council:

Dr. med., Professor **Guntis Karelis**

Table of Contents

Abbreviations used in the Thesis	5
Introduction	6
Aim of the Thesis	6
Tasks of the Thesis	7
Hypotheses of the Thesis	7
Novelty of the Thesis	7
1 Literature review	9
1.1 Cognitive impairment and dementia	9
1.2 Brain structure and cortical parcellation	10
1.3 MRI scan in patients with cognitive impairment	11
1.4 Qualitative visual assessment scales MR	13
1.4.1 Global cortical atrophy scale	14
1.4.2 Parietal atrophy scale	16
1.4.3 Medial temporal atrophy scale	17
1.4.4 Entorhinal cortical atrophy scale	18
1.4.5 White matter hyperintensities or Fazekas scale	20
1.4.6 Microhaemorrhage evaluation	21
1.4.7 Perivascular space dilatation evaluation	22
1.5 Quantitative brain measurements	24
2 Materials and methods	26
2.1 Patient selection and demographics	26
2.2 Magnetic resonance imaging protocol	29
2.3 Cortical and subcortical quantitative measurement acquisition	30
2.4 Diffusion tensor imaging (DTI) sequence analysis	30
2.5 Statistical analysis of data	31
3 Results	32
3.1 Visual rating scales	32
3.1.1 Global Cortical Atrophy Scale	32
3.1.2 Medial temporal lobe atrophy (MTA) scale	33
3.1.3 White Matter Hyperintensity Scale (Fazekas Scale)	35
3.1.4 Parietal atrophy scale or Koedam scale	37
3.1.5 Entorhinal cortical atrophy scale	39
3.1.6 Microhaemorrhage evaluation	40
3.1.7 Perivascular space evaluation	41
3.1.8 Correlation of MoCA scores with visual rating scales	43

3.2	Quantitative brain evaluation.....	44
3.2.1	Volumetric characteristics of brain structures	45
3.2.2	Cortical thickness measurements	49
3.2.3	Correlation of volumetric data and cortical thickness data with MoCA results	53
3.3	Quantitative assessment of brain DTI.....	55
3.3.1	DTI quantitative data assessing participants in 2 groups.	57
3.3.2	DTI quantitative data assessing participants in 4 groups.	58
3.4	Principal Component Analysis (PCA) for visual assessment scales and quantitative data.....	60
3.4.1	Principal component analysis for visual rating scales	62
3.4.2	Principal component analysis for volume measurements and cortical thickness measurements	69
4.	Discussion.....	74
	Limitations and constraints in the evaluation of quantitative brain MRI data in cognitive impairment	85
	Conclusions	88
	Recommendations	90
	References	94
	Annexes.....	113
	Annex 1	114
	Annex 2	115
	Annex 3	116
	Annex 4	117
	Annex 5	118
	Annex 6	119
	Annex 7	120
	Annex 8	121
	Annex 9	122

Abbreviations used in the Thesis

MR	Magnetic resonance imaging.
CT	Computed Tomography.
FLAIR	Fluid attenuation inversion recovery.
mm ³	Cubic millimetres.
MoCA	The Montreal Cognitive Assessment.
DWM	Deep white matter.
PVWM	Periventricular white matter.
MPRAGE	Magnetization-prepared rapid acquisition gradient-echo.
SD	Standard deviation.
SE	Standard error.
ERICA	Entorhinal atrophy scale.
ADNI	The Alzheimer's Disease Neuroimaging Initiative.
FA	Fractional anisotropy.
DTI	Diffusion tensor imaging.
CF	Cognitive function.
CI	Cognitive impairment.
PVS	Perivascular spaces.
MTA	Medial temporal atrophy
DKT	<i>Desikan-Killiany-Tourville</i> cortical parcellation atlas.
sMRI	Structural MRI.
fMRI	Functional MRI.
PCA	Principal Component Analysis.
GCA	Global Cortical Atrophy Scale.
BOMBS	Brain Observer MicroBleed scale.
ASL	Arterial Spin Labelling.
GRE	Gradient Echo.

Introduction

Neuroradiological evaluation in cognitive impairment was initially used to exclude pathologies associated with cognitive impairment, for example, to exclude such pathologies as brain tumors (both intra-axial and extra-axial), ischemic or haemorrhagic stroke and other pathologies such as hydrocephalus.

Nowadays, thanks to the development of MRI machines and new brain evaluation sequences, MRI scans provide much more information. Different processing software can detect changes that are not visible by visual assessment, and these neuroradiological findings can help to refine the diagnosis and, in certain cases, confirm the diagnosis.

A specific neuroradiological examination could also assess disease progression and identify patients at higher risk of cognitive impairment progressing to dementia.

In summary, brain MRI, in combination with specific sequences and appropriate software, provides a wide range of radiological biomarkers. The biggest challenge in neuroradiological assessment is to identify which of these biomarkers are most relevant and which biomarkers might indicate an early stage or preclinical state of the disease.

Aim of the Thesis

To determine the relationship of qualitative and quantitative biomarkers of the brain with cognitive function in patients with cognitive impairment and dementia.

Tasks of the Thesis

To achieve the goal of the doctoral thesis, the following tasks have been set:

1. Determine the qualitative and quantitative brain biomarkers of the control group.
2. Determine the qualitative and quantitative brain biomarkers of the study group.
3. Compare the obtained qualitative and quantitative biomarkers in the control group and the study group.
4. Analyse the relationship of cognitive test results with quantitative brain biomarkers.
5. Analyse the correlation of the data obtained.

Hypotheses of the Thesis

- In case of cognitive impairment and dementia there are structural changes which can be detected by quantitative analysis of brain structures.
- Cognitive impairment is associated with specific changes in the quantitative brain biomarkers.

Novelty of the Thesis

Currently, one of the most important research areas in neurodegenerative diseases is the use of magnetic resonance imaging (MRI) biomarkers to identify patients with cognitive impairment at preclinical and early stage, to start interventions much earlier. The study used both – well-known methods for the analysis of brain MR images and methods that have not yet entered routine clinical practice (e.g. the use of quantitative measurements) and which role and application are under investigation (e.g. the analysis of DTI images and

interpretation of the data). Overall, the results of the work contribute to the existing knowledge on the diagnosis of cognitive impairment and provide new knowledge on both DTI analysis and MRI biomarker analysis using multiparametric data analysis.

1 Literature review

Cognitive impairment, including mild cognitive impairment and dementia, is a growing public health problem worldwide. Although the neuropathological mechanism of cognitive impairment is complex and involves many factors, imaging has become an important diagnostic method to analyse structural and functional changes in the brain. Magnetic resonance imaging (MRI) of the brain is nowadays widely used in the diagnosis of cognitive disorders.

However, routine MRI evaluation and imaging methods are largely based on qualitative assessment of brain structure or function, which often does not provide sufficient sensitivity and specificity to detect early changes (Custodio et al., 2022; Harper et al., 2016; Yuan et al., 2019). The use of quantitative MRI biomarkers has entered clinical practice and provides more detailed and objective measurements of brain structures (Pemberton et al., 2021).

The aim of this thesis is to investigate the use of quantitative brain MRI biomarkers in the diagnosis of cognitive impairment. Overall, the use of quantitative brain MRI biomarkers has the potential to improve our understanding of the neuropathological mechanisms of cognitive impairment, improve diagnostic options, and evaluate intervention outcomes.

1.1 Cognitive impairment and dementia

Cognitive impairment is defined as a disruption in cognitive functions, such as memory, attention, language, problem-solving, and executive functioning. If cognitive impairment limits the person's performance in everyday life and the person is no longer able to participate in everyday social life, the cognitive impairment may have progressed to dementia. **Dementia** is defined as

a cognitive impairment severe enough that person is no longer able to participate in social and/or work life.

Cognitive tests, such as the Montreal Cognitive Assessment Scale (MoCA), are used to assess the presence of cognitive impairment. The MoCA assesses visual-spatial function/control, memory, attention, language, orientation in time and space. The maximum score that can be obtained on the MoCA is 30. According to the original normative data, the MoCA value for normal cognitive function was defined as a score equal to or higher than 26 (control group patients had a mean score of 27.4, mild cognitive impairment patients had a mean score of 22.1 and Alzheimer's dementia patients had a mean score of 16.2) (Nasreddine et al., 2005).

Cognitive tests provide a way to detect the presence of cognitive impairment, as well as to determine its severity, which is essential for selecting an appropriate follow-up intervention strategy and evaluating the effectiveness of the intervention. However, individual differences and interactions between different factors can complicate this process, thus highlighting the need for accurate and objective diagnostic tools, such as the use of quantitative biomarkers for brain MRI.

1.2 Brain structure and cortical parcellation.

The brain consists of two hemispheres connected by the corpus callosum, with four lobes in each hemisphere (frontal, parietal, occipital and parietal lobes). In addition to the four lobes, some authors also distinguish the insular lobe and the limbic lobe (Kortz and Lillehei, 2023; Pessoa and Hof, 2015; Purves et al., 2001; Torrico and Abdijadid, 2023). Each of these lobes has a different function and together they perform different cognitive functions.

In each lobe gyri and sulci can be distinguished. The structure of the gyri and sulci varies from person to person, i.e. while it is possible to distinguish most of the anatomically defined gyri and sulci in all people, there is variability in the thickness, surface area, volume, folding, etc. (Heidekum et al., 2020; Lin et al., 2021). Various structural anatomy models have been developed, dividing the brain into smaller units based on the structural structure of the gyri and sulci.

The DKT (Desikan-Killiany-Tourville) cortical parcellation atlas is a widely used brain atlas that provides a detailed delineation of the cerebral cortex into different regions or parcels. It was developed based on high-resolution structural magnetic resonance imaging (MRI) data from a large group of individuals. The DKT atlas divides the cerebral cortex into 34 distinct regions per hemisphere, resulting in a total of 68 parcels. The DKT atlas is widely used in neuroimaging research and clinical practice to identify and analyse specific cortical regions. It serves as a valuable tool for studying brain structure and function, investigating the effects of neurological disorders on different brain regions, and guiding surgical planning and interventions (Desikan et al., 2006).

The DKT cortical parcellation atlas was used for the analysis of the participants in the thesis study.

1.3 MRI scan in patients with cognitive impairment

In the context of cognitive impairment, MRI can be used in several ways to study structural and functional changes in the brain.

Structural magnetic resonance imaging (sMRI) provides detailed images of the brain anatomy, including grey matter, white matter and cerebrospinal fluid. sMRI can be used to detect changes in brain volume, such as atrophy, and to identify specific brain regions that may be affected in cognitive impairment.

Cognitive impairment studies typically use multiple sMRI sequences. T1-weighted (T1) images provide high-resolution images of the brain with the ability to distinguish between white and grey matter and are useful for detecting changes in brain volume and cortical thickness. T2-weighted images are sensitive to changes in myelination and can be used, for example, to detect changes in white matter integrity. FLAIR images are sensitive to changes in tissue water content and are used to assess white matter damage commonly seen in cognitive impairment. In addition, Magnetization Prepared RAPid Gradient Echo (MPRAGE) sequences and 3D T1-weighted gradient echo sequences (3D-T1 GRE) are commonly used to obtain high-resolution brain images (Brant-Zawadzki et al., 1992).

Functional magnetic resonance imaging (fMRI) measures changes in blood flow to the brain (BOLD, or blood-oxygen-level-dependent), which is an indirect indicator of brain activity. fMRI can be used at rest (resting-state fMRI) and to identify areas of the brain that are activated during specific tasks, such as memory or language tasks.

The Alzheimer's Disease Neuroimaging Initiative (ADNI) is a research project aimed at identifying biomarkers for the early diagnosis of Alzheimer's disease (AD). The ADNI MRI protocol consists of a standardized set of MRI sequences including 3D T1, 3D FLAIR, T2* GRE, high-resolution hippocampal structure assessment sequence, arterial spin labelling sequence, diffusion tensor imaging (DTI) and fMRI sequence (Jack et al., 2008; Weiner et al., 2017).

Quantitative MRI biomarkers can provide accurate and unbiased measurements. These measurements are more sensitive to small changes in the brain compared to qualitative MRI evaluations, making them a valuable tool in the diagnosis of cognitive impairment. Analyzing MRI data from multiple sequences can provide information about the structural and functional changes in the brain that occur in cognitive impairment.

1.4 Qualitative visual assessment scales MR

Different rating scales were used to analyse the brain. Visual rating scales in MRI scans allow the qualitative finding of the brain to be translated into quantified values based on defined scales.

The advantages of using visual assessment scales are interpretable and reproducible data that allow comparison between patients and assessment of the progression of pathological changes. However, the disadvantages of using such scales include inter-rater variability and reliability. Visual rating scales also fail to show small changes in volume or cortical thickness, which may be clinically relevant when assessing patients with cognitive impairment (Vernooij et al., 2019).

In the context of cognitive impairment, brain assessment using rating scales is recommended in several studies and guidelines (Festari et al., 2022; Harper et al., 2016, 2015; Vernooij et al., 2019; Yuan et al., 2019).

The most used visual rating scales for brain assessment are:

- Global Cortical Atrophy Scale (GCA),
- Medial temporal lobe atrophy scale (MTA),
- Parietal Lobe Atrophy Scale,
- Entorhinal Cortex Atrophy Scale (ERICA),
- White Matter Hyperintensity Scale (or Fazekas Scale),
- Perivascular space dilation assessment,
- Microhaemorrhage assessment.

As part of the thesis, all participant MRI scans were analysed with above mentioned qualitative visual assessment scales.

1.4.1 Global cortical atrophy scale

The Global Cortical Atrophy Scale was one of the first atrophy scales used to assess the brain. It was originally described and introduced by Pasquier et al. (Pasquier et al., 1996a; Scheltens et al., 1997), to assess the degree of brain atrophy in patients after ischemic stroke. The brain is assessed in 13 regions. Each brain region is scored from 0 to 3 (0 – no atrophy, 1 – dilatation of sulci, 2 – reduction of gyral volume, 3 – severe atrophy with “knife blade” type atrophy) and the enlargement of the cerebral ventricles in each region is assessed (0 – no enlargement, 1 – slight ventricular enlargement, 2 – moderate ventricular enlargement, 3 – marked ventricular enlargement). The regions included are:

1. Right frontal lobe,
2. Left frontal lobe,
3. Right lateral ventricle frontal horns,
4. Left lateral ventricle frontal horns,
5. Right parietal lobe,
6. Left parietal lobe,
7. Right lateral ventricle temporal horns,
8. Left lateral ventricle temporal horns,
9. Right parietal-occipital lobe,
10. Left parietal-occipital lobe,
11. Right lateral ventricle occipital horns,
12. Left lateral ventricle occipital horns,
13. III ventricle.

Accordingly, the number of points varies from 0 to 39 (see Figures 1.1 and 1.2).

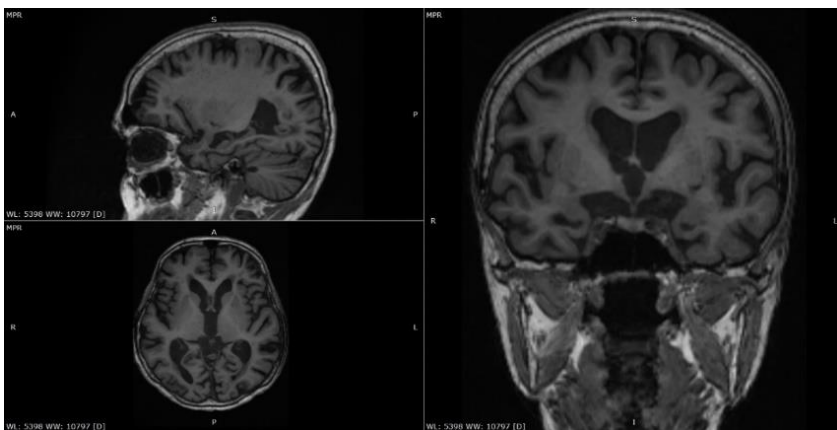


Figure 1.1 Participant with Global Cortical Atrophy Scale score 27 – cortical sulci widening, volume loss and marked enlargement of the ventricular system (author's image)

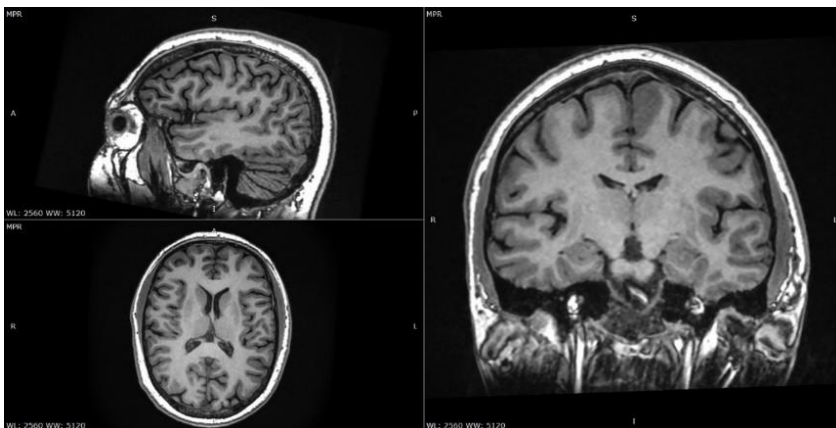


Figure 1.2 Participant with Global Cortical Atrophy Scale score 2 – slight enlargement of the lateral ventricle occipital horns in both lobes (author's image)

Nowadays, some authors also use a simplified global cortical atrophy scale, or GCA, defined as an approximate average value assessing widening of sulci, volume loss and the presence of “knife blade” atrophy.

The analysis of the brain using the global cortical atrophy scale requires the use of T1 sequence in different planes (at least 2). Nowadays, 3D thin-slice T1 sequences are commonly used for evaluation, which allow examination and evaluation of the brain in all planes, including oblique planes.

1.4.2 Parietal atrophy scale

The parietal lobe atrophy scale or Koedam atrophy scale assesses the width, height of cortical gyri and volume loss of the parietal lobe. To assess parietal lobe atrophy, the sagittal, axial and coronal planes must be assessed. In these planes, the posterior cingulum, the parietal-occipital gyri, including the praecuneus, are assessed (see Figure 1.3).

The scale of atrophy of the parietal lobe is divided into 3 grades:

- Grade 0 – no cortical atrophy, no widening of the sulci,
- Grade 1 – slight atrophy of the parietal lobe, slight enlargement of the sulci in the posterior cingulum and the parieto-occipital lobes,
- Grade 2 – marked atrophy of the parietal lobe, widening of sulci in the posterior cingulum and parieto-occipital lobes,
- Grade 3 – marked atrophy with a 'knife-blade' atrophy pattern, marked widening of the sulci in the posterior cingulum and parieto-occipital lobes.

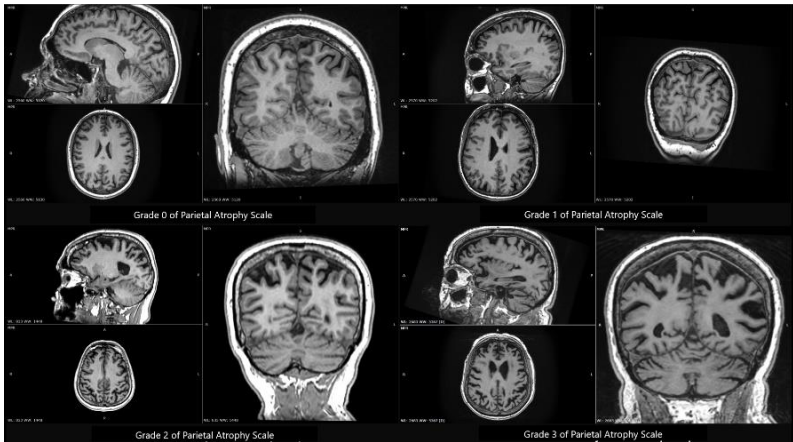


Figure 1.3 **Grades 0 to 3 on the scale of parietal lobe atrophy**

Assessment of the parietal lobe is important because in early Alzheimer's disease initial atrophy may develop in the parietal lobe and such patients may have normal hippocampal volume values and normal values on the medial temporal lobe atrophy scale (Karas et al., 2007).

1.4.3 Medial temporal atrophy scale

The medial temporal lobe includes the hippocampus, the nucleus accumbens and the parahippocampal part of the brain. These regions are important for episodic and spatial memory, as well as for memory encoding, consolidation and recall (Baars and Gage, 2013; Cutsuridis and Yoshida, 2017; LaRocque and Wagner, 2015). All these processes play an important role in the development of cognitive impairment, making the assessment of medial temporal lobe atrophy one of the most important assessment scales. The medial temporal lobe atrophy scale assesses both hemispheres of the brain (see Figure 1.4):

- Grade 1 – widening of the choroidal fissure,
- Grade 2 – enlargement of the lateral ventricle temporal horn,

- Grade 3 – loss of hippocampal volume (or reduction in height),
- Grade 4 – marked loss of hippocampal volume.



Figure 1.4 **Grades 0 to 4 on the medial temporal lobe atrophy scale**

On the medial temporal lobe atrophy scale, an abnormal value is considered to be grade 2 or higher if the patient is younger than 75 years and grade 3 or higher if the patient is older than 75 years (Claus et al., 2017; Scheltens et al., 1997, 1995, 1992; Velickaite et al., 2018). It should be noted that these thresholds are being revised in some studies and MTA scale values are proposed for several age groups (Claus et al., 2017).

1.4.4 Entorhinal cortical atrophy scale

The Entorhinal Cortical Atrophy Scale (ERICA) was developed to measure the degree of atrophy in the entorhinal cortex, a part of the cortex that is localised in the medial temporal lobe, is an important link between the hippocampus and the neocortex, and plays an important role in memory and spatial navigation (Enkirch et al., 2018). The scale ranges from 0 (no atrophy) to 3 (severe atrophy):

- Grade 0 – no atrophy, normal entorhinal cortex,
- Grade 1 – slight atrophy and enlargement of the collateral fissure,

- Grade 2 – moderate atrophy with separation of the entorhinal cortex from the tentorium cerebelli,
- Grade 3 – severe atrophy with atrophy of the parahippocampal cortex, wide gap between the tentorium cerebelli and the entorhinal cortex (see Figure 1.5).

The ERICA scale has been validated in studies of Alzheimer's disease and other neurodegenerative conditions. Its diagnostic accuracy in Alzheimer's disease is 91 %, sensitivity 83 %, specificity 98 %. The scale may also be useful in other neurodegenerative diseases, such as Parkinson's disease (Enkirch et al., 2018).

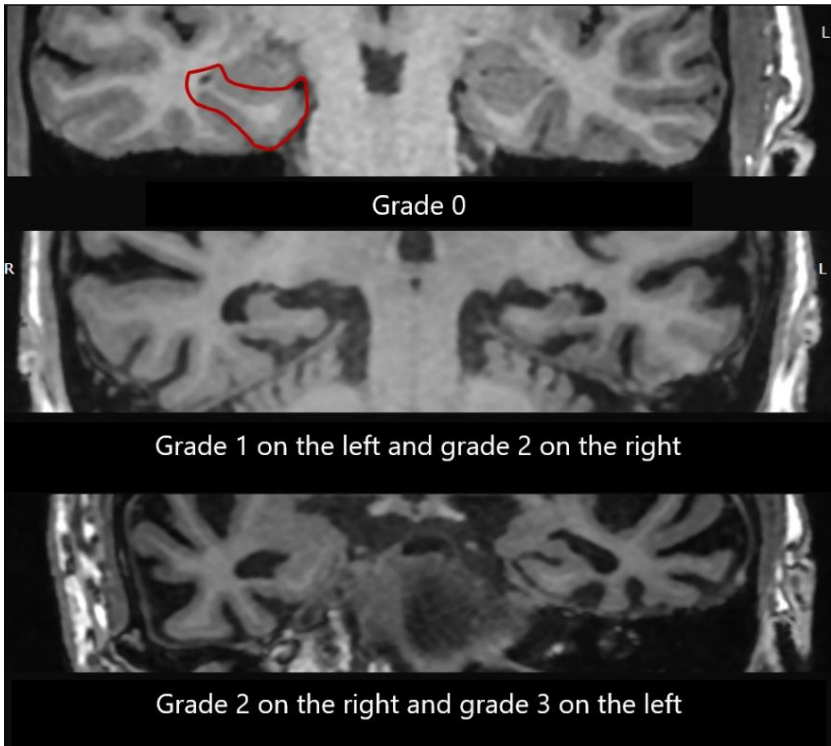


Figure 1.5 **Grades 0 to 3 on the scale of entorhinal cortical atrophy**

1.4.5 White matter hyperintensities or Fazekas scale

The Fazekas scale is used to assess the severity of changes in the white matter of the brain. The T2 FLAIR sequence is used to assess white matter. This sequence reduces the signal intensity from the cerebrospinal fluid, thus providing better resolution of brain lesions compared to the T2 sequence (Kates et al., 1996).

The Fazekas scale was described by Fazekas et al. separately distinguishing between deep white matter (DWM) and periventricular white matter (PVWM). In describing PVWM, 3 grades are distinguished (see Figure 1.6):

- Grade 0 – no white matter hyperintensity periventricularly,
- Grade 1 – small “caps” or thin lines periventricularly,
- Grade 2 – 'halo' periventricularly,
- Grade 3 – periventricular hyperintensity extending to the deep white matter.

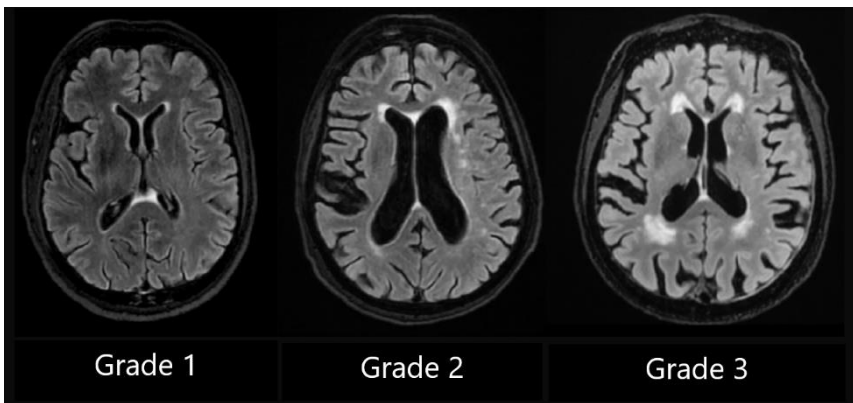


Figure 1.6 Fazekas scale grades for assessing PVWM – from left to right grade 1, grade 2, grade 3

There are 3 stages in describing DWM (see Figure 1.7):

- Grade 0 – no white matter hyperintensities,
- Grade 1 – punctate hyperintensities,
- Grade 2 – part of the punctate hyperintensities converge,
- Grade 3 – extensive hyperintensities converging into each other.

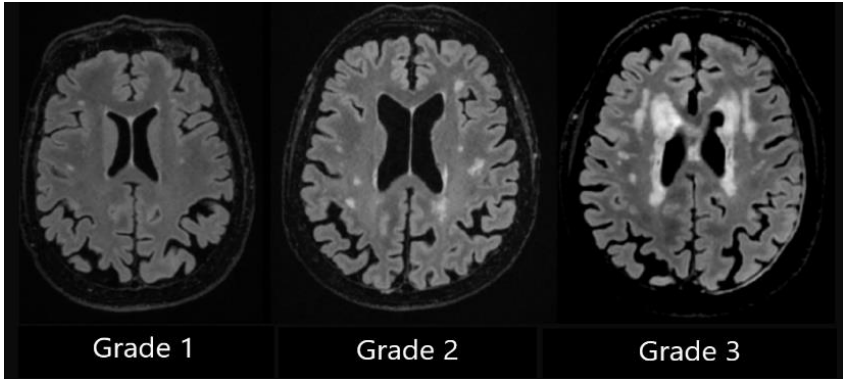


Figure 1.7 Fazekas scale grades for assessing DWM – from left to right grade 1, grade 2, grade 3

1.4.6 Microhaemorrhage evaluation

Microhaemorrhages are small haemorrhages in the brain that can form during lifetime without a severe clinical symptom. Microhaemorrhages can be detected by MRI examinations and are associated with various neurodegenerative diseases, including Alzheimer's disease and cognitive impairment (Juyoun Lee et al., 2018).

On MRI, microhaemorrhages are evaluated on SWI, SWAN or T2* GRE sequences. These sequences are the most sensitive for microhaemorrhage detection.

Microhaemorrhages can contribute to cognitive impairment in several ways - by directly damaging the white and grey matter of the brain, by damaging the white matter tracts of the brain, and by causing inflammation and oxidative stress. In patients with mild cognitive impairment, the presence of microhaemorrhages is also associated with an increased risk of developing dementia in the future (Akoudad et al., 2016; Donaghy et al., 2020; Liu et al., 2020).

Currently, there is no common approach to the assessment of microhaemorrhages in clinical practice. It should be noted that not all patients with microhaemorrhages develop cognitive impairment, so it is important to assess the presence of microhaemorrhages in the context of the clinical signs and other radiological assessment scales.

1.4.7 Perivascular space dilatation evaluation

The perivascular spaces of the brain (PVS or Robin-Wirch spaces) are part of the microvascular structure of the brain, surrounded by vascular adventitia and astrocytic processes as they move from the subarachnoid space through the brain parenchyma (Kwee and Kwee, 2007; Ramirez et al., 2016). The presence of PVS in the brain is associated with increased amyloid- β (A β) deposition in leptomeningeal arteries (Bakker et al., 2016; Hampel et al., 2021; Murphy and LeVine, 2010; Weller et al., 2009)

Perivascular spaces are divided into four subtypes (Lim et al., 2015; Potter et al., 2015; Rawal et al., 2014; Rudie et al., 2018) :

- Type 1 – located in the basal ganglia along the perforating lenticulostriate arteries.
- Type 2 – located in the centrum semiovale along the perforating medullary arterial pathway in white matter.

- Type 3 – located in the midbrain at the pontomesencephalic junction.
- Type 4 – PVS dilatation in the anterior part of the temporal lobe.

At present, the clinical relevance of perivascular dilatation in the development of cognitive impairment is not fully understood and some studies have found an association between PVS enlargement and cognitive impairment, but some studies have not found such association (Arba et al., 2018; Hurford et al., 2014; Paradise et al., 2021; Smeijer et al., 2019; Zanon Zotin et al., 2021).

To assess PVS, three regions are evaluated: the midbrain, centrum semiovale, and basal ganglia. In the midbrain, the presence or absence of perivascular space extension is determined without further subdivision. In the basal ganglia (see Figure 1.8) and centrum semiovale (see Figure 1.9), PVS dilatation is divided into four grades:

- Grade 0 – no PVS dilatation,
- Grade 1 – 1 to 10 PVS dilated,
- Grade 2 – 11 to 20 PVS dilated,
- Grade 3 – 21 to 40 PVS dilated,
- Grade 4 – more than 40 PVS dilated.

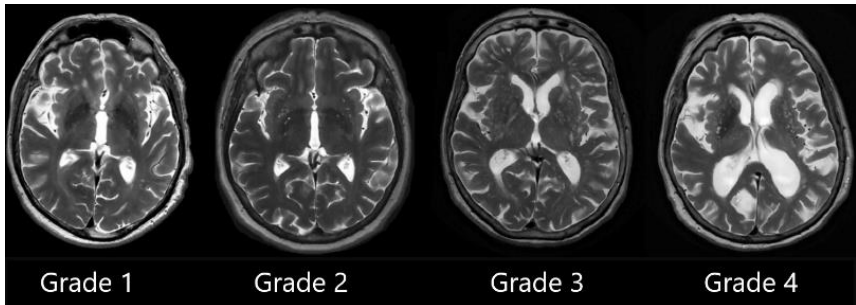


Figure 1.8 Perivascular space dilatation in the basal ganglia and division into grades from 1 to 4

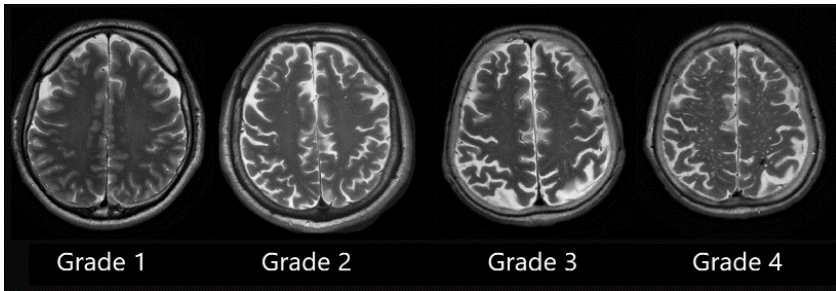


Figure 1.9 **Perivascular space dilatation in *centrum semiovale* and subdivision into grades**

1.5 Quantitative brain measurements

Quantitative brain measurements are a numerical measure derived from MRI scan and provide objective and quantitative information for the analysis. Although quantitative measurements have been around for a long time, automatic, standardized and clinically validated quantitative brain measurements are a recent development in the field.

Quantitative brain measurements can be divided into several subtypes. We used structural quantitative measurements from various brain structures and diffusion tensor imaging quantitative measurements.

Structural quantitative measurements – are detected in anatomical sequences such as T1, T2 or FLAIR. (Chalavi et al., 2012; McEvoy and Brewer, 2010). Structural quantitative measurements of the brain include the thickness, volume, curvature and other quantitative parameters of certain brain structures or lesions. In the context of cognitive impairment, several brain structures have been analysed that can be used as early biomarkers in the diagnosis of cognitive impairment and dementia (Frisoni et al., 2010; Lombardi et al., 2020; Vemuri and Jack, 2010).

Structural quantitative measures were the first biomarkers to evolve after the use of qualitative rating scales, and now clinically validated tools have been developed that allow these quantitative measures to be used with greater confidence in clinical practice (Pemberton et al., 2021), therefore it is important to identify which of all structural MRI biomarkers are most relevant for the early diagnosis of cognitive impairment.

Diffusion tensor and tractography measurements. Diffusion tensor imaging (DTI) is a type of diffusion MRI that provides information about the direction and anisotropy of water diffusion in the brain. DTI is commonly used to define brain tracts, to assess their structure qualitatively and could be used for quantitative measurements. From the DTI data, quantitative parameters can be extracted for the specific tract evaluation. The quantitative parameters that could be extracted are fractional anisotropy (FA), mean diffusivity (MD), axial diffusivity (AD), radial diffusivity (RD) (Oishi et al., 2011; Zhang et al., 2022).

The analysis and application of DTI in cognitive impairment is currently under investigation and there is no consensus on its usefulness. Some of the limitations would be the lack of standardization (there are wide technical variations that also influence the acquisition time), the lack of standardization in the post-processing (post-processing involves several steps such as noise reduction and signal optimization), the variations in interpretation (depending on the post-processing software chosen, different results may be obtained). Also, in the case of DTI, white matter is primarily analysed, but changes in grey matter cannot be judged from a DTI examination.

2 Materials and methods

2.1 Patient selection and demographics

A total of 90 participants (68 women, 22 men) were included in the study. Of the initially enrolled patients, 5 were unable to undergo an MRI scan. To equate the mean age of the control group and the cognitive impairment group, 4 patients (aged 30, 35, 36 and 43 years) were excluded from the control group. Further analysis and correlation of cognitive function with MRI findings was performed in 81 participants: 64 women (mean age 73,0 years, standard deviation 7,659, youngest participant 51 years, oldest participant 96 years), 17 men (mean age 70 years, standard deviation 9,129, youngest participant 48 years, oldest participant 86 years).

All patients underwent cognitive testing using the Montreal Cognitive Assessment (MoCA). Based on the cognitive test results, patients were divided into 2 different ways:

1. Patients were divided into 2 groups: patients without cognitive impairment (MoCA score 26 and above) and patients with cognitive impairment (MoCA score 25 and below), see Table 2.1. (Nasreddine et al., 2012)
2. Patients were divided into 4 groups (see Table 2.2):
 - patients without cognitive impairment (MoCA score 26 or higher),
 - mild cognitive impairment (MoCA score between 19 and 25),
 - moderate cognitive impairment (MoCA score between 10 and 18),
 - severe cognitive impairment (MoCA score below 9).

Table 2.1

**Participant demographics and MoCA results by group
(patients divided into 2 groups)**

	Participants with normal cognition	Participants with cognitive impairment
Number of participants	24	57
Average age and standard deviation	70.3 ± 8.2	73.4 ± 7.8
Mean MoCA score and standard deviation	27.3 ± 1.2	18.6 ± 6.6
Women: Men	22: 2	42: 15

A Mann-Whitney U test was performed to assess differences between groups and no statistically significant differences by age were observed ($p = 0.298$) and statistically significant differences between MoCA results were observed ($p < 0.001$). When patients were divided into 2 groups (with and without cognitive impairment) and a Chi-square test was performed and sex differences were assessed, no statistically significant differences were found between groups ($X^2(1, N = 81) = 3.29, p = 0.0696$). Accordingly, when evaluating the patients in the 2 groups, sex differences were not significant.

Table 2.2

**Participant demographics and MoCA results by group
(patients divided into 4 groups)**

	Normal cognition	Mild cognitive impairment	Moderate cognitive impairment	Severe cognitive impairment
Number of participants	24	38	10	9
Average age and standard deviation	70.3 ± 8.2	72.7 ± 6.7	73 ± 5.6	77.1 ± 12.8
Mean MoCA score and standard deviation	27.3 ± 1.2	22.7 ± 2.1	14.3 ± 2.4	6.1 ± 1.8
Women: Men	22: 2	31:7	4:6	7:2

When patients were divided into 4 groups (Normal cognition, Mild cognitive impairment, Moderate cognitive impairment, Severe cognitive impairment) and Chi-square test was performed to assess sex differences between groups, statistically significant differences were found ($X^2(4, N = 81) = 11.65, p = 0.0087$). Accordingly, when evaluating the patients in the 4 groups, it should be noted that the sex differences are statistically significant, and this should be considered when interpreting the results. A Kruskal-Wallis H test was performed to assess differences between groups and no statistically significant differences by age were observed ($H(3) = 1.482, p = 0.686$) and statistically significant differences between MoCA results were observed ($H(3) = 69.377, p < 0.001$). In the post-hoc Dunn analysis, statistically significant differences were found between all groups except in the moderate CI – severe CI group (see Table 2.3).

Table 2.3

Dunn Post Hoc analysis of MoCA scores between patient groups

	z	W_i	W_j	p	p_{bonf}
Normal CF – Mild CI	5.028	69.354	38.592	< 0.001	< 0.001
Normal CF – Moderate CI	6.211	69.354	14.500	< 0.001	< 0.001
Normal CF – Severe CI	7.016	69.354	5.000	< 0.001	< 0.001
Mild CI – Moderate CI	2.889	38.592	14.500	0.004	0.023
Mild CI – Severe CI	3.862	38.592	5.000	< 0.001	< 0.001
Moderate CI – Severe CI	0.881	14.500	5.000	0.378	1.000

Exclusion criteria for participants were clinically significant neurological diseases (tumors, severe strokes, vascular malformations, etc.), drug use and alcohol abuse. All patients in the study had no other significant abnormalities on MRI. Based on available clinical information, none of the participants had

uncontrolled hypertension, diabetes mellitus or clinically proven depression. All participants were university graduates with at least 16 years of education.

2.2 Magnetic resonance imaging protocol

All patients underwent an MRI scan based on the Alzheimer's Disease Neuroimaging Initiative. The Alzheimer's Disease Neuroimaging Initiative (ADNI) recommended sequences, which include:

- 3D T1 SPGR (technical parameters – Flip Angle 11, TE Min Full, TI 400, FOV 25.6, layer thickness 1 mm),
- 3D FLAIR (technical parameters – TE 119, TR 4800, TI 1473, Echo 182, FOV 25.6, layer thickness 1.2 mm),
- High-resolution hippocampal structure assessment sequence (technical parameters - Flip angle 122, TE 50, Echo 1, TR 8020, FOV 17.5, layer thickness 2, coronal direction perpendicular to the hippocampus),
- DTI (technical parameters – 32 directions, diffusion direction – tensor, FOV 23.2, layer thickness 2 mm, TE 100)
- SWI,
- DWI,

In our research work ASL and fMRI sequences were not performed.

2.3 Cortical and subcortical quantitative measurement acquisition

Quantitative values for cortical and subcortical regions were obtained by 3D T1 sequence analysis with Freesurfer 7.2 software (<http://surfer.nmr.mgh.harvard.edu/>). To obtain quantitative measurements following steps were conducted:

- Conversion of DICOM files to NIFTI format.
- Start of the recon-all command in Freesurfer 7.2 software, which performs several actions, including motion correction, intensity normalization, Talairach transformation, cranial subtraction, cervical subtraction, white matter segmentation, automatic topology correction, cortical analysis, cortical quantitative data output, etc. Technical details, accuracy and repeatability data are described in previous publications (Dale et al., 1999; Fischl et al., 2004, 2002, 2001; Fischl and Dale, 2000; Han et al., 2006; Jovicich et al., 2006; Reuter et al., 2012, 2010; Segonne et al., 2004).
- After the analysis, the quantitative values obtained are reviewed, the cortical and subcortical images obtained are evaluated and quality controlled. Where necessary, the images were corrected and refined.

Accurate quantitative data extraction and image processing are described in previous studies using FreeSurfer 7.2 (Fischl et al., 2004, 2004; Han et al., 2006; Jovicich et al., 2006; Reuter et al., 2012, 2010).

2.4 Diffusion tensor imaging (DTI) sequence analysis

DTI sequences were analysed by using *Icometrix* pipeline which standardizes, homogenizes and provides quantitative measurements for structural analysis of DTI. DTI data processing included tract segmentation with TractSeg to create a binary tract mask and calculate a mean fractional anisotropy

(FA) value (Collier et al., 2015; Wasserthal et al., 2018). As a result, fractional anisotropy quantitative measurements were obtained (including age normative percentiles) for the:

- Whole brain,
- Corpus callosum,
- *tractus corticospinalis* (both hemispheres with additional asymmetry index),
- *fasciculus longitudinalis superior* (both hemispheres with additional asymmetry index),
- *fasciculus frontooccipitalis inferior* (both hemispheres with an additional asymmetry index),
- *cingulum* (both hemispheres with an additional asymmetry index).

The FA quantitative results and the normative percentiles were compared between the groups.

2.5 Statistical analysis of data

For the statistical analysis Microsoft Excel 2023, JASP 0.18.1, and Orange Data Mining 3.34 were used.

Due to the small number of participants in the study cohort, non-parametric tests were used to assess the association of radiological findings with cognitive impairment using the Mann Whitney U test (assessing 2 groups), Kruskal-Wallis H test (assessing 4 groups) with post-hoc tests including adjustment for multiple comparisons (Bonferoni). In addition, the correlation of MoCA with biomarkers was assessed and principal component analysis (PCA) was performed.

3 Results

3.1 Visual rating scales

3.1.1 Global Cortical Atrophy Scale

The global cortical atrophy scale was evaluated in all patients according to the method described in the literature review section, where 13 brain regions are evaluated and scored according to changes.

When the patients were divided into 2 groups and the results were evaluated using the Mann-Whitney U test, statistically significant differences were found between participants with cognitive impairment and participants without cognitive impairment ($p = 0.006$). The mean Global Cortical Atrophy Scale score was 11.7 ($n = 24$, standard deviation 3.345, standard error 0.683) for patients without cognitive impairment and 15,4 ($n = 57$, standard deviation 5.707, standard error 0.756) for patients with cognitive impairment.

When the patients were divided into 4 groups and the results were evaluated by Kruskal-Wallis test, statistically significant differences were found ($H(3) = 29.008$, $p < 0.001$). Distribution of mean GCA scale values by group:

- 11.7 (standard deviation 3.3) in the normal CF group,
- 12.8 (standard deviation 3.4) in the mild CI group,
- 18.1 (standard deviation 4.4) in the moderate CI group,
- 23.3 (standard deviation 5.2) in the severe CI group.

See Figure 3.1 for the distribution of GCA scale scores across participant groups.

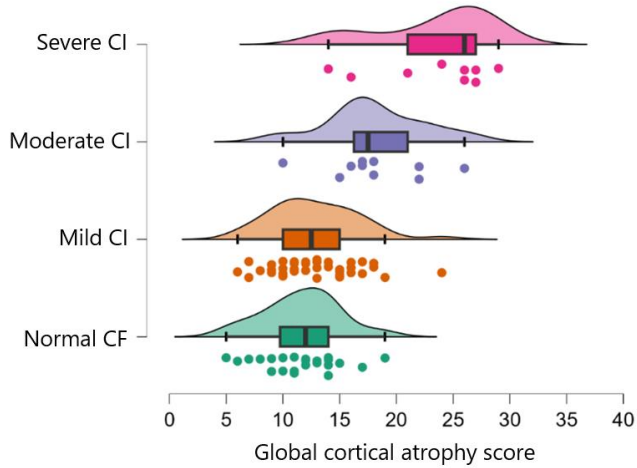


Figure 3.1 Distribution of Global Cortical Atrophy Scale scores between groups of participants with normal cognitive function, mild cognitive impairment, moderate cognitive impairment, and severe cognitive impairment

In Dunn post-hoc analysis, statistically significant differences were observed between normal CF-moderate CI ($p < 0.001$), normal CF-severe CI ($p < 0.001$), mild CF-moderate CI ($p = 0.003$) and mild CF-severe CI ($p < 0.001$).

3.1.2 Medial temporal lobe atrophy (MTA) scale

The medial temporal lobe atrophy scale was assessed in all patients in a 3D T1 sequence according to the method described in the literature review section, where MTA score was given for each lobe and score from 0 to 4 was given.

By dividing the patients into 2 groups and evaluating the results with the Mann-Whitney U test, statistically significant differences were found between participants with cognitive impairment and participants without cognitive impairment in the right side, left side and total MTA scale value ($p = 0.032$,

$p = 0.010$ and $p = 0.017$). Mean MTA scale score in patients without cognitive impairment on right side was 0.917 (SD 0.654, SE 0.683), left side 0.875 (SD 0.797, SE 0.163), total score 0.896 (SD 0.675, SE 0.138), patients with cognitive impairment right side 1.632 (SD 1.318, SE 0.175), left side 1.684 (SD 1.284, SE 0.170), total score 1.658 (SD 1.279, SE 0.169).

By dividing the patients into 4 groups and evaluating the results by performing the Kruskal-Wallis test, statistically significant differences were found between the participants in right hemisphere MTA scale ($H(3) = 25.335$, $p < 0.001$), on the left side ($H(3) = 33.782$, $p < 0.001$) and total MTA scale value ($H(3) = 30.442$, $p < 0.001$). By performing Dunn's post-hoc analysis for the right, left side and evaluating the total MTA values, statistically significant differences were observed between:

- normal CF – moderate CI (right side $p = 0.002$, left side $p = 0.003$, total value $p < 0.001$),
- normal CF – severe CI (right side $p < 0.001$, left side $p < 0.001$, total value $p < 0.001$),
- mild CI – moderate CI (right side $p = 0.003$, left side $p < 0.001$, total value $p < 0.001$)
- mild CI – severe CI (right side $p < 0.001$, left side $p < 0.001$, total value $p < 0.001$).

The obtained results by groups with indication of the average value and standard deviation can be seen in Figure 3.2.

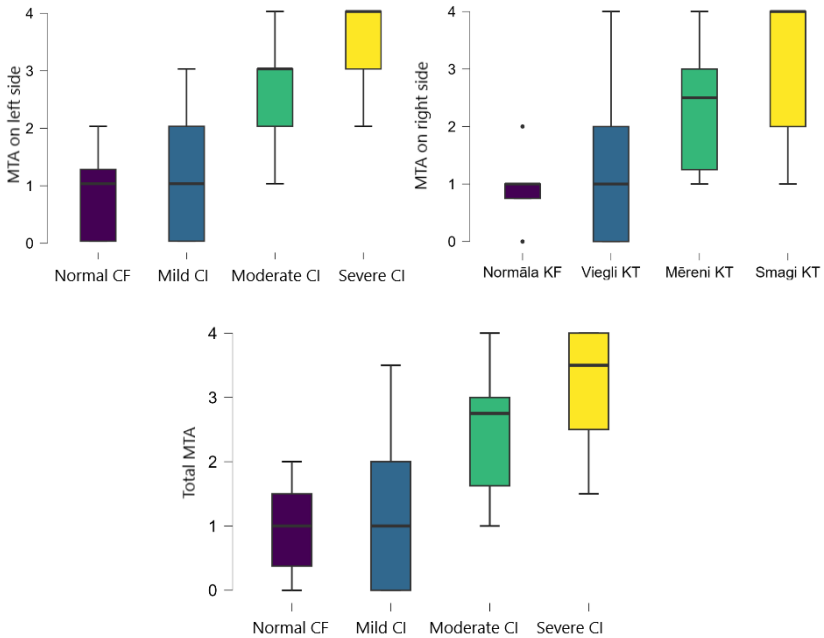


Figure 3.2 Distribution of the mean value of the medial temporal lobe atrophy scale (MTA) in both lobes and total score between groups of participants with normal CF, mild CI, moderate CI and severe CI

3.1.3 White Matter Hyperintensity Scale (Fazekas Scale)

White matter hyperintensities were assessed by T2 FLAIR sequence and white matter was assessed periventricularly and subcortically as well as by total Fazekas score. A detailed evaluation is described in the literature review section.

When the patients were divided into 2 groups and the results were evaluated with the Mann-Whitney U test, no statistically significant differences in white matter hyperintensities were found between participants with cognitive impairment and participants without cognitive impairment in PVWM, DWM and total Fazekas score ($p = 0.711$, $p = 0.209$ and $p = 0.885$, respectively).

When the patients were divided into 4 groups and the results were evaluated by Kruskal-Wallis test, statistically significant differences were found in PVWM ($H(3) = 11.588$, $p = 0.009$) and total Fazekas scale ($H(3) = 9.415$, $p = 0.024$), while no statistically significant differences were observed in DWM ($H(3) = 5.221$, $p = 0.156$).

In Dunn's post-hoc analysis of the PVWM and the overall Fazekas scale, statistically significant differences were observed (see Figure 3.3):

- PVWM between normal CF – severe CI ($p = 0.010$), mild CI – severe CI ($p = 0.002$), no significant differences were found in other group comparisons,
- No significant differences were found in the overall Fazekas score between normal CF-severe CI ($p = 0.011$), mild CI – severe CI ($p = 0.010$) and other group comparisons,

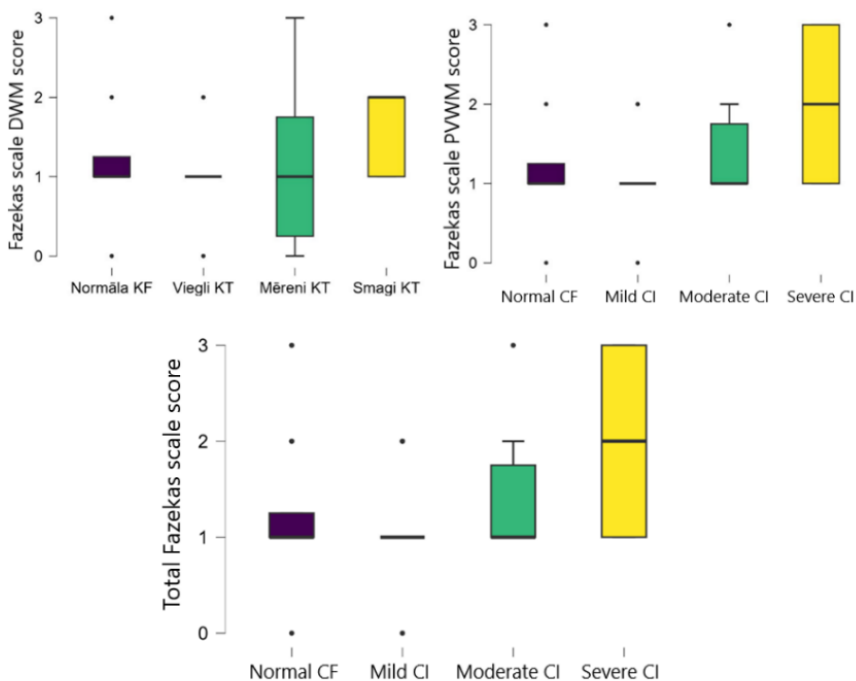


Figure 3.3 Distribution of the mean of the Fazekas score in deep white matter (DWM), periventricular white matter (PVWM) and total score between groups of participants with normal CF, mild CI, moderate CI and severe CI

3.1.4 Parietal atrophy scale or Koedam scale

The parietal lobe atrophy scale was evaluated in all patients in 3D T1 sequence according to the method described in the literature review section. The temporal lobe was assessed in axial, coronal and sagittal planes and values from 0 to 4 were assigned to each hemisphere according to the degree of atrophy.

When the patients were divided into 2 groups and the results were evaluated using the Mann-Whitney U test, statistically significant differences were found between participants with cognitive impairment and participants without cognitive impairment in the right and left hemispheres ($p < 0.001$ and

$p = 0.003$, respectively). The mean score on the Parietal Lobe Atrophy Scale was 1.083 (SD 0.584, SE 0.119) in patients without cognitive impairment on the right, 1.125 (SD 0.612, SE 0.125) on the left and 1.596 (SD 0.563, SE 0.075) in patients with cognitive impairment on the right and 0.596 (SD 0.563, SE 0.075) on the left.

When the patients were divided into 4 groups and the results were evaluated by Kruskal-Wallis test, statistically significant differences were found between participants on the right ($H(3) = 18.782$, $p < 0.001$) and left ($H(3) = 16.796$, $p < 0.001$) side of the parietal lobe.

In Dunn's post-hoc analysis of the right and left sides of the parietal lobe atrophy scale, statistically significant differences were observed (see Figure 3.4):

- in the right parietal lobe between normal CF – mild CI ($p = 0.030$), normal CF – moderate CI ($p = 0.006$), normal CF – severe CI ($p < 0.001$) and mild CI – severe CI ($p = 0.007$),
- in the left parietal lobe between normal CF – moderate CI ($p = 0.012$), normal CF – severe CI ($p < 0.001$) and mild CI – severe CI ($p = 0.007$).

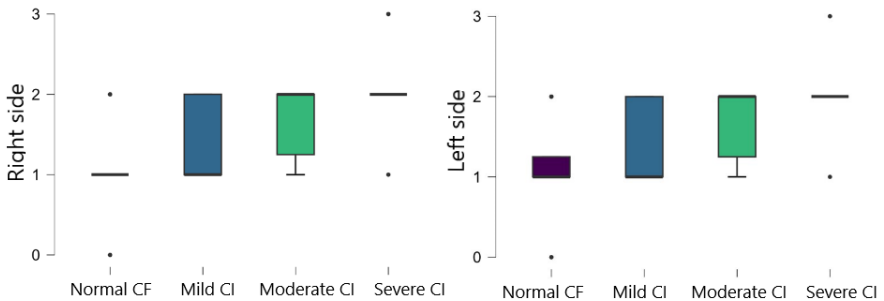


Figure 3.4 Mean values of the parietal lobe atrophy scale in the right and left hemispheres between groups of participants with normal CF, mild CI, moderate CI and severe CI

3.1.5 Entorhinal cortical atrophy scale

The entorhinal cortical atrophy scale was evaluated in all patients in a 3D T1 sequence according to the method described in the literature review section. The entorhinal cortex was assessed in the coronal plane and values from 0 to 4 were assigned to each hemisphere according to the degree of atrophy.

Dividing the patients into 2 groups and evaluating the results with the Mann-Whitney U test revealed statistically significant differences between participants with cognitive impairment and participants without cognitive impairment in the right and left hemispheres ($p = 0.013$ and $p = 0.001$, respectively). Mean entorhinal cortex atrophy scale score in patients without cognitive impairment on right side was 0.583 (SD 0.584, SE 0.119), left side 0.542 (SD 0.588, SE 0.120), patients with cognitive impairment right side 1.140 (SD 0.934, SE 0.124), left side 1.228 (SD 0.887, SE 0.117).

By dividing the patients into 4 groups and evaluating the results by performing the Kruskal-Wallis test, statistically significant differences were obtained between the participants in the right side of the entorhinal cortex ($H(3) = 27.825$, $p < 0.001$) and the left side ($H(3) = 28.014$, $p < 0.001$).

When performing Dunn's post-hoc analysis, statistically significant differences were observed for the entorhinal cortex atrophy scale in (see Figure 3.5):

- in the right entorhinal cortex between normal CF – moderate CI ($p = 0.003$), normal CF – severe CI ($p < 0.001$), mild CI – moderate CI ($p = 0.008$) and mild CI – severe CI ($p < 0.001$),
- in the left entorhinal cortex between normal CF – moderate CI ($p < 0.001$), normal CF – severe CI ($p < 0.001$), mild CI – moderate CI ($p = 0.003$) and mild CI – severe CI ($p < 0.001$).

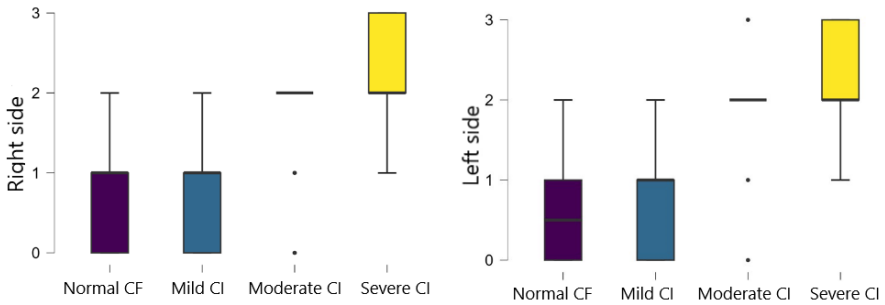


Figure 3.5 Entorhinal cortical atrophy scale values in the right and left hemispheres between groups of participants with normal CF, mild CI, moderate CI and severe CI.

3.1.6 Microhaemorrhage evaluation

All study participants were screened for the presence of microhaemorrhages based on the SWI sequence. No participants had more than 2 microhaemorrhages and no clinically significant lobar haemorrhages.

When the results were analysed in 2 groups (patients with cognitive impairment and patients without cognitive impairment), there were no statistically significant differences between the groups ($p = 0.725$). In the group without cognitive impairment, microhaemorrhages were found in 5 people (20.8 %) and were not found in 19 people (79.2 %). In the group with cognitive impairment, microhaemorrhages were found in 14 people (24.6 %) and were absent in 43 people (75.4 %).

When the results were evaluated in the 4 groups (patients with normal CF, mild CI, moderate CI and severe CI), no statistically significant differences were observed ($p = 0.953$, see figure 3.6).

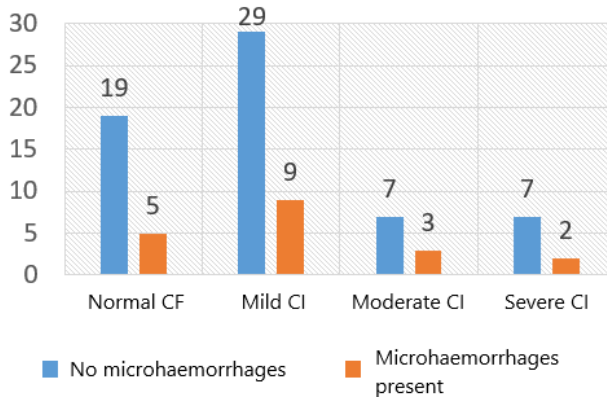


Figure 3.6 **Incidence of microhaemorrhages in participant groups**

3.1.7 Perivascular space evaluation

Perivascular spaces were evaluated in the midbrain, basal nuclei, and centrum semiovale. The evaluation was performed in T2 and T2 FLAIR sequences, and in the basal nuclei, the dilatation of the perivascular spaces was determined without grading (it was stated whether it is dilated or not), in the basal nuclei and centrum semiovale, the expansion of the perivascular spaces was graded from grades 0 to 4.

When evaluating the dilatation of perivascular spaces in 2 groups (with cognitive impairment and without cognitive impairment), no statistically significant differences were found in the midbrain ($p = 0.348$), centrum semiovale ($p = 0.699$) and basal nuclei ($p = 0.497$). A detailed breakdown by grades, locations and groups is given in Table 3.1.

Table 3.1

**Assessment of perivascular space dilatation
by dividing patients into 2 groups**

	Grade	Participants with normal cognition	Participants with cognitive impairment
Perivascular space dilatation in centrum semiovale	Grade 0	2	4
	Grade 1	8	22
	Grade 2	13	21
	Grade 3	1	6
	Grade 4	0	4
Perivascular space dilatation in basal nuclei	Grade 0	2	0
	Grade 1	9	27
	Grade 2	11	18
	Grade 3	1	9
	Grade 4	1	3
Perivascular space dilatation in midbrain	No dilatation	12	22
	Dilatation present	12	35

When perivascular space dilatation was assessed in the 4 groups (Normal CF, Mild CI, Moderate CI, Severe CI) by Kruskal-Wallis test, no statistically significant differences were observed in the midbrain ($p = 0.456$), centrum semiovale ($p = 0.083$) and basal nuclei ($p = 0.091$). The detailed breakdown by grade, localization and group is shown in Table 3.2.

Table 3.2

**Assessment of perivascular space dilation
by dividing patients into 4 groups**

	Grade	Normal CF	Mild CI	Moderate CI	Severe CI
Perivascular space dilatation in centrum semiovale	Grade 0	2	4	0	0
	Grade 1	8	16	4	2
	Grade 2	13	15	3	3
	Grade 3	1	1	2	3
	Grade 4	0	2	1	1

Table 3.2 continued

	Grade	Normal CF	Mild CI	Moderate CI	Severe CI
Perivascular space dilatation in basal nuclei	Grade 0	2	0	0	0
	Grade 1	9	21	4	2
	Grade 2	11	11	5	2
	Grade 3	1	5	1	3
	Grade 4	1	1	0	2
Perivascular space dilatation in midbrain	No dilatation	12	16	2	4
	Dilatation present	12	22	8	5

3.1.8 Correlation of MoCA scores with visual rating scales

The relationship of the qualitative assessment scales with the MoCA results was analysed by Spearman correlation, where the correlation coefficient, p-value, upper and lower 95 % confidence level effect sizes (Fisher's z) and standard error effect sizes were determined (see Table 3.3).

A moderately strong statistically significant correlation (correlation coefficient below 0.4) was observed when correlating MoCA scores with the medial temporal lobe atrophy scale, the temporal lobe atrophy scale, the entorhinal cortical atrophy scale and the global cortical atrophy scale score.

A weak statistically significant correlation (correlation coefficient below 0.2) was observed when correlating the MoCA results with the total value of the Fazekas scale and the PVT extension in the centrum semiovale localization.

Table 3.3

Correlation of MoCA with qualitative rating scales

	Spearman's correlation coefficient	P value	Lower 95% CI	Upper 95% CI	Effect size (Fisher z)	SD
MoCA – MTA scale on the right	-0.489	< 0.001	-0.639	-0.303	-0.535	0.117
MoCA – MTA scale on the left	-0.570	< 0.001	-0.701	-0.402	-0.648	0.118
MoCA – MTA total value	-0.538	< 0.001	-0.677	-0.362	-0.601	0.118
MoCA – Parietal Lobe Atrophy Scale on the right	-0.507	< 0.001	-0.653	-0.324	-0.558	0.117
MoCA – Parietal lobe atrophy scale on the left	-0.456	< 0.001	-0.613	-0.264	-0.492	0.117
MoCA – ERICA scale on the right	-0.542	< 0.001	-0.680	-0.368	-0.608	0.118
MoCA – ERICA scale on the left	-0.594	< 0.001	-0.719	-0.431	-0.683	0.118
MoCA – GCA	-0.577	< 0.001	-0.706	-0.410	-0.658	0.118
MoCA – PVWM	-0.321	0.399	-0.307	0.126	-0.095	0.113
MoCA – DWM	-0.095	0.067	-0.405	0.015	-0.207	0.114
MoCA – Total value of the Fazekas scale	-0.204	< 0.001	0.625	0.827	0.956	0.121
MoCA – PVS BG	-0.187	0.095	-0.389	0.033	-0.189	0.114
MoCA – PVS CS	-0.227	0.042	-0.424	-0.009	-0.231	0.115

3.2 Quantitative brain evaluation

Quantitative brain data were evaluated in 80 participants (one participant did not have the required sequence quality due to movement artefacts). The evaluation of the quantitative data was divided into 3 sections:

1. General quantitative brain characteristics (*corpus callosum* volume, white and grey matter volume of both cerebellar hemispheres, thalamus, *lobus caudatus*, putamen, pallidum, hippocampus,

nucleus accumbens, cortical volume, white matter volume, subcortical grey matter volume and total grey matter volume).

2. Quantitative measurements of cortical areas based on the DKT cortical parcellation atlas, which divides the cerebral cortex into 31 regions in each hemisphere.
3. Quantitative evaluation of diffusion tensor imaging by determining fractional anisotropy (FA) characteristics of the whole brain, *corpus callosum*, *tractus corticospinalis* (both hemispheres), *fasciculus longitudinalis superior* (both hemispheres), *fasciculus frontooccipitalis inferior* (both hemispheres), cingulum (both hemispheres).

3.2.1 Volumetric characteristics of brain structures

To evaluate the quantitative volume of the brain structures, a comparison of quantitative values was made in 2 groups and 4 groups.

When quantitative values were compared between the 2 groups using the Mann-Whitney U test, statistically significant differences were observed in the left hippocampus, the left amygdala and the right amygdala (see Table 3.4).

Table 3.4

**Differences in general quantitative measures between the groups
with and without cognitive impairment**

Anatomical structure	Left hemisphere		Right hemisphere	
	W	p value	W	p value
Hippocampus	888.000	0.024	820.000	0.121
Amygdala	962.000	0.002	880.000	0.029
Cerebellar white matter	755.000	0.386	741.000	0.472
Cortical part of cerebellum	668.000	0.971	666.000	0.954
Thalamus	661.000	0.912	671.000	0.996
Nucleus Caudatus	603.000	0.472	649.000	0.813
Putamen	828.000	0.103	725.500	0.578
Pallidum	654.000	0.854	722.000	0.603
Nucleus accumbens	837.000	0.084	719.000	0.533
Cortical volume of the hemisphere	812.000	0.143	781.000	0.255
White matter volume	771.000	0.301	774.000	0.287
Overall differences in both hemispheres				
Anatomical structure	W	p value		
Total cortical volume	805.000	0.164		
Total white matter volume	767.000	0.321		
Posterior part of the corpus callosum	682.000	0.921		
Posterior part of middle part of corpus callosum	795.500	0.197		
The central part of the corpus callosum	841.000	0.077		
Anterior part of the middle part of the corpus callosum	817.500	0.128		
The anterior part of the corpus callosum	690.000	0.854		

The mean left hippocampal volume for participants without cognitive impairment was 3597.117 mm³, for participants with cognitive impairment 3340.770 mm³; the mean left amygdala volume for participants without cognitive impairment was 1495.558 mm³, for participants with cognitive impairment 1274.145 mm³; the mean right amygdala volume for participants without cognitive impairment was 1663.125 mm³, for participants with cognitive impairment 1499.213 mm³. See Table 3.5 for the mean, SD and SE of the results.

**Quantitative results of statistically significant structures
comparing group means, standard deviation and standard error**

	Group	N	Mean	SD	SE
Left hippocampal volume, mm ³	No cognitive impairment	24	3597.117	406.570	82.991
	With cognitive impairment	56	3340.770	598.105	79.925
Left amygdala volume, mm ³	No cognitive impairment	24	1495.558	251.821	51.403
	With cognitive impairment	56	1274.145	297.404	39.742
Right amygdala volume, mm ³	No cognitive impairment	24	1663.125	228.110	46.563
	With cognitive impairment	56	1499.213	307.881	41.142

General quantitative brain characteristics were compared between 4 groups (Normal CF, Mild CI, Moderate CI, Severe CI) using the Kruskal-Wallis test. Statistically significant differences between groups were observed:

- Left hippocampus ($H(3) = 18.318, p < 0.001$),
- Left amygdala ($H(3) = 24.800, p < 0.001$),
- Left *nucleus accumbens* ($H(3) = 10.861, p = 0.012$),
- Right cerebellar cortical volume ($H(3) = 8.188, p = 0.042$),
- Right hippocampus ($H(3) = 18.318, p = 0.003$),
- Right amygdala ($H(3) = 21.719, p < 0.001$),

No statistically significant differences were observed between groups in other quantitative volume parameters.

Dunn's post hoc analysis of hippocampal volumes showed statistically significant differences between groups:

- Left side: Normal CF – Moderate CI ($p = 0.009$), Normal CF – Severe CI ($p < 0.001$), Mild CI – Moderate CI ($p = 0.032$) and Mild CI – Severe CI ($p < 0.001$).
- Right side: Normal CF – Severe CI ($p < 0.001$) and Mild CI – Severe CI ($p < 0.001$).

The hippocampal volume values by group are given in Table 3.6.

Table 3.6

**Hippocampal volume mean values on both sides with standard deviation
and standard error values**

		N	Mean (cm³)	SD	SE
Left hippocampus	Normal CF	24	3597.117	406.570	82.991
	Mild CI	37	3548.668	536.484	88.197
	Moderate CI	10	3149.950	294.341	93.079
	Severe CI	9	2698.100	597.232	199.077
Right hippocampus	Normal CF	24	3751.200	439.016	89.614
	Mild CI	38	3760.157	565.380	92.948
	Moderate CI	10	3413.210	413.630	130.801
	Severe CI	9	2764.489	744.916	248.305

Dunn's post hoc analysis of amygdala volumes showed statistically significant differences between groups:

- Left side: Normal CF – Moderate CI ($p < 0.001$), Normal CF – Severe CI ($p < 0.001$), Mild CI – Moderate CI ($p = 0.003$) and Mild CI – Severe CI ($p = 0.002$).
- Right side: Normal CF – Moderate CI ($p = 0.004$), Normal CF – Severe CI ($p < 0.001$), Mild CI – Moderate CI ($p = 0.009$) and Mild CI – Severe CI ($p < 0.001$).

The values of the amygdala volume per group are given in Table 3.7.

Table 3.7

**Mean values of the amygdala on both sides
with standard deviation and standard error values**

		Group	N	Mean (cm³)	SD	SE
Left amygdala volume	Normal CF	24	1495.558	199.051	62.946	
	Mild CI	37	1389.857	259.931	42.732	
	Moderate CI	10	1065.580	199.051	62.946	
	Severe CI	9	1030.178	276.075	92.025	
Right amygdala volume	Normal CF	24	1663.125	226.464	71.614	
	Mild CI	38	1623.078	239.308	39.342	
	Moderate CI	10	1358.870	226.464	71.614	
	Severe CI	9	1145.922	316.680	105.560	

Dunn post hoc analysis of left *nucleus accumbens* volume showed statistically significant differences between the groups Normal CF – Moderate CI ($p = 0.044$), Normal CF – Severe CI ($p = 0.004$) and Mild CI – Severe CI ($p = 0.011$). *Nucleus accumbens* volume values per group are shown in Table 3.8.

Table 3.8

**Nucleus accumbens mean values with standard deviation
and standard error values**

	Group	N	Mean (cm³)	SD	SE
<i>Nucleus accumbens</i> volume	Normal CF	24	441.879	120.984	0.274
	Mild CI	37	429.270	115.897	19.053
	Moderate CI	10	357.350	73.470	23.233
	Severe CI	9	303.433	116.742	38.914

Dunn's post hoc analysis of the cortical part of the right cerebellum showed statistically significant differences between groups – Normal CF – Moderate CI ($p = 0.035$), Mild CI – Moderate CI ($p = 0.013$) and Moderate CI – Severe CI ($p = 0.008$).

3.2.2 Cortical thickness measurements

Cortical thickness was determined using the Desikan-Killiany-Tourville DKT cortical parcellation atlas. In this atlas, each hemisphere is divided into 32 regions. Cortical thicknesses were compared between 2 groups (without and with cognitive impairment) using the Mann-Whitney U test and statistically significant differences were observed in the left entorhinal cortex.

Cortical thickness was compared in 4 groups (Normal CF, Mild CI, Moderate CI, Severe CI) using the Kruskal-Wallis test. Statistically significant differences between groups were observed:

- Temporal lobe:
 - Entorhinal cortex on the left side ($H(3) = 25.224$, $p < 0.001$) and right side ($H(3) = 13.127$, $p = 0.004$),
 - Parahippocampal cortex on the left side ($H(3) = 20.459$, $p < 0.001$) and right side ($H(3) = 18.229$, $p < 0.001$),
 - Middle temporal gyrus cortex on the left side ($H(3) = 12.508$, $p = 0.006$) and right side ($H(3) = 9.909$, $p = 0.019$),
 - Fusiform cortex on the left side ($H(3) = 14.176$, $p = 0.003$) and right side ($H(3) = 7.812$, $p = 0.050$),
 - Superior temporal gyrus cortex on the left side ($H(3) = 14.274$, $p = 0.003$) and right side ($H(3) = 14.286$, $p = 0.003$),
 - Transverse temporal gyrus cortex on the right side ($H(3) = 9.155$, $p = 0.027$).
- Parietal lobe:
 - Supramarginal cortex on the left side ($H(3) = 12.693$, $p = 0.005$) and right side ($H(3) = 9.466$, $p = 0.024$),
 - Cingulum isthmic part on the right side ($H(3) = 8.336$, $p = 0.04$),
 - Left inferior parietal gyrus cortex ($H(3) = 9.078$, $p = 0.028$),
- Occipital lobe:
 - Pericalcarine gyrus on the right side ($H(3) = 11.351$, $p < 0.010$),

Dunn's post-hoc analysis of the entorhinal cortex showed statistically significant differences between the groups:

- on the left side Normal CF – Moderate CI ($p < 0.001$), Normal CF – Severe CI ($p < 0.001$), Mild CI – Moderate CI ($p < 0.001$) and Mild CI – Severe CI ($p = 0.004$),
- on the right-side Normal CF – Severe CI ($p = 0.005$), Mild CI – Moderate CI ($p = 0.036$) and Mild CI – Severe CI ($p = 0.002$)

Dunn's post-hoc analysis in the parahippocampal cortex showed statistically significant differences between groups:

- on the left side Normal CF – Moderate CI ($p = 0.038$), Normal CF – Severe CI ($p = 0.005$), Mild CI – Moderate CI ($p = 0.002$) and Mild CI – Severe CI ($p < 0.001$).
- on the right-side Normal CF – Moderate CI ($p = 0.007$), Normal CF – Severe CI ($p = 0.002$), Mild CI – Moderate CI ($p = 0.004$) and Mild CI – Severe CI ($p < 0.001$).

Dunn's post-hoc analysis in the middle temporal gyrus cortex showed statistically significant differences between groups:

- on the left side Normal CF – Moderate CI ($p = 0.010$), Normal CF – Severe CI ($p = 0.029$), Mild CI – Moderate CI ($p = 0.006$) and Mild CI – Severe CI ($p = 0.018$).
- on the right-side Normal CF – Moderate CI ($p = 0.022$) and Mild CI – Moderate CI ($p = 0.004$).

Dunn's post-hoc analysis in the fusiform cortex showed statistically significant differences between the groups:

- on the left side Normal CF – Moderate CI ($p = 0.031$), Normal CF – Severe CI ($p = 0.009$), Mild CI – Moderate CI ($p = 0.010$) and Mild CI – Severe CI ($p = 0.002$).
- on the right-side Mild CI – Severe CI ($p = 0.011$).

Dunn's post-hoc analysis of the upper cortex of the temporal lobe showed statistically significant differences between groups:

- on the left side Normal CF – Moderate CI ($p = 0.022$), Normal CF – Severe CI ($p = 0.012$), Mild CI – Moderate CI ($p = 0.007$) and Mild CI – Severe CI ($p = 0.003$).
- on the right-side Mild CI – Moderate CI ($p = 0.003$) and Mild CI – Severe CI ($p = 0.003$).

Dunn's post-hoc analysis of the transverse cortex of the right temporal lobe showed statistically significant differences between groups Mild CI – Moderate CI ($p = 0.034$) and Mild CI – Severe CI ($p = 0.011$).

Dunn's post-hoc analysis of the cortical parts of the temporal lobe showed statistically significant differences in several groups. Statistically significant differences between groups were observed in the supramarginal cortex of the left lobe:

- on the left side Normal CF – Moderate CI ($p = 0.030$), Normal CF – Severe CI ($p = 0.003$), Mild CI – Moderate CI ($p = 0.044$) and Mild CI – Severe CI ($p = 0.005$).
- on the right-side Mild CI – Moderate CI ($p = 0.021$) and Mild CI – Severe CI ($p = 0.029$).

Statistically significant were observed on the right side of cingulum isthmus part between groups Normal CF – Severe CI ($p = 0.021$), Mild CI – Severe CI ($p = 0.010$).

Statistically significant differences between groups were found in the inferior cortex of the left temporal lobe – Normal CF – Severe CI ($p = 0.024$), Mild CI – Moderate CI ($p = 0.049$), Mild CI – Severe CI ($p = 0.020$).

Dunn's post-hoc analysis showed statistically significant differences between groups in the right pericalcarine cortex in Normal CF – Mild CI ($p = 0.005$) and Mild CI – Severe CI ($p = 0.009$).

Overall, the quantitative brain data showed statistically significant differences between several groups, but the small cohort and the Bonferroni correction results should be noted, indicating the need to validate the results with a larger number of participants. Statistically significant quantitative data for cerebral cortex measurements are available in Annex 1.

3.2.3 Correlation of volumetric data and cortical thickness data with MoCA results

The aim of the study was to determine the relationship of quantitative measurements with cognitive function, as a result correlation analysis was performed between the volumetric data, cortical thickness and MoCA results (statistically significant correlations are indicated in Annex No. 8 and Annex No. 9).

When assessing the correlation of **brain structure volume** with MoCA results, a strong, positive correlation was observed:

- Left hippocampus (Spearman's rho coefficient 0.473, $p < 0.001$),
- Left amygdala (Spearman's rho coefficient 0.532, $p < 0.001$),
- Right hippocampus (Spearman's rho coefficient 0.372, $p < 0.001$),
- Right amygdala (Spearman's rho coefficient 0.467, $p < 0.001$),

A moderate positive correlation was observed:

- Left putamen (Spearman's rho coefficient 0.310, $p = 0.005$)
- Left nucleus accumbens (Spearman's rho coefficient 0.302, $p = 0.006$),

Other structures showed weaker correlations and higher p-values.

When assessing the correlation of **cortical thickness** with MoCA results, a strong, positive correlation was observed:

- Left entorhinal cortex (Spearman's rho coefficient 0.515, $p < 0.001$)

A moderate positive correlation was observed for the following structures:

- Right entorhinal cortex thickness (Spearman's rho coefficient 0.345, $p = 0.002$),
- Right parahippocampal cortex thickness (Spearman's rho coefficient 0.382, $p < 0.001$),
- Left fusiform cortex thickness (Spearman's rho coefficient 0.323, $p = 0.003$),
- Left inferior parietal gyrus cortex thickness (Spearman's rho coefficient 0.326, $p = 0.003$),
- Left middle temporal gyrus cortex thickness (Spearman's rho coefficient 0.328, $p = 0.003$),
- Left superior temporal gyrus cortex thickness (Spearman's rho coefficient 0.364, $p < 0.001$),
- Left supramarginal cortex thickness (Spearman's rho coefficient 0.348, $p = 0.002$),
- Right *praecuneus* cortex thickness (Spearman's rho coefficient 0.310, $p = 0.005$).

For other structures, cortical thicknesses showed weaker correlations and higher p-values.

3.3 Quantitative assessment of brain DTI

Participants underwent DTI examinations on two 3T machines. Due to technical differences in the equipment, movement artefacts and failed sequences, DTI data were evaluated in 44 patients (see Tables 3.9 and 3.10 for group distribution and demographic data).

The evaluation was performed using the Icometrix DTI software package, which detects changes in fractional anisotropy in specific brain tracts. The examinations were performed on a single MRI machine, images were preprocessed, and DTI data was processed to acquire FA values for whole brain and specific tracts. These steps were performed by using validated methods combined with machine learning techniques (Timmermans et al., 2019). After all steps have been completed, the resulting FA data are standardized and compared to age- and gender-normative data obtained from 900 participants without cognitive impairment aged 16 to 86 years, and a normative percentile for age is obtained.

Table 3.9

Demographic characteristics of DTI quantitative assessment participants and MoCA results by group (dividing patients into 2 groups)

	Normal cognition	Cognitive impairment
Number of participants	12	32
Mean age and standard deviation	70.3 ± 17.5	72.8 ± 9.5
Mean MoCA score and standard deviation	28.7 ± 1.2	17.0 ± 7.3
Female : Male	9:3	20:12

A Mann-Whitney U test was performed to assess differences between groups and statistically significant differences were observed by age ($p = 0.01$), which should be considered when evaluating the absolute values obtained by FA,

and statistically significant differences were observed after MoCA results ($p < 0.001$).

Table 3.10

Demographic characteristics of DTI quantitative evaluation participants and MoCA results by group (patients in 4 groups)

	Normal cognition	Mild cognitive impairment	Moderate cognitive impairment	Severe cognitive impairment
Number of participants	12	16	9	7
Mean age and standard deviation	57,0 ± 17,5	69,6 ± 7,3	73,1 ± 7,3	79,6 ± 13,3
Mean MoCA score and standard deviation	28,7 ± 1,2	23,3 ± 1,6	14,6 ± 2,4	5,9 ± 1,9
Female : Male	9:3	10:6	4:5	6:1

A Kruskal Wallis H test was performed to assess differences between groups and statistically significant differences were observed by age ($H(3) = 10.124$, $p = 0.018$) and statistically significant differences were observed between MoCA results ($H(3) = 39.735$, $p < 0.001$). In the post-hoc Dunn analysis, statistically significant differences were found between all groups except Moderate CI – Severe CI.

Analysed tracts include – the whole brain , *corpus callosum* (report example is shown in Annex 3), Corticospinal tract in both hemispheres, Superior longitudinal fasciculus (SLF) – arcuate fasciculus in both hemispheres, inferior fronto-occipital (IFO) tract in both hemispheres un *cingulum* in both hemispheres (report example is shown in Annex 4). For tractography of the whole brain and corpus callosum, fractional anisotropy data, normalized amplitude and percentile of the result are obtained.

For other tracts analysed in both hemispheres, in addition to the fractional anisotropy data, the normalized amplitude and the percentile of the result, an asymmetry index is also obtained (a negative asymmetry index value indicates a higher FA value in the left hemisphere, a positive value of the asymmetry index

indicates a higher FA value in the right hemisphere), the normal amplitude of the asymmetry index and the normalized percentile, and the deviation of the normalized percentile from 50 was calculated to assess the bias of the asymmetry on both sides.

3.3.1 DTI quantitative data assessing participants in 2 groups

Quantitative DTI data were compared in patients with and without cognitive impairment. Comparisons between groups were performed using the Mann-Whitney U test and the results are shown in Annex 7.

Statistically significant differences between groups were observed in the normative percentage of whole brain FA, the normative percentage of right-sided corticospinal tract and the normative percentage of left-sided corticospinal tract. The differences between groups, mean, standard deviation and standard error are shown in Table 3.11.

Table 3.11

Statistically significant differences in fractional anisotropy (FA) between groups comparing group means, standard deviation and standard error

	Group	N	Mean value	SD	SE
Normative percentile for whole brain FA	Without cognitive impairment	12	58.2	21.5	6.2
	With cognitive impairment	32	76.9	20.4	3.6
Normative percentile of the left-sided corticospinal tract	Without cognitive impairment	12	62.3	26.7	7.7
	With cognitive impairment	32	83.8	16.6	2.9
Normative percentile of the right-sided corticospinal tract	Without cognitive impairment	12	62.4	27.7	7.9
	With cognitive impairment	32	83.2	15.9	2.8

In this case, lower values of the normative FA percentile were observed in the group without cognitive impairment. The reason for these results and an explanation are discussed in the Discussion section.

3.3.2 DTI quantitative data assessing participants in 4 groups

Quantitative DTI data were compared for patients with no cognitive impairment, mild cognitive impairment, moderate cognitive impairment, and severe cognitive impairment. Comparisons between groups were performed using the Kruskal-Wallis test and statistically significant differences between groups were found:

- Changes in whole brain FA ($H(3) = 8.342, p = 0.039$) and normative percentile for whole brain FA ($H(3) = 13.866, p = 0.003$). In the Dunn post-hoc analysis, statistically significant differences were observed in whole-brain FA scores between mild CI – Severe CI ($p = 0.007$), and statistically significant differences were also maintained after Bonferroni correction ($p = 0.044$); when assessing the normative percentile of whole brain FA, statistically significant differences were observed between the groups normal CF – mild CI ($p < 0.001$) and mild CI – Severe CI ($p = 0.016$, after Bonferroni correction $p = 0.098$).
- Left SLF – arcuate fasciculus FA ($H(3) = 14.580, p = 0.002$) and FA normative percentile ($H(3) = 14.734, p = 0.002$). In Dunn's post-hoc analysis, statistically significant differences were observed in FA scores between normal CF – severe CI ($p = 0.05$), mild CI – moderate CI ($p = 0.005$), and mild CI – severe CI ($p < 0.001$); when assessing the normative FA percentile, statistically significant differences were observed between normal CF - mild CI ($p < 0.011$),

mild CI – moderate CI ($p = 0.005$) and mild CI and severe CI ($p = 0.001$).

- Right SLF – arcuate fasciculus FA ($H(3) = 11.881$, $p = 0.008$) and FA in the normative percentile ($H(3) = 13.796$, $p = 0.003$). In the Dunn post-hoc analysis, statistically significant differences were observed in FA scores between the normal CF-severe CF groups ($p = 0.038$), mild CF – moderate CF ($p = 0.023$) and mild CF – severe CF ($p = 0.002$) in both cases; when assessing the normative FA percentile, statistically significant differences were observed between the normal CF – mild CI ($p < 0.006$), mild CI – moderate CI ($p = 0.013$) and mild CI and severe CI ($p = 0.002$) groups.
- SLF – arcuate fasciculus asymmetry normative percentile ($H(3) = 8.898$, $p = 0.031$). In Dunn's post-hoc analysis, statistically significant differences were observed between the Mild CI – Moderate CI ($p = 0.031$) and Mild CI – Severe CI ($p = 0.008$) groups.
- Left inferior fronto-occipital fasciculus FA ($H(3) = 16.119$, $p = 0.001$) and normative percentile ($H(3) = 15.928$, $p = 0.001$). In the Dunn post-hoc analysis, statistically significant differences were observed in FA scores between mild CI-moderate CI ($p < 0.001$), mild CI – severe CI ($p = 0.002$) in both cases; when FA normative percentile was assessed, statistically significant differences were observed between mild CI – moderate CI ($p = 0.001$), mild CI – severe CI ($p = 0.001$) and normal CF – mild CI ($p = 0.024$) groups.
- Right inferior fronto-occipital (IFO) fasciculus FA ($H(3) = 15.349$, $p = 0.002$) and normative percentile ($H(3) = 15.854$, $p = 0.001$). In Dunn's post-hoc analysis, statistically significant differences were observed in FA scores between normal CF – severe CI ($p = 0.050$),

mild CI – moderate CI ($p = 0.002$), mild CI – severe CI ($p = 0.001$) in both cases; when assessing the normative FA percentile, statistically significant differences were observed between the groups Normal CF – mild CI ($p = 0.020$), mild CI – moderate CI ($p = 0.002$) and mild CI – severe CI ($p < 0.001$).

- Left cingulum FA ($H(3) = 8.256$, $p = 0.041$) and normative percentile ($H(3) = 10.430$, $p = 0.015$). In the Dunn post-hoc analysis, statistically significant differences were observed in FA scores between mild CI – moderate CI ($p = 0.013$), mild CI – severe CI ($p = 0.032$) in both cases; when FA normative percentile was assessed, statistically significant differences were observed between normal CF – mild CI ($p = 0.004$), mild CI – moderate CI ($p = 0.017$) groups.
- Right cingulum FA normative percentile ($H(3) = 8.857$, $p = 0.031$). In Dunn's post-hoc analysis, statistically significant differences were observed between normal CF – mild CI ($p = 0.016$) and mild CI – severe CI ($p = 0.013$).

3.4 Principal Component Analysis (PCA) for visual assessment scales and quantitative data

Given the multidimensionality and multicollinearity of the data (see Annex 2), as well as the relatively small number of participants in the groups, the data were analysed using principal components analysis. Orange Data Mining software was used for the PCA (Demšar et al., 2013).

This analysis was conducted on visual rating scales and quantitative data including brain volume and cortical thickness values. Several limitations of principal component analysis must be considered when applying PCA, which include:

- Data linearity assumption – The PCA analysis assumes that the structure of the data to be analysed is linear. Brain atrophy, brain volume and cortical thickness measures are assumed to be linearly related to age and cognitive impairment in many studies and clinically validated software (Cavedo et al., 2022; Pemberton et al., 2021).
- Data interpretation – Although PCT helps to reduce the number of variables, the principal components obtained are not always clinically useful as they are a linear combination of the original variables relative to the target outcome.
- Effects of outliers – Principal components obtained with a small number of participants may be sensitive to variables that do not follow a linear relationship. Such atypical data are possible in the analysis of brain structures.
- Loss of important data – single variables that play a significant role in diagnostics of cognitive impairment may be lost in the principal component analysis.
- Independence of components – The principal components from the PCA analysis are independent, i.e., they are unrelated to each other.

Therefore, the data obtained in the principal components analysis are treated with caution to assess possible correlations between variables.

3.4.1 Principal component analysis for visual rating scales

Ordinal scales of the visual rating scales were subjected to PCA to reduce the dimensionality of the data and to identify factors that might affect cognitive function. The software automatically processes the data and applies a weighted mean of 0 with a standard deviation of 1. The PCA was performed using singular value decomposition (SVD) to identify principal components. The MoCA score was set as the target value for the PCA. Using a value scree plot, 3 principal components were identified, explaining 71 % of the variance (see Figure 3.7).

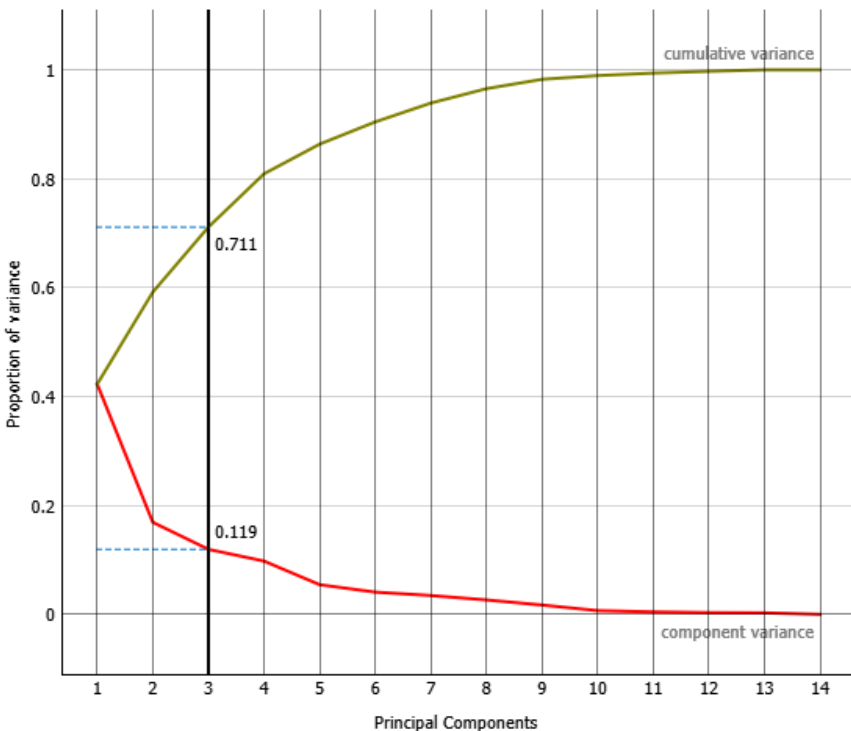
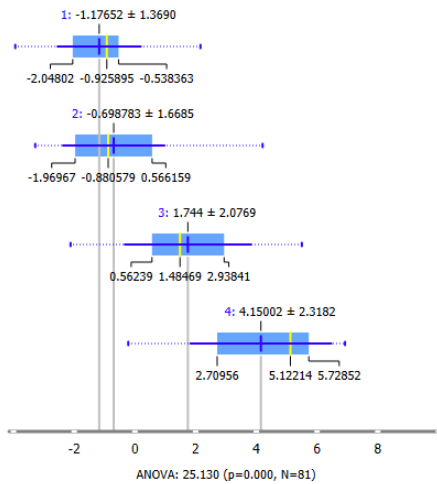
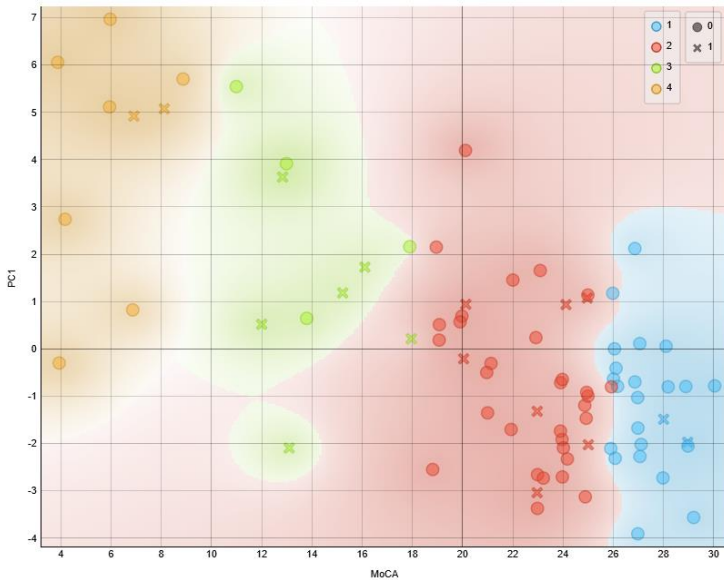


Figure 3.7 Scree plot with explained variance and principal component quantities

The value of principal component 1 (PC1) explained 42.2 % of the variance and was characterized mainly by the GCA scale, the MTA scale, and the ERICA scale, with a smaller measure of PVWM hyperintensities, which could be relevant for participants with mainly non-vascular cognitive impairment (see figure 3.8, left). The results were also compared between groups and statistically significant differences were observed (see Figure 3.8, right). The largest differences between groups were observed when comparing the normal CF and mild CI groups with the moderate CI and severe CI groups.



**Figure 3.8 On the left MoCA score association with PC1;
On the right PC1 differences between groups**

1 – patients without cognitive impairment in blue, 2 – patients with mild cognitive impairment in red, 3 – patients with moderate cognitive impairment in green and 4 – patients with severe cognitive impairment in orange; X – males, O – females.

The value of principal component 2 explained 16.9 % of the variance and was mainly characterized by the PVWM hyperintensity scale and the DWM hyperintensity scale, which could be relevant mainly for patients with vascular cognitive impairment (see Figure 3.9, left). The results were also compared between groups and statistically significant differences were observed ($p = 0.044$), see Figure 3.9 on the right. The largest differences between groups were observed when comparing the normal CF and mild CI groups with the moderate CI and severe CI groups.

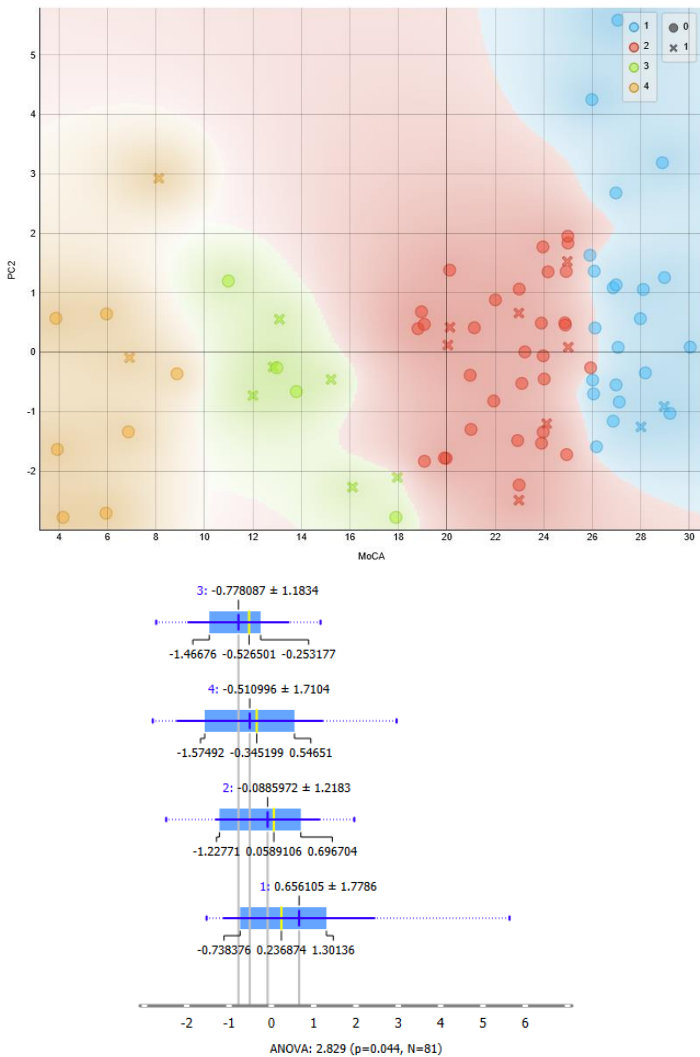


Figure 3.9 On the left MoCA score association with principal component 2 (PC2); On the right PC2 differences between groups

1 – patients without cognitive impairment in blue, 2 – patients with mild cognitive impairment in red, 3 – patients with moderate cognitive impairment in green and 4 – patients with severe cognitive impairment in orange; X – males, O – females.

The value of principal component 3 (PC3) explained 11.9 % of the variance and was characterized mainly by microhaemorrhages, which could be relevant mainly in patients with cerebral amyloid angiopathy or mainly microvascular lesions leading to cognitive impairment (see Figure 3.10, on the left). In contrast, no statistically significant differences were observed when comparing component 3 between groups ($p = 0.710$).

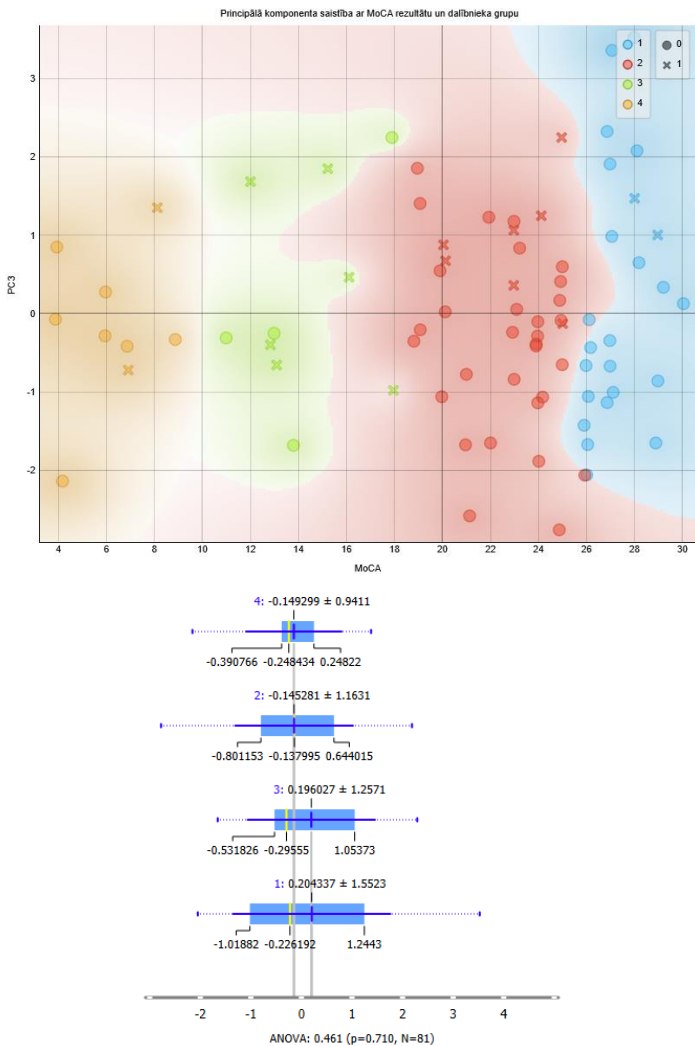


Figure 3.10 **On the left MoCA score association with principal component 3 (PC3); on the right PC3 differences between groups**

1 – patients without cognitive impairment in blue, 2 – patients with mild cognitive impairment in red, 3 – patients with moderate cognitive impairment in green and 4 – patients with severe cognitive impairment in orange; X – males, O – females.

3.4.2 Principal component analysis for volume measurements and cortical thickness measurements

Brain volume and cortical thickness were assessed using Principal Component Analysis (PCA) to perform a general exploratory analysis of the quantitative data. 95 variables were used for the analysis and the MoCA score was set as the target value for principal components. Using a scree plot, 9 principal components were identified, explaining 71 % of the variance (see Figure 3.11).

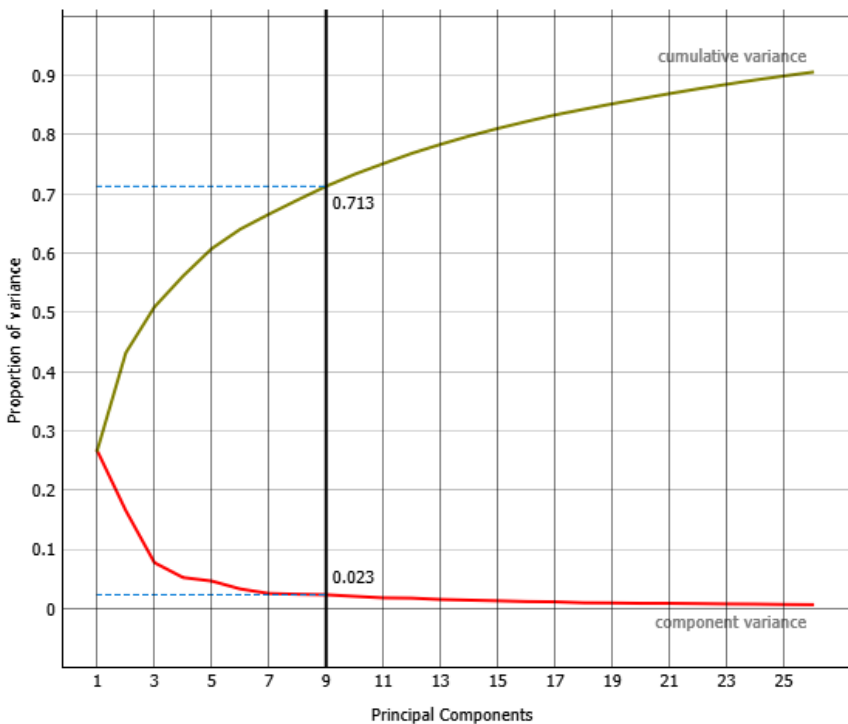


Figure 3.11 Scree plot explained variance and number of principal components for PCA

After identifying the principal components, the ability of each principal component to explain the variance in the data was assessed – PC1: Explains 26.66 % of the total variance in the data, PC2: Explains 16.51 % of the total variance in the data, PC3: Explains 7.73 % of the total variance in the data, PC4: Explains 5.22 % of the total data variance, PC5: Explains 4.63 % of the total data variance, PC6: Explains 3.29 % of the total data variance, PC7: Explains 2.53 % of the total data variance, PC8: Explains 2.40 % of the total data variance, PC9: Explains 2.31 % of the total data variance.

The relationship of the principal components to the MoCA score and the participant group is shown in Figure 3.12.

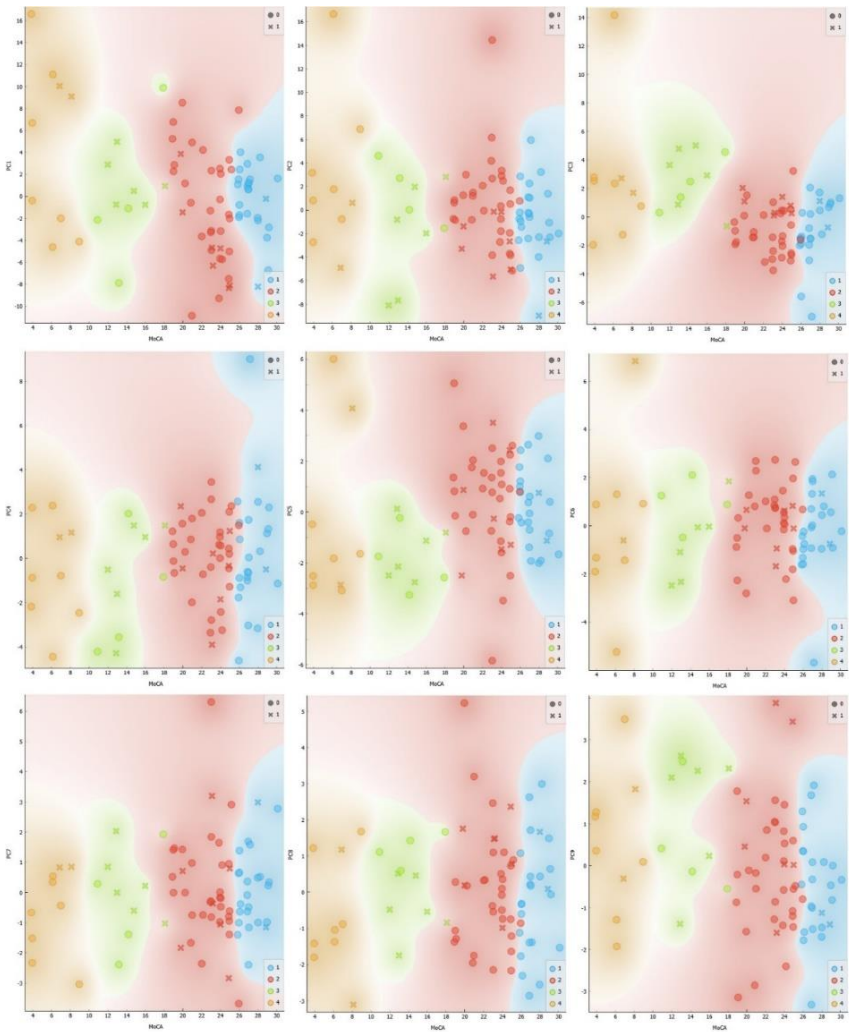


Figure 3.12 Relationship of MoCA score to principal components from PC1 to PC9 – first row left to right from PC1 to PC3, second row left to right from PC4 to PC6, third row left to right from PC7 to PC9

Blue – patients without cognitive impairment, red - patients with mild cognitive impairment, green – patients with moderate cognitive impairment and orange – patients with severe cognitive impairment; X – males, O – females.

Given the relatively large number of principal components and given that some of the principal components explain only a small proportion of the variance in the data, FreeViz data visualization was used to identify possible relationships between the PK and MoCA test results (Demšar et al., 2007). The result of the FreeViz data visualization is shown in Figure 3.13.

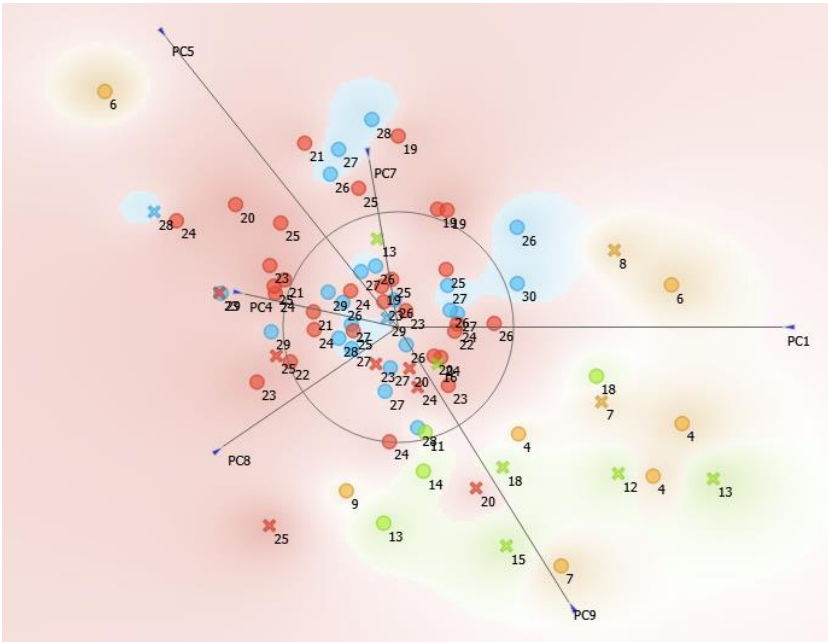


Figure 3.13. FreeViz data visualization shows the distribution of data based on the PCA analysis

Blue – participants with no cognitive impairment, red – participants with mild cognitive impairment, green – participants with moderate cognitive impairment and orange – participants with severe cognitive impairment; X – men, O – women; the value at the dot is the MoCA test score.

When visualizing the FreeViz data, it can be observed that higher MoCA values are centrally localized, indicating an association between PC and MoCA results. Possible explanation for this distribution:

- ***Central concentration of higher MoCA scores*** – Participants with higher MoCA scores have similar values for brain structures covered by PK. This may indicate a cluster of brain structures that is associated with better cognitive function.
- ***Lower MoCA scores further from the central part*** – lower MoCA scores further from the central part indicate higher variability. This may indicate the involvement of several clusters of brain structures in the development of cognitive impairment.

In addition to the above-mentioned relationships, it can be observed that lower MoCA values in the moderate CI and severe CI groups are observed in the PC1 and PC9 directions, indicating a stronger association of these PC. On the other hand, when assessing the localization between normal CF and mild CI, it can be observed that there is a slightly stronger shift towards PC4, PC5 and PC7 for mild CI, so if it is necessary to differentiate normal CF from mild CI, the combinations of these PC might be more relevant.

Overall, the Principal Components Analysis in combination with the FreeViz data visualization outlines several possible future research directions where quantitative data could be combined to build predictive models.

Discussion

Cognitive impairment and dementia diagnostics are a complex process involving a variety of diagnostic tools and techniques, including brain MRI. In general, brain MRI plays a vital role in the diagnosis of cognitive impairment, but the use of quantitative biomarkers has the potential to increase its role and improve early diagnosis of cognitive impairment and dementia. By providing objective measurements of brain structures, biomarkers can help in early diagnosis and assessment of progression, as well as in the development of personalized interventions (Cummings et al., n.d.; Silva-Spínola et al., 2022).

Qualitative visual rating scales were introduced to assess brain structures more objectively and to standardize findings on brain MR images. After their introduction, reference values were developed and their association with cognitive impairment and dementia was assessed (Ferreira et al., 2015). Qualitative rating scales have the advantage of being relatively quick and easy to use, no specific software requirements and low costs. Although in some studies visual assessment scales show good reliability, reproducible scores between radiologists and satisfactory correlation with quantitative measurements, it should be noted that there may be differences between radiologists' assessments, which may be due to inexperience, inaccurate projection selection, incorrect sequence selection and also due to differences in image quality between different MRI machines. (Pasquier et al., 1996b; Scheltens et al., 1997; Wahlund et al., 2016). It should be noted that visual rating scales are ordinal and do not reflect small changes in the brain, which may be clinically significant in certain cases. Despite all the limitations, visual assessment scales are now more widely used in clinical practice than quantitative brain measurements. In this thesis, participants' brain MRI scans were evaluated using the global cortical atrophy scale, medial temporal lobe atrophy scale, white matter hyperintensity scale or Fazekas scale,

temporal lobe atrophy or Koedam scale, entorhinal cortical atrophy scale and perivascular space dilation assessment scale.

The Global Cortical Atrophy (GCA) scale showed statistically significant differences when participants were divided into 2 groups (normal cognition and cognitive impairment groups) and statistically significant differences when participants were divided into 4 groups (between groups normal CF – moderate CI, normal CF – severe CI, mild CF – moderate CI and mild CI – severe CI). Overall, the results show an association of the GCA scale with cognitive impairment, but problems in differentiating cognitive impairment arise when comparing scores between normal CF and mild CI – differentiation between these groups is difficult not only radiologically, but also with cognitive tests and clinical assessment (Thomann et al., 2020).

The results observed in this thesis are consistent with the literature – higher scores on the GCA scale may indicate existing cognitive impairment or a risk of developing cognitive impairment in the future (Al-Janabi et al., 2018; Chan et al., 2001; Harper et al., 2015; Yew et al., 2017). It should be noted that the original GCA scale with analysis of each region and ventricle dilatation was used in the thesis (with a maximum score of 37), but nowadays a simplified approach with the GCA scale score (1 – opening of sulci or mild ventricular enlargement; 2 – volume loss of gyri or moderate ventricular enlargement, 3 – marked volume loss or “knife blade” atrophy) is often used (Harper et al., 2015; Muzio, n.d.).

Given the non-specific nature of the GCA scale and the fact that specific brain regions are known to be more specific in terms of cognitive impairment diagnostics, region-specific visual rating (qualitative) scales have also been developed, i.e. the medial temporal lobe atrophy scale (MTA), the parietal lobe atrophy scale and the entorhinal cortex atrophy scale (ERICA).

The medial temporal lobe atrophy scale mainly assesses the hippocampus, the lateral ventricle width (*fissura chorioidea*) and the parahippocampal cortex. In our study, statistically significant differences were observed when participants were divided into 2 groups (with and without cognitive impairment), with a mean value of 0.896 for patients without cognitive impairment and 1.658 for patients with cognitive impairment. Statistically significant differences were observed between normal CF-moderate CI, normal CF-severe CI, mild CF-moderate CI and mild CI-severe CI when participants were divided into 4 groups. With overall mean values of normal CF - 0.896, mild CI - 1.066, moderate CI 2.450 and severe CI 3.278. In the literature, the cut-off value for an abnormal finding on the MTA scale varies, with sources citing a score of 2 (up to 75 years of age) as an abnormal finding, other authors suggesting a cut-off value of 1.5, but most studies now recommend the use of age-appropriate values, i.e. a value ≥ 1.0 is considered abnormal in the < 65 age group, ≥ 1.5 in the 65–74 age group, ≥ 2.0 in the 75–84 age group and ≥ 2.0 in the > 85 age group (Barkhof and van Buchem, 2016; Claus et al., 2017; Ferreira et al., 2015).

Closely related to the MTA scale is the **entorhinal cortical atrophy scale (ERICA)**. The entorhinal cortical atrophy scale is a relatively newer scale and is less commonly used in clinical practice. The entorhinal cortex provides signal transmission from the hippocampus to the neocortex, is involved in memory consolidation processes and visuospatial navigation, and entorhinal atrophy has been observed to precede hippocampal atrophy in AD (Braak and Braak, 1991; Du et al., 2004; Enkirch et al., 2018; Khan et al., 2014; van Strien et al., 2009). Studies using the ERICA scale were able to distinguish Alzheimer's disease from subjective cognitive impairment with a sensitivity of 83 % and a specificity of 98 % (Enkirch et al., 2018). The ERICA scale showed statistically significant differences in both hemispheres when participants were divided into 2 groups:

those without cognitive impairment had a mean score of 0.583 on the right and 0.542 on the left, those with cognitive impairment had a mean score of 1.140 on the right and 1.228 on the left. Thus, our finding is different from that reported in the studies and patients with ERICA scale values below 2 were found to have cognitive impairment. When the ERICA scale was assessed in the 4 groups, statistically significant differences were observed between normal CF-moderate CI, normal CF-severe CI, mild CF-moderate CI and mild CI-severe CI. When considering the mean values per group, participants in the moderate CI and severe CI groups were closer to grade 2 of the ERICA scale. In contrast, no statistically significant differences were observed between normal CF and mild CI. In summary, the ERICA scale can be used as an additional tool to assess the brain in patients with subjective cognitive impairment, but findings in other assessment scales should also be considered.

The assessment of the **parietal lobe atrophy scale** is important because in early Alzheimer's disease, parietal lobe atrophy can be one of the first signs of cognitive impairment (Jacobs et al., 2011; Lehmann et al., 2012; Silhan et al., 2020). In our study group, statistically significant differences were observed between the cognitive impairment group and the no cognitive impairment group with mean values of 1.596 and 1.115, respectively. Statistically significant differences were also observed between the 4 patient groups, with statistically significant differences in the values of the parietal lobe. Atrophy Scale between the patient groups on both the right and left side. In contrast to previous visual assessment scales, statistically significant differences were also observed between normal CF and mild CI in the right parietal lobe, and no statistically significant differences were observed between mild CI and moderate CI. These differences point to the possible importance of parietal lobe atrophy in cognitive impairment and dementia, as suggested by several authors, especially in early dementia (Jacobs et al., 2011; Lehmann et al., 2012; Silhan et al., 2020).

The **microvascular structure** of the brain plays an important role in the pathogenesis of cognitive impairment. On structural MRI, the microvascular status can be assessed by detecting perivascular space enlargement, the presence of microhaemorrhages and white matter hyperintensities (Wardlaw et al., 2013).

Some authors suggest that **perivascular space enlargement** plays an important role in the functioning of the glymphatic system of the brain and could serve as a structural biomarker to identify individuals at increased risk of developing cognitive impairment (Jie et al., 2020; MacLulich et al., 2004; Wardlaw et al., 2013). However, as with other MRI biomarkers, perivascular space enlargement may be observed in patients with arterial hypertension, diabetes mellitus, and normal ageing (Choi et al., 2021; Gutierrez et al., 2017; Wardlaw et al., 2013).

Perivascular space enlargement was assessed in centrum semiovale, basal nuclei and midbrain using the scoring system proposed by Potter et al. (Potter et al., 2015). No statistically significant differences were observed in the perivascular space enlargement in the participant groups. Given that perivascular enlargement can also occur in normal ageing, it should be assessed together with other structural biomarkers, thus providing more insight into brain changes in cognitive impairment.

Although **microhaemorrhages** in the brain can affect cognitive function (Akoudad et al., 2016; Martinez-Ramirez et al., 2014) no statistically significant differences were observed when assessing microhaemorrhages in the participants of our study. This could be due to the exclusion criteria, as the patients with a history of haemorrhagic stroke were not included in the study.

The White Matter Hyperintensity Rating Scale is one of the oldest scales in use. When white matter hyperintensities were assessed in periventricular and deep white matter and participants were divided into 2 groups (with and without cognitive impairment), no statistically significant differences

between groups were observed. When patients were divided into 4 groups, statistically significant differences in PVWM and total Fazekas scale score were observed between normal CF-severe CI, mild CI-severe CI. Overall, white matter hyperintensities are a known risk factor for the development of cerebrovascular and neurodegenerative diseases (Brickman et al., 2012; Chen et al., 2021; Veldsman et al., 2020). PVWM and DWM hyperintensities are associated with cognitive impairment in domains such as information processing speed, executive function and attention (Prins and Scheltens, 2015). In some longitudinal studies, increases in white matter hyperintensities are associated with progression of cognitive impairment and reduction in cortical thickness (Boyle et al., 2016; Jiang et al., 2022; Kim et al., 2020; J. Lee et al., 2018). Despite several studies indicating an association of white matter hyperintensities with cognitive impairment, there are studies that attribute such an association to other conditions or observe only a small association when adjusting for confounding factors (Mortamais et al., 2013). In general, white matter hyperintensities could be one of the biomarkers for cognitive impairment, especially vascular cognitive impairment. In our study group, vascular cognitive impairment was an exclusion criterion and this could partly explain why no statistically significant differences were observed between our groups.

Overall, the results of the **visual assessment scales** suggest that the scales used are complementary and are representative of a particular brain region or observation that may affect cognitive function. The limiting factors of visual rating scales must be considered, i.e., the subjectivity of the rater, the experience of the rater in using the scales, the relatively lower sensitivity in the evaluation of small structures and the amount of time required for the evaluation. Therefore, the use of visual assessment scales in combination with quantitative brain data such as subcortical structure volume measurements, cortical thickness measurements and white matter tract analysis should be considered. Using

quantitative brain measurements it is possible to assess changes in the brain more objectively, and it is possible to assess changes in cortical thickness or volume that are not possible in qualitative assessment (Sangha et al., 2021; Schwarz et al., 2016).

When **subcortical brain structure volumes** were measured and participants were divided into 2 groups, statistically significant differences were observed in left hippocampal volume and bilaterally in the nucleus accumbens. In contrast, when the participants were divided into 4 groups, statistically significant differences were observed in the volumes of the hippocampus bilaterally, amygdala bilaterally, the left nucleus accumbens and the right cerebellar cortex. Similar results have been observed in other studies where significant differences in cognitive impairment are observed in the hippocampus and the amygdala (Dawe et al., 2020; Nobis et al., 2019; Sangha et al., 2021; Schwarz et al., 2016). The role of the hippocampus and amygdala in the development of cognitive impairment has been widely studied and to some extent explained, i.e. the hippocampus plays an important role in memory formation, memory consolidation, visuospatial processing (Braak and Braak, 1991; Dawe et al., 2020; Devanand et al., 2007; Lee et al., 2012; van Strien et al., 2009) and amygdala is responsible for emotion processing and emotion regulation - atrophy or damage to the amygdala can lead to emotional and behavioural changes that are common in people with dementia, such as apathy, anxiety and aggression (Belkhiria et al., 2020; Braak and Braak, 1991; Poulin et al., 2011; Prieto del Val et al., 2016).

Nucleus accumbens atrophy is less frequently reported in studies, but there are a number of studies showing similar changes with nucleus accumbens atrophy in patients with cognitive impairment and dementia (Kawakami et al., 2014; Nie et al., 2017), its atrophy is associated with clinical manifestations such as limbic dysfunction, depression, apathy, anxiety and nucleus accumbens

atrophy is also associated with symptoms of Parkinson's disease, which include hypokinesia and akinesia (Mavridis et al., 2011; Mavridis, 2015; Nie et al., 2017).

While historically cerebellar function was mainly associated with motor functions, coordination and balance, it has now become clear that the cerebellum is the associative centre for higher cognitive functions, and, thanks to fMRI scans, the association between cognition and specific regions of the cerebellum has been found (Allen and Courchesne, 1998; Koziol et al., 2014; Leiner et al., 1993), but it should be noted that several studies found no statistically significant differences with cognitive impairment (Bernard et al., 2014; Hoogendam et al., 2014; Paradiso et al., 1997; Zdanovskis et al., 2021). In contrast, the papers by Mitoma et al. and Bordignon et al. view the cerebellum as a structure that provides cognitive reserve, i.e., the cerebellar cognitive reserve is defined as the cerebellum's ability to compensate and restore some function in response to damage or atrophy in other parts of the brain. In the context of cognitive impairment, there may be no structural differences in the cerebellum between study groups, but there is a reorganization of compensatory signal transduction, which may result in improved cognitive function (Bordignon et al., 2021; Mitoma et al., 2020).

In addition to volumetric measures, **cortical thickness** in different brain regions was also analysed to identify possible differences between groups. Statistically significant differences in left entorhinal cortical thickness were observed when participants were divided into 2 groups. In contrast, when the participants were divided into 4 groups, statistically significant differences in cortical thickness were observed in the **temporal lobe** (bilateral entorhinal cortex, bilateral parahippocampal cortex, bilateral medial temporal lobe cortex, bilateral fusiform cortex, bilaterally in the superior cortex of the temporal lobe, in the right transverse cortex of the temporal lobe), the **parietal lobe** (bilaterally

in the supramarginal cortex, right cingulum isthmus part and left inferior cortex of the parietal lobe) and the right pericalcarine cortex of the **occipital lobe**.

The involvement of the entorhinal cortex in the development of cognitive impairment and the relationship of entorhinal cortex thickness measurements to it are well established (Holbrook et al., 2020; Velayudhan et al., 2013). Similar observations are also found in the parahippocampal cortex and other parts of the temporal lobe, which in combination with loss of cortical thickness in the temporal lobe may indicate a higher risk of developing dementia (Du et al., 2007; Machulda et al., 2020; Verfaillie et al., 2016; Zarei et al., 2013).

Our cortical measurements are partly consistent with other studies looking for “Alzheimer's disease signature cortex” (Bakkour et al., 2009; Dickerson et al., 2009; Schwarz et al., 2016). For example, the Schwarz et al study recommended 6 cortical regions to be evaluated in Alzheimer's disease – entorhinal cortex, fusiform cortex, parahippocampal cortex, medial temporal lobe, inferior temporal cortex and angular cortex – compared with our data, we have similar results, with 5 of 6 cortical regions showing the largest differences between groups. In general, other studies have also cited the entorhinal cortex, parahippocampal cortex and temporal lobe cortex as the main cortical areas to be assessed in cognitive impairment (Bakkour et al., 2009; Dickerson et al., 2009; Machulda et al., 2020; Schwarz et al., 2016).

In our study, a DTI sequence was used to evaluate quantitative tractography data, in this case fractional anisotropy (FA) data. DTI is a relatively newer technique used to assess white matter in the brain, i.e., to assess not only the presence of lesions (as in the case of white matter hyperintensities), but to determine to what extent these lesions may affect the integrity of the brain tracts. In the context of cognitive impairment, quantitative FA measurements are associated with changes in the nerve fibres of the tract, which also result in changes in the direction of diffusion of water molecules. Several studies have

observed changes in FA in specific brain regions that have been linked to the development of cognitive impairment, for example in the whole brain (Xing et al., 2021) and *corpus callosum* (Raghavan et al., 2020).

Fractional Anisotropy (FA) measurements were performed, and participants were divided into 2 groups and statistically significant differences were observed between the normative percentiles of the whole brain, right-sided and left-sided corticospinal tracts, with lower normative percentile values in the group without cognitive impairment. Limitations in the interpretation of these results should be mentioned. The normative percentile value is calculated as the value from the standardized control group, which assumes a linear relationship between FA and age change, some studies confirm this, but an examination of longitudinal data on FA and DTI assessment has concluded that there is a very wide variability in FA across the life course and also at the individual level (Sexton et al., 2014). In addition to individual variation, FA outcomes may be influenced by the development of the crossed tracts and changes in the microstructural organization of the tracts. Another important factor is the high heterogeneity in the group of patients with cognitive impairment, which makes comparison of FA difficult if milder and more severe cognitive impairment are not separated. Therefore, FA data were also compared by dividing patients into 4 groups.

When patients were divided into 4 groups, statistically significant differences were observed in whole-brain FA, whole-brain FA normative percentile score, bilaterally in SLF-arcuate FA and FA normative percentile, in the asymmetry of SLF-arcuate FA, bilaterally in inferior frontal-occipital fasciculus FA and normative percentile, left cingulum FA and normative percentile, and right cingulum FA normative percentile.

Comparing the results with studies by other authors, Xing et al. concluded that whole-brain FA changes are a better predictor of cognitive impairment than tract-specific FA measurements and brain volume measurements (Xing et al., 2021). The SLF-arcuate fasciculus connect different lobes of the brain, thus affecting several cognitive domains that also provide visuospatial function and speech perception and memory, but the relationship with cognitive function is not straightforward across studies, i.e., Hoeft et al. found that increased FA was associated with poorer visuospatial function performance (Hoeft et al., 2007; Koshiyama et al., 2020; Koyama and Domen, 2017). In contrast, a decrease in cingulum FA in cognitive impairment has been observed in several studies (Dalboni da Rocha et al., 2020; Hall et al., 2021; Xiao et al., 2022). As before, FA results should be interpreted with caution. DTI provides additional information on the structure of the white matter of the brain, but there are several limitations in the evaluation and reproducibility of these results, i.e., the quantitative value of FA is a general measure of the localization of a specific region/tract and the analysis does not take into account fibre crossing or damage in another tract; the DTI sequence has a relatively higher signal-to-noise ratio (SNR) compared to other sequences, which can be partially corrected by choosing appropriate scan parameters (increasing scan time) and performing appropriate image post-processing; The DTI sequence is sensitive to motion and other artefacts that can lead to inaccurate diffusion measurements resulting in inaccurate fractional anisotropy results; differences in equipment, post-processing algorithms and data acquisition methods make DTI results difficult to reproduce (Tax et al., 2022).

Despite its limitations, the use of DTI sequences in the diagnosis of cognitive impairment provides additional information that potentially could be used in future.

Limitations and constraints in the evaluation of quantitative brain MRI data in cognitive impairment

In general, the assessment and diagnosis of cognitive impairment, both clinically and radiologically, is a complex process and requires multidisciplinary collaboration and active patient follow-up to differentiate at-risk patients early. Several limitations of cognitive impairment studies, including the one performed, can have a significant impact on the interpretation of results:

1. **Participant selection and heterogeneity.** Patient selection and patient heterogeneity may affect the results of a study. Most participants in the control group presented to a neurologist with complaints unrelated to cognitive impairment or with subjective cognitive impairment. In certain cases, this cohort of control participants may not be representative of the general population and the values from controls may be inaccurate, leading to inaccurate interpretation of results and erroneous conclusions.
2. **Insufficient number of participants.** A limited number of participants affects the statistical power of the results. Within the framework of the thesis, appropriate statistical analysis methods were used to confirm or reject the hypotheses. Based on the statistical power calculations and the effect sizes of the existing variables, the required number of patients to achieve 80 % statistical power when dividing patients into 2 groups (with and without cognitive impairment) and assessing them by visual rating scales requires between 70 and 145 participants per group, whereas when assessing patients quantitative measures the required number of participants per group (depending on the variable chosen) is between 100 and 1000. Further research on cognitive impairment should consider the number of participants needed to achieve greater statistical power.

3. **Software and software development.** All MR images of the study participants were analysed with the latest version of Freesurfer software and the latest Icometrix software package. The data generated by this software are applicable to the current version of the software and are not applicable to older versions and are unlikely to be applicable to newer versions of the software. Note that the brain data obtained are only comparable to the results analysed in the specific software. If other software is used - using other segmentation algorithms or machine learning algorithms - the results may differ. With software development - new results may be discovered related to changes in cognitive function and dementia.
4. **Technological differences in MR equipment.** The magnetic field strength of the MR equipment, the MR equipment from different manufacturers, the chosen MR sequences and sequence parameters can all affect the quantitative MR results and make the data difficult to compare, reproduce and interpret.
5. **Subjective assessment of cognitive function.** Although cognitive tests are designed to reduce subjectivity, the communication between the test-taker and the performer and possible communication problems that may lead to inaccurate cognitive assessment must be considered.
6. **Control group and study participant differences.** Without a properly matched control group that is as similar as possible to the study participants, it may be difficult to identify which radiological changes are associated with cognitive changes and dementia.
7. **Lack of longitudinal data.** Quantitative changes in brain structure over time are influenced by a variety of factors with wide individual variability, so it should be noted that longitudinal data may be more

useful in certain cases than a cross-sectional measure of age-matched normalized values or a control group.

8. **Impact of biological and environmental factors.** Several biological and environmental factors, such as heredity, education, medication use, diet, and lifestyle, can influence both changes in brain biomarkers and the development of cognitive function and dementia. It can be difficult to exclude or control the influence of all these factors in a study.
9. **Co-morbidities of participants.** Other medical conditions and diseases that may be associated with cognitive changes and dementia may cause problems in the interpretation of the study results, such as depression, diabetes, hypertension, other undiagnosed psychiatric conditions, etc.

Despite several limitations, thanks to the software developments, improvements in standardization and the introduction of new clinically validated tools into clinical practice, quantitative MRI biomarkers offer the opportunity to assess the brain objectively and comprehensively, including cortical thicknesses, subcortical volumes and assessment of white matter structure.

Overall, the use of quantitative MRI biomarkers in cognitive impairment and dementia is a relatively new and evolving area of research that could in the near future improve the accuracy of diagnostics.

Conclusions

The aim of this thesis was to determine the association of qualitative and quantitative changes in radiological biomarkers in the brain with changes in cognitive function and dementia. The aims of the thesis were achieved, and the hypotheses were confirmed:

- In cognitive impairment and dementia there are structural changes that can be assessed by both visual rating scales and quantitative brain analysis.
- In cognitive impairment, changes in quantitative values are observed in specific brain regions.

Based on the analysis of the *visual assessment scales*, an association with cognitive impairment was observed by assessing Global Cortical Atrophy Scale, Medial Lobe Atrophy Scale, Entorhinal Cortical Atrophy Scale, Parietal Lobe Atrophy Scale scores.

Based on the quantitative measurements identified, the following conclusions were drawn for **quantitative biomarkers of MR**:

- By performing **volumetric measurements** association with cognitive impairment was observed in hippocampal volume, amygdala volume and *nucleus accumbens* volume.
- By performing **cortical thickness measurements** association with cognitive impairment was observed in entorhinal cortex bilaterally, parahippocampal cortex bilaterally, middle temporal lobe cortex bilaterally, fusiform cortex bilaterally, superior temporal lobe cortex bilaterally, transversal temporal lobe cortex on the right side, supramarginal cortex bilaterally, *isthmus cinguli* cortex on the right side, lower parietal lobe cortex on the left side and pericalcarine cortex on the right side.

Principal Component Analysis (PCA) was used to identify relationships between multiple quantitative variables and to derive several principal components that could be used in further research to explain differences between cognitive impairment groups.

Based on the DTI FA quantitative measures the association with cognitive impairment was observed in whole-brain FA results, SLF-arcuate fasciculus FA results bilaterally, inferior frontal-occipital fasciculus FA results bilaterally and cingulum FA results bilaterally.

Recommendations

1. In patients with cognitive impairment, MRI scans should include sequences that allow image post-processing and quantitative assessment of structures, i.e., 3D T1, 3D FLAIR. Additional sequences for further studies should also be considered including diffusion imaging (with multiple b-values and multiple directions), arterial spin labelling (ASL) and functional magnetic resonance imaging (fMRI).
2. Based on our findings, MRI reports for patients with suspected cognitive impairment should include:
 - Fazekas scale,
 - Medial temporal atrophy scale,
 - Parietal atrophy scale,
 - Global cortical atrophy scale,
 - Entorhinal cortical atrophy scale,
3. In patients with suspected cognitive impairments, using clinically validated quantification software (depending on the software's capabilities), assess:
 - Hippocampal volume,
 - Amygdala volume,
 - Entorhinal cortex thickness,
 - Parahippocampal cortex,
 - Temporal and parietal cortex thickness and volumetric data (depending on software capabilities).
4. If applicable, give possible etiological cause of cognitive impairment based on MRI findings, i.e., vascular cognitive impairment, neurodegenerative disease, mixed cognitive impairment.

5. The observed relationships based on the analysis of the principal components could be used in future studies to create predictive models and analyse the relationship of principal components with diagnosis of cognitive disorders.

Publications and thesis

Publications:

1. **Zdanovskis, N.**, Platkājis, A., Kostiks, A., Šneidere, K., Stepens, A., Naglis, R., & Karelis, G. 2022. Combined Score of Perivascular Space Dilatation and White Matter Hyperintensities in Patients with Normal Cognition, Mild Cognitive Impairment, and Dementia. *Medicina*, 58(7), 887. MDPI AG. Retrieved from <http://dx.doi.org/10.3390/medicina58070887>
2. **Zdanovskis, N.**, Platkājis, A., Kostiks, A., Grigorjeva, O., & Karelis, G. 2021. Cerebellar Cortex and Cerebellar White Matter Volume in Normal Cognition, Mild Cognitive Impairment, and Dementia. *Brain Sciences*, 11(9), 1134. MDPI AG. Retrieved from <http://dx.doi.org/10.3390/brainsci11091134>
3. **Zdanovskis, N.**, Platkājis, A., Kostiks, A., Karelis, G., & Grigorjeva, O. 2021. Brain Structural Connectivity Differences in Patients with Normal Cognition and Cognitive Impairment. *Brain Sciences*, 11(7), 943. MDPI AG. Retrieved from <http://dx.doi.org/10.3390/brainsci11070943>
4. **Zdanovskis, N.**, Platkājis, A., Kostiks, A., & Karelis, G. 2020. Structural Analysis of Brain Hub Region Volume and Cortical Thickness in Patients with Mild Cognitive Impairment and Dementia. *Medicina*, 56(10), 497. MDPI AG. Retrieved from <http://dx.doi.org/10.3390/medicina56100497>

International oral presentations:

1. **Zdanovskis, N.** 2023. Combined Score of Perivascular Space Dilatation and White Matter Hyperintensities in Patients with Normal Cognition, Mild Cognitive Impairment and Dementia. *RSU Research Week 2023, Knowledge for Use in Practice*. 30.03.2023.
2. **Zdanovskis, N.** 2023. Current Approach to Alzheimer's Disease in Radiology and Other Neurodegenerative Diseases and Importance of Radiology in Clinical Trials of AD Drugs. *RSU Research Week 2023, Knowledge for Use in Practice*. 29.03.2023.
3. **Zdanovskis, N.** 2023. MR diagnostics in Parkinson's disease – structural, functional and biochemical imaging biomarkers. *Latvian Association of Neurodegenerative Diseases meeting in 2023 “Challenges of Parkinson’s Disease Management”*
4. **Zdanovskis, N.**, Platkājis, A., Kostiks, A., Šneidere, K., Naglis, R., Stepens, A., Karelis, G. 2022. Brain Hub Cortical Thickness in Patients with Normal Cognition and Cognitive Impairment. *Annual Congress RSNA 2022, Chicago, USA*.
5. **Zdanovskis, N.**, Platkājis, A. Brain Imaging in Neuroscience – Corticometry, Volumetry and Tractometry. 2021. *Veselība un personības attīstība: starpdisciplinārā pieeja, 7. starptautiskā zinātniski praktiskā konference 2021. gada 22.–24. aprīlī*, 23.04.2021.

6. **Zdanovskis, N.**, Platkājis, A., Kostiks, A., Karelis, G. 2021. MRI whole-brain connectometry analysis in patients with mild cognitive impairment and dementia. *Rīga Stradiņš University International Research Conference On Medical And Healthcare Sciences «Knowledge for Use in Practice»*, 25.03.2021.

International posters:

1. **Zdanovskis, N.**, Platkājis, A., Kostiks, A., Šneidere, K., Stepens, A., Karelis, G. 2022. Multiparametric Brain MRI Evaluation in Patients with Cognitive Impairment. *European Congress of Radiology 2022*, EPOS C-10232, Vienna, Austria, DOI-Link: <https://dx.doi.org/10.26044/ecr2022/C-10232>

Local scientific meetings:

1. **Zdanovskis., N.**, Platkājis, A. Radiological diagnostics in cases of cognitive disorders and dementia. 2021. Meeting of the Association of Neurodegenerative Diseases of Latvia, report 16.04.2021.
2. **Zdanovskis., N.** Tractography of the brain, connectometry, graph analysis – possibilities today and application in the future. 2021. Meeting of the Association of Radiologists of Latvia, report.
3. **Zdanovskis., N.**, Platkājis, A. Radiological diagnosis and image interpretation of neurodegenerative diseases of the brain. 2020. Meeting of the Association of Radiologists of Latvia, report.

References

1. Akoudad, S., Wolters, F.J., Viswanathan, A., de Bruijn, R.F., van der Lugt, A., Hofman, A., Koudstaal, P.J., Ikram, M.A., Vernooij, M.W., 2016. Cerebral microbleeds are associated with cognitive decline and dementia: the Rotterdam Study. *JAMA Neurol.* 73, 934–943. <https://doi.org/10.1001/jamaneurol.2016.1017>
2. Al-Janabi, O.M., Panuganti, P., Abner, E.L., Bahrani, A.A., Murphy, R., Bardach, S.H., Caban-Holt, A., Nelson, P.T., Gold, B.T., Smith, C.D., Wilcock, D.M., Jicha, G.A., 2018. Global Cerebral Atrophy Detected by Routine Imaging: Relationship with Age, Hippocampal atrophy, and White Matter Hyperintensities. *J. Neuroimaging Off. J. Am. Soc. Neuroimaging* 28, 301–306. <https://doi.org/10.1111/jon.12494>
3. Allen, G., Courchesne, E., 1998. The cerebellum and non-motor function: clinical implications. *Mol. Psychiatry* 3, 207–210. <https://doi.org/10.1038/sj.mp.4000395>
4. Arba, F., Quinn, T.J., Hankey, G.J., Lees, K.R., Wardlaw, J.M., Ali, M., Inzitari, D., 2018. Enlarged perivascular spaces and cognitive impairment after stroke and transient ischemic attack. *Int. J. Stroke* 13, 47–56. <https://doi.org/10.1177/1747493016666091>
5. Baars, B.J., Gage, N.M. (Eds.), 2013. Chapter 9 - Learning and memory, in: *Fundamentals of Cognitive Neuroscience*. Academic Press, San Diego, pp. 253–288. <https://doi.org/10.1016/B978-0-12-415805-4.00009-6>
6. Bakker, E.N.T.P., Bacskai, B.J., Arbel-Ornath, M., Aldea, R., Bedussi, B., Morris, A.W.J., Weller, R.O., Carare, R.O., 2016. Lymphatic Clearance of the Brain: Perivascular, Paravascular and Significance for Neurodegenerative Diseases. *Cell. Mol. Neurobiol.* 36, 181–194. <https://doi.org/10.1007/s10571-015-0273-8>
7. Bakkour, A., Morris, J.C., Dickerson, B.C., 2009. The cortical signature of prodromal AD. *Neurology* 72, 1048–1055. <https://doi.org/10.1212/01.wnl.0000340981.97664.2f>
8. Barkhof, F., van Buchem, M.A., 2016. Neuroimaging in Dementia, in: Hodler, J., Kubik-Huch, R.A., von Schulthess, G.K. (Eds.), *Diseases of the Brain, Head and Neck, Spine 2016-2019*. Springer International Publishing, Cham, pp. 79–85. https://doi.org/10.1007/978-3-319-30081-8_10
9. Becerra-Laparra, I., Cortez-Conradis, D., Garcia-Lazaro, H.G., Martinez-Lopez, M., Roldan-Valadez, E., 2020. Radial diffusivity is the best global biomarker able to discriminate healthy elders, mild cognitive impairment, and Alzheimer’s disease: A diagnostic study of DTI-derived data. *Neurol. India* 68, 427–434. <https://doi.org/10.4103/0028-3886.284376>
10. Belkhiria, C., Vergara, R.C., San Martin, S., Leiva, A., Martinez, M., Marcenaro, B., Andrade, M., Delano, P.H., Delgado, C., 2020. Insula and Amygdala Atrophy Are Associated With Functional Impairment in Subjects With Presbycusis. *Front. Aging Neurosci.* 12.

11. Bernard, J.A., Leopold, D.R., Calhoun, V.D., Mittal, V.A., 2014. Regional cerebellar volume and cognitive function from adolescence to late middle age. *Hum. Brain Mapp.* 36, 1102–1120. <https://doi.org/10.1002/hbm.22690>
12. Bernardin, F., Maheut-Bosser, A., Paille, F., 2014. Cognitive Impairments in Alcohol-Dependent Subjects. *Front. Psychiatry* 5.
13. Bolandzadeh, N., Davis, J.C., Tam, R., Handy, T.C., Liu-Ambrose, T., 2012. The association between cognitive function and white matter lesion location in older adults: a systematic review. *BMC Neurol.* 12, 126. <https://doi.org/10.1186/1471-2377-12-126>
14. Bordignon, A., Devita, M., Sergi, G., Coin, A., 2021. “Cerebellar cognitive reserve”: a possible further area of investigation. *Aging Clin. Exp. Res.* 33, 2883–2886. <https://doi.org/10.1007/s40520-021-01795-1>
15. Boyle, P.A., Yu, L., Fleischman, D.A., Leurgans, S., Yang, J., Wilson, R.S., Schneider, J.A., Arvanitakis, Z., Arfanakis, K., Bennett, D.A., 2016. White matter hyperintensities, incident mild cognitive impairment, and cognitive decline in old age. *Ann. Clin. Transl. Neurol.* 3, 791–800. <https://doi.org/10.1002/acn3.343>
16. Braak, H., Braak, E., 1991. Neuropathological staging of Alzheimer-related changes. *Acta Neuropathol. (Berl.)* 82, 239–259. <https://doi.org/10.1007/BF00308809>
17. Brant-Zawadzki, M., Gillan, G.D., Nitz, W.R., 1992. MP RAGE: a three-dimensional, T1-weighted, gradient-echo sequence—initial experience in the brain. *Radiology* 182, 769–775. <https://doi.org/10.1148/radiology.182.3.1535892>
18. Brickman, A.M., Provenzano, F.A., Muraskin, J., Manly, J.J., Blum, S., Apa, Z., Stern, Y., Brown, T.R., Luchsinger, J.A., Mayeux, R., 2012. Regional white matter hyperintensity volume, not hippocampal atrophy, predicts incident Alzheimer’s disease in the community. *Arch. Neurol.* 69, 1621–1627. <https://doi.org/10.1001/archneurol.2012.1527>
19. Buckner, R.L., 2013. The brain’s default network: origins and implications for the study of psychosis. *Dialogues Clin. Neurosci.* 15, 351–358.
20. Buie, J.J., Watson, L.S., Smith, C.J., Sims-Robinson, C., 2019. Obesity-related cognitive impairment: The role of endothelial dysfunction. *Neurobiol. Dis.* 132, 104580. <https://doi.org/10.1016/j.nbd.2019.104580>
21. Cavedo, E., Tran, P., Thoprakarn, U., Martini, J.-B., Movschin, A., Delmaire, C., Gariel, F., Heidelberg, D., Pyatigorskaya, N., Ströer, S., Krolak-Salmon, P., Cotton, F., dos Santos, C.L., Dormont, D., 2022. Validation of an automatic tool for the rapid measurement of brain atrophy and white matter hyperintensity: QyScore®. *Eur. Radiol.* 32, 2949–2961. <https://doi.org/10.1007/s00330-021-08385-9>
22. Chalavi, S., Simmons, A., Dijkstra, H., Barker, G.J., Reinders, A.S., 2012. Quantitative and qualitative assessment of structural magnetic resonance imaging data in a two-center study. *BMC Med. Imaging* 12, 27. <https://doi.org/10.1186/1471-2342-12-27>

23. Chan, D., Fox, N.C., Jenkins, R., Schill, R.I., Crum, W.R., Rossor, M.N., 2001. Rates of global and regional cerebral atrophy in AD and frontotemporal dementia. *Neurology* 57, 1756–1763. <https://doi.org/10.1212/WNL.57.10.1756>
24. Chao, L.L., Buckley, S.T., Kornak, J., Schuff, N., Madison, C., Yaffe, K., Miller, B.L., Kramer, J.H., Weiner, M.W., 2010. ASL Perfusion MRI Predicts Cognitive Decline and Conversion From MCI to Dementia. *Alzheimer Dis. Assoc. Disord.* 24, 19–27. <https://doi.org/10.1097/WAD.0b013e3181b4f736>
25. Chen, Y., Wang, X., Guan, L., Wang, Y., 2021. Role of White Matter Hyperintensities and Related Risk Factors in Vascular Cognitive Impairment: A Review. *Biomolecules* 11, 1102. <https://doi.org/10.3390/biom11081102>
26. Choi, E.Y., Park, Y.W., Lee, M., Kim, M., Lee, C.S., Ahn, S.S., Kim, J., Lee, S.-K., 2021. Magnetic Resonance Imaging-Visible Perivascular Spaces in the Basal Ganglia Are Associated With the Diabetic Retinopathy Stage and Cognitive Decline in Patients With Type 2 Diabetes. *Front. Aging Neurosci.* 13, 666495. <https://doi.org/10.3389/fnagi.2021.666495>
27. Claus, J.J., Staekenborg, S.S., Holl, D.C., Roorda, J.J., Schuur, J., Koster, P., Tielkes, C.E.M., Scheltens, P., 2017. Practical use of visual medial temporal lobe atrophy cut-off scores in Alzheimer’s disease: Validation in a large memory clinic population. *Eur. Radiol.* 27, 3147–3155. <https://doi.org/10.1007/s00330-016-4726-3>
28. Collier, Q., Veraart, J., Jeurissen, B., den Dekker, A.J., Sijbers, J., 2015. Iterative reweighted linear least squares for accurate, fast, and robust estimation of diffusion magnetic resonance parameters. *Magn. Reson. Med.* 73, 2174–2184. <https://doi.org/10.1002/mrm.25351>
29. Cordonnier, C., Potter, G.M., Jackson, C.A., Doubal, F., Keir, S., Sudlow, C.L.M., Wardlaw, J.M., Al-Shahi Salman, R., 2009. Improving interrater agreement about brain microbleeds: development of the Brain Observer MicroBleed Scale (BOMBS). *Stroke* 40, 94–99. <https://doi.org/10.1161/STROKEAHA.108.526996>
30. Cummings, J., Ritter, A., Zhong, K., n.d. Clinical Trials for Disease-Modifying Therapies in Alzheimer’s Disease: A Primer, Lessons Learned, and a Blueprint for the Future. *J. Alzheimers Dis.* 64, S3–S22. <https://doi.org/10.3233/JAD-179901>
31. Custodio, N., Malaga, M., Chamberg-Michilot, D., Montesinos, R., Moron, E., Vences, M.A., Huilca, J.C., Lira, D., Failoc-Rojas, V.E., Diaz, M.M., 2022. Combining visual rating scales to identify prodromal Alzheimer’s disease and Alzheimer’s disease dementia in a population from a low and middle-income country. *Front. Neurol.* 13, 962192. <https://doi.org/10.3389/fneur.2022.962192>
32. Cutsuridis, V., Yoshida, M., 2017. Editorial: Memory Processes in Medial Temporal Lobe: Experimental, Theoretical and Computational Approaches. *Front. Syst. Neurosci.* 11.

33. Dalboni da Rocha, J.L., Bramati, I., Coutinho, G., Tovar Moll, F., Sitaram, R., 2020. Fractional Anisotropy changes in Parahippocampal Cingulum due to Alzheimer's Disease. *Sci. Rep.* 10, 2660. <https://doi.org/10.1038/s41598-020-59327-2>
34. Dale, A., Fischl, B., Sereno, M.I., 1999. Cortical Surface-Based Analysis: I. Segmentation and Surface Reconstruction. *NeuroImage* 9, 179–194.
35. Dawe, R.J., Yu, L., Arfanakis, K., Schneider, J.A., Bennett, D.A., Boyle, P.A., 2020. Late-life cognitive decline is associated with hippocampal volume, above and beyond its associations with traditional neuropathologic indices. *Alzheimers Dement.* 16, 209–218. <https://doi.org/10.1002/alz.12009>
36. Demšar, J., Curk, T., Erjavec, A., Gorup, Č., Hočevar, T., Milutinovič, M., Možina, M., Polajnar, M., Toplak, M., Starič, A., Štajdohar, M., Umek, L., Žagar, L., Žbontar, J., Žitnik, M., Zupan, B., 2013. Orange: Data Mining Toolbox in Python. *J. Mach. Learn. Res.* 14, 2349–2353.
37. Demšar, J., Leban, G., Zupan, B., 2007. FreeViz—An intelligent multivariate visualization approach to explorative analysis of biomedical data. *J. Biomed. Inform., Intelligent Data Analysis in Biomedicine* 40, 661–671. <https://doi.org/10.1016/j.jbi.2007.03.010>
38. Desikan, R.S., Ségonne, F., Fischl, B., Quinn, B.T., Dickerson, B.C., Blacker, D., Buckner, R.L., Dale, A.M., Maguire, R.P., Hyman, B.T., Albert, M.S., Killiany, R.J., 2006. An automated labeling system for subdividing the human cerebral cortex on MRI scans into gyral based regions of interest. *NeuroImage* 31, 968–980. <https://doi.org/10.1016/j.neuroimage.2006.01.021>
39. DESTRIEUX, C., FISCHL, B., DALE, A., HALGREN, E., 2010. Automatic parcellation of human cortical gyri and sulci using standard anatomical nomenclature. *NeuroImage* 53, 1–15. <https://doi.org/10.1016/j.neuroimage.2010.06.010>
40. Devanand, D.P., Pradhaban, G., Liu, X., Khandji, A., De Santi, S., Segal, S., Rusinek, H., Pelton, G.H., Honig, L.S., Mayeux, R., Stern, Y., Tabert, M.H., de Leon, M.J., 2007. Hippocampal and entorhinal atrophy in mild cognitive impairment: prediction of Alzheimer disease. *Neurology* 68, 828–836. <https://doi.org/10.1212/01.wnl.0000256697.20968.d7>
41. Dickerson, B.C., Bakkour, A., Salat, D.H., Feczko, E., Pacheco, J., Greve, D.N., Grodstein, F., Wright, C.I., Blacker, D., Rosas, H.D., Sperlberg, R.A., Atri, A., Growdon, J.H., Hyman, B.T., Morris, J.C., Fischl, B., Buckner, R.L., 2009. The Cortical Signature of Alzheimer's Disease: Regionally Specific Cortical Thinning Relates to Symptom Severity in Very Mild to Mild AD Dementia and is Detectable in Asymptomatic Amyloid-Positive Individuals. *Cereb. Cortex N. Y. NY* 19, 497–510. <https://doi.org/10.1093/cercor/bhn113>
42. Dolz, J., Desrosiers, C., Wang, L., Yuan, J., Shen, D., Ben Ayed, I., 2020. Deep CNN ensembles and suggestive annotations for infant brain MRI segmentation. *Comput. Med. Imaging Graph. Off. J. Comput. Med. Imaging Soc.* 79, 101660. <https://doi.org/10.1016/j.compmedimag.2019.101660>

43. Donaghy, P.C., Firbank, M., Mitra, D., Petrides, G., Lloyd, J., Barnett, N., Olsen, K., Thomas, A.J., O'Brien, J.T., 2020. Microbleeds in dementia with Lewy bodies. *J. Neurol.* 267, 1491–1498. <https://doi.org/10.1007/s00415-020-09736-0>
44. Du, A.T., Schuff, N., Kramer, J.H., Ganzer, S., Zhu, X.P., Jagust, W.J., Miller, B.L., Reed, B.R., Mungas, D., Yaffe, K., Chui, H.C., Weiner, M.W., 2004. Higher atrophy rate of entorhinal cortex than hippocampus in AD. *Neurology* 62, 422–427.
45. Du, A.-T., Schuff, N., Kramer, J.H., Rosen, H.J., Gorno-Tempini, M.L., Rankin, K., Miller, B.L., Weiner, M.W., 2007. Different regional patterns of cortical thinning in Alzheimer's disease and frontotemporal dementia. *Brain J. Neurol.* 130, 1159–1166. <https://doi.org/10.1093/brain/awm016>
46. Eickhoff, S.B., Müller, V.I., 2015. Functional Connectivity, in: Toga, A.W. (Ed.), *Brain Mapping*. Academic Press, Waltham, pp. 187–201. <https://doi.org/10.1016/B978-0-12-397025-1.00212-8>
47. Enkirch, S.J., Traschütz, A., Müller, A., Widmann, C.N., Gielen, G.H., Heneka, M.T., Jurcoane, A., Schild, H.H., Hattingen, E., 2018. The ERICA Score: An MR Imaging-based Visual Scoring System for the Assessment of Entorhinal Cortex Atrophy in Alzheimer Disease. *Radiology* 288, 226–333. <https://doi.org/10.1148/radiol.2018171888>
48. Erickson, K.I., Hillman, C., Stillman, C.M., Ballard, R.M., Bloodgood, B., Conroy, D.E., Macko, R., Marquez, D.X., Petruzzello, S.J., Powell, K.E., 2019. Physical Activity, Cognition, and Brain Outcomes: A Review of the 2018 Physical Activity Guidelines. *Med. Sci. Sports Exerc.* 51, 1242–1251. <https://doi.org/10.1249/MSS.0000000000001936>
49. Eubank, J.M., Oberlin, D.J., Alto, A., Sahyoun, N.R., Asongwed, E., Monroe-Lord, L., Harrison, E.A., 2022. Effects of Lifestyle Factors on Cognition in Minority Population of Older Adults: A Review. *Front. Nutr.* 9, 841070. <https://doi.org/10.3389/fnut.2022.841070>
50. Fazekas, F., Chawluk, J.B., Alavi, A., Hurtig, H.I., Zimmerman, R.A., 1987. MR signal abnormalities at 1.5 T in Alzheimer's dementia and normal aging. *AJR Am. J. Roentgenol.* 149, 351–356. <https://doi.org/10.2214/ajr.149.2.351>
51. Ferreira, D., Cavallin, L., Larsson, E.-M., Muehlboeck, J.-S., Mecocci, P., Vellas, B., Tsolaki, M., Kłoszewska, I., Soininen, H., Lovestone, S., Simmons, A., Wahlund, L.-O., Westman, E., AddNeuroMed consortium and the Alzheimer's Disease Neuroimaging Initiative, 2015. Practical cut-offs for visual rating scales of medial temporal, frontal and posterior atrophy in Alzheimer's disease and mild cognitive impairment. *J. Intern. Med.* 278, 277–290. <https://doi.org/10.1111/joim.12358>

52. Festari, C., Massa, F., Cotta Ramusino, M., Gandolfo, F., Nicolosi, V., Orini, S., Aarsland, D., Agosta, F., Babiloni, C., Boada, M., Borroni, B., Cappa, S., Dubois, B., Frederiksen, K.S., Froelich, L., Garibotto, V., Georges, J., Haliassos, A., Hansson, O., Jessen, F., Kamondi, A., Kessels, R.P.C., Morbelli, S., O'Brien, J.T., Otto, M., Perret-Liaudet, A., Pizzini, F.B., Ritchie, C.W., Scheltens, P., Vandenberghe, M., Vanninen, R., Verhey, F., Vernooij, M.W., Yousry, T., Van Der Flier, W.M., Nobili, F., Frisoni, G.B., 2022. European consensus for the diagnosis of MCI and mild dementia: Preparatory phase. *Alzheimers Dement. J. Alzheimers Assoc.* <https://doi.org/10.1002/alz.12798>
53. Fischl, B., Dale, A.M., 2000. Measuring the thickness of the human cerebral cortex from magnetic resonance images. *Proc. Natl. Acad. Sci. U. S. A.* 97, 11050–11055.
54. Fischl, B., Liu, A., Dale, A.M., 2001. Automated manifold surgery: constructing geometrically accurate and topologically correct models of the human cerebral cortex. *IEEE Med. Imaging* 20, 70–80.
55. Fischl, B., Salat, D.H., Busa, E., Albert, M., Dieterich, M., Haselgrove, C., van der Kouwe, A., Killiany, R., Kennedy, D., Klaveness, S., Montillo, A., Makris, N., Rosen, B., Dale, A.M., 2002. Whole brain segmentation: automated labeling of neuroanatomical structures in the human brain. *Neuron* 33, 341–355.
56. Fischl, B., Salat, D.H., Kouwe, A.J.W. van der, Makris, N., Ségonne, F., Quinn, B.T., Dale, A.M., 2004. Sequence-independent segmentation of magnetic resonance images. *NeuroImage* 23, S69–S84. [https://doi.org/DOI: 10.1016/j.neuroimage.2004.07.016](https://doi.org/DOI:10.1016/j.neuroimage.2004.07.016)
57. Francis, F., Ballerini, L., Wardlaw, J.M., 2019. Perivascular spaces and their associations with risk factors, clinical disorders and neuroimaging features: A systematic review and meta-analysis. *Int. J. Stroke* 14, 359–371. <https://doi.org/10.1177/1747493019830321>
58. Frisoni, G.B., Fox, N.C., Jack, C.R., Scheltens, P., Thompson, P.M., 2010. The clinical use of structural MRI in Alzheimer disease. *Nat. Rev. Neurol.* 6, 67–77. <https://doi.org/10.1038/nrneurol.2009.215>
59. Gordon, B.A., Blazey, T., Su, Y., Fagan, A.M., Holtzman, D.M., Morris, J.C., Benzinger, T.L.S., 2016. Longitudinal β -Amyloid Deposition and Hippocampal Volume in Preclinical Alzheimer Disease and Suspected Non-Alzheimer Disease Pathophysiology. *JAMA Neurol.* 73, 1192–1200. <https://doi.org/10.1001/jamaneurol.2016.2642>
60. Grafton, S.T., Volz, L.J., 2019. Chapter 13 - From ideas to action: The prefrontal–premotor connections that shape motor behavior, in: D'Esposito, M., Grafman, J.H. (Eds.), *Handbook of Clinical Neurology, The Frontal Lobes*. Elsevier, pp. 237–255. <https://doi.org/10.1016/B978-0-12-804281-6.00013-6>
61. Gregoire, S.M., Chaudhary, U.J., Brown, M.M., Yousry, T.A., Kallis, C., Jäger, H.R., Werring, D.J., 2009. The Microbleed Anatomical Rating Scale (MARS): reliability of a tool to map brain microbleeds. *Neurology* 73, 1759–1766. <https://doi.org/10.1212/WNL.0b013e3181c34a7d>

62. Grieve, S.M., Williams, L.M., Paul, R.H., Clark, C.R., Gordon, E., 2007. Cognitive Aging, Executive Function, and Fractional Anisotropy: A Diffusion Tensor MR Imaging Study. *Am. J. Neuroradiol.* 28, 226–235.
63. Griffanti, L., Jenkinson, M., Suri, S., Zsoldos, E., Mahmood, A., Filippini, N., Sexton, C.E., Topiwala, A., Allan, C., Kivimäki, M., Singh-Manoux, A., Ebmeier, K.P., Mackay, C.E., Zamboni, G., 2018. Classification and characterization of periventricular and deep white matter hyperintensities on MRI: A study in older adults. *NeuroImage, Segmenting the Brain* 170, 174–181. <https://doi.org/10.1016/j.neuroimage.2017.03.024>
64. Gutierrez, J., Elkind, M.S.V., Dong, C., Di Tullio, M., Rundek, T., Sacco, R.L., Wright, C.B., 2017. Brain Perivascular Spaces as Biomarkers of Vascular Risk: Results from the Northern Manhattan Study. *AJNR Am. J. Neuroradiol.* 38, 862–867. <https://doi.org/10.3174/ajnr.A5129>
65. Hall, J.R., Johnson, L.A., Zhang, F., Petersen, M., Toga, A.W., Shi, Y., Mason, D., Rissman, R.A., Yaffe, K., O'Bryant, S.E., for the HABLE Study, 2021. Using Fractional Anisotropy Imaging to Detect Mild Cognitive Impairment and Alzheimer's Disease among Mexican Americans and Non-Hispanic Whites: A HABLE Study. *Dement. Geriatr. Cogn. Disord.* 50, 266–273. <https://doi.org/10.1159/000518102>
66. Hampel, H., Hardy, J., Blennow, K., Chen, C., Perry, G., Kim, S.H., Villemagne, V.L., Aisen, P., Vendruscolo, M., Iwatsubo, T., Masters, C.L., Cho, M., Lannfelt, L., Cummings, J.L., Vergallo, A., 2021. The Amyloid- β Pathway in Alzheimer's Disease. *Mol. Psychiatry* 26, 5481–5503. <https://doi.org/10.1038/s41380-021-01249-0>
67. Han, X., Jovicich, J., Salat, D., van der Kouwe, A., Quinn, B., Czanner, S., Busa, E., Pacheco, J., Albert, M., Killiany, R., Maguire, P., Rosas, D., Makris, N., Dale, A., Dickerson, B., Fischl, B., 2006. Reliability of MRI-derived measurements of human cerebral cortical thickness: The effects of field strength, scanner upgrade and manufacturer. *NeuroImage* 32, 180–194.
68. Harper, L., Barkhof, F., Fox, N.C., Schott, J.M., 2015. Using visual rating to diagnose dementia: a critical evaluation of MRI atrophy scales. *J. Neurol. Neurosurg. Psychiatry* 86, 1225–1233. <https://doi.org/10.1136/jnnp-2014-310090>
69. Harper, L., Fumagalli, G.G., Barkhof, F., Scheltens, P., O'Brien, J.T., Bouwman, F., Burton, E.J., Rohrer, J.D., Fox, N.C., Ridgway, G.R., Schott, J.M., 2016. MRI visual rating scales in the diagnosis of dementia: evaluation in 184 post-mortem confirmed cases. *Brain J. Neurol.* 139, 1211–1225. <https://doi.org/10.1093/brain/aww005>
70. Heidekum, A.E., Vogel, S.E., Grabner, R.H., 2020. Associations Between Individual Differences in Mathematical Competencies and Surface Anatomy of the Adult Brain. *Front. Hum. Neurosci.* 14.

71. Hoefft, F., Barnea-Goraly, N., Haas, B.W., Golarai, G., Ng, D., Mills, D., Korenberg, J., Bellugi, U., Galaburda, A., Reiss, A.L., 2007. More Is Not Always Better: Increased Fractional Anisotropy of Superior Longitudinal Fasciculus Associated with Poor Visuospatial Abilities in Williams Syndrome. *J. Neurosci.* 27, 11960–11965. <https://doi.org/10.1523/JNEUROSCI.3591-07.2007>
72. Holbrook, A.J., Tustison, N.J., Marquez, F., Roberts, J., Yassa, M.A., Gillen, D.L., Alzheimer’s Disease Neuroimaging Initiative§, 2020. Anterolateral entorhinal cortex thickness as a new biomarker for early detection of Alzheimer’s disease. *Alzheimers Dement. Amst. Neth.* 12, e12068. <https://doi.org/10.1002/dad2.12068>
73. Hoogendam, Y.Y., van der Geest, J.N., Niessen, W.J., van der Lugt, A., Hofman, A., Vernooij, M.W., Ikram, M.A., 2014. The role of cerebellar volume in cognition in the general elderly population. *Alzheimer Dis. Assoc. Disord.* 28, 352–357. <https://doi.org/10.1097/WAD.0000000000000024>
74. Hurford, R., Charidimou, A., Fox, Z., Cipolotti, L., Jager, R., Werring, D.J., 2014. MRI-visible perivascular spaces: relationship to cognition and small vessel disease MRI markers in ischaemic stroke and TIA. *J. Neurol. Neurosurg. Psychiatry* 85, 522–525. <https://doi.org/10.1136/jnnp-2013-305815>
75. Jack, C.R., Bernstein, M.A., Fox, N.C., Thompson, P., Alexander, G., Harvey, D., Borowski, B., Britson, P.J., L Whitwell, J., Ward, C., Dale, A.M., Felmlee, J.P., Gunter, J.L., Hill, D.L.G., Killiany, R., Schuff, N., Fox-Bosetti, S., Lin, C., Studholme, C., DeCarli, C.S., Krueger, G., Ward, H.A., Metzger, G.J., Scott, K.T., Mallozzi, R., Blezek, D., Levy, J., Debbins, J.P., Fleisher, A.S., Albert, M., Green, R., Bartzokis, G., Glover, G., Mugler, J., Weiner, M.W., 2008. The Alzheimer’s Disease Neuroimaging Initiative (ADNI): MRI methods. *J. Magn. Reson. Imaging JMRI* 27, 685–691. <https://doi.org/10.1002/jmri.21049>
76. Jacobs, H.I.L., Van Boxtel, M.P.J., Uylings, H.B.M., Gronenschild, E.H.B.M., Verhey, F.R., Jolles, J., 2011. Atrophy of the parietal lobe in preclinical dementia. *Brain Cogn.* 75, 154–163. <https://doi.org/10.1016/j.bandc.2010.11.003>
77. Jiang, J., Yao, K., Huang, X., Zhang, Y., Shen, F., Weng, S., 2022. Longitudinal white matter hyperintensity changes and cognitive decline in patients with minor stroke. *Aging Clin. Exp. Res.* 34, 1047–1054. <https://doi.org/10.1007/s40520-021-02024-5>
78. Jie, W., Lin, G., Liu, Z., Zhou, H., Lin, L., Liang, G., Ou, M., Lin, M., 2020. The Relationship Between Enlarged Perivascular Spaces and Cognitive Function: A Meta-Analysis of Observational Studies. *Front. Pharmacol.* 11, 715. <https://doi.org/10.3389/fphar.2020.00715>
79. Jovicich, J., Czanner, S., Greve, D., Haley, E., Kouwe, A. van der, Gollub, R., Kennedy, D., Schmitt, F., Brown, G., MacFall, J., Fischl, B., Dale, A., 2006. Reliability in multi-site structural MRI studies: Effects of gradient non-linearity correction on phantom and human data. *NeuroImage* 30, 436–443. <https://doi.org/DOI: 10.1016/j.neuroimage.2005.09.046>

80. Karas, G., Scheltens, P., Rombouts, S., van Schijndel, R., Klein, M., Jones, B., van der Flier, W., Vrenken, H., Barkhof, F., 2007. Precuneus atrophy in early-onset Alzheimer's disease: a morphometric structural MRI study. *Neuroradiology* 49, 967–976. <https://doi.org/10.1007/s00234-007-0269-2>
81. Kates, R., Atkinson, D., Brant-Zawadzki, M., 1996. Fluid-attenuated inversion recovery (FLAIR): clinical prospectus of current and future applications. *Top. Magn. Reson. Imaging TMRI* 8, 389–396.
82. Kawakami, I., Hasegawa, M., Arai, T., Ikeda, K., Oshima, K., Niizato, K., Aoki, N., Omi, K., Higashi, S., Hosokawa, M., Hirayasu, Y., Akiyama, H., 2014. Tau accumulation in the nucleus accumbens in tangle-predominant dementia. *Acta Neuropathol. Commun.* 2, 40. <https://doi.org/10.1186/2051-5960-2-40>
83. Khan, U.A., Liu, L., Provenzano, F.A., Berman, D.E., Profaci, C.P., Sloan, R., Mayeux, R., Duff, K.E., Small, S.A., 2014. Molecular drivers and cortical spread of lateral entorhinal cortex dysfunction in preclinical Alzheimer's disease. *Nat. Neurosci.* 17, 304–311. <https://doi.org/10.1038/nm.3606>
84. Kim, K.W., MacFall, J.R., Payne, M.E., 2008. Classification of White Matter Lesions on Magnetic Resonance Imaging in Elderly Persons. *Biol. Psychiatry, Stress and Synaptic Plasticity* 64, 273–280. <https://doi.org/10.1016/j.biopsych.2008.03.024>
85. Kim, S.J., Lee, D.K., Jang, Y.K., Jang, H., Kim, S.E., Cho, S.H., Kim, J.P., Jung, Y.H., Kim, E.-J., Na, D.L., Lee, J.-M., Seo, S.W., Kim, H.J., 2020. The Effects of Longitudinal White Matter Hyperintensity Change on Cognitive Decline and Cortical Thinning over Three Years. *J. Clin. Med.* 9, 2663. <https://doi.org/10.3390/jcm9082663>
86. Kortz, M.W., Lillehei, K.O., 2023. Insular Cortex, in: *StatPearls*. StatPearls Publishing, Treasure Island (FL).
87. Koshiyama, D., Fukunaga, M., Okada, N., Morita, K., Nemoto, K., Yamashita, F., Yamamori, H., Yasuda, Y., Matsumoto, J., Fujimoto, M., Kudo, N., Azechi, H., Watanabe, Y., Kasai, K., Hashimoto, R., 2020. Association between the superior longitudinal fasciculus and perceptual organization and working memory: A diffusion tensor imaging study. *Neurosci. Lett.* 738, 135349. <https://doi.org/10.1016/j.neulet.2020.135349>
88. Koyama, T., Domen, K., 2017. Diffusion Tensor Fractional Anisotropy in the Superior Longitudinal Fasciculus Correlates with Functional Independence Measure Cognition Scores in Patients with Cerebral Infarction. *J. Stroke Cerebrovasc. Dis.* 26, 1704–1711. <https://doi.org/10.1016/j.jstrokecerebrovasdis.2017.03.034>
89. Koziol, L.F., Budding, D., Andreasen, N., D'Arrigo, S., Bulgheroni, S., Imamizu, H., Ito, M., Manto, M., Marvel, C., Parker, K., Pezzulo, G., Ramnani, N., Riva, D., Schmähmann, J., Vandervert, L., Yamazaki, T., 2014. Consensus Paper: The Cerebellum's Role in Movement and Cognition. *Cerebellum Lond. Engl.* 13, 151–177. <https://doi.org/10.1007/s12311-013-0511-x>

90. Kwee, R.M., Kwee, T.C., 2007. Virchow-Robin Spaces at MR Imaging. *RadioGraphics* 27, 1071–1086. <https://doi.org/10.1148/rg.274065722>
91. Lara, E., Caballero, F.F., Rico-Urbe, L.A., Olaya, B., Haro, J.M., Ayuso-Mateos, J.L., Miret, M., 2019. Are loneliness and social isolation associated with cognitive decline? *Int. J. Geriatr. Psychiatry* 34, 1613–1622. <https://doi.org/10.1002/gps.5174>
92. LaRocque, K.F., Wagner, A.D., 2015. The Medial Temporal Lobe and Episodic Memory, in: Toga, A.W. (Ed.), *Brain Mapping*. Academic Press, Waltham, pp. 537–541. <https://doi.org/10.1016/B978-0-12-397025-1.00281-5>
93. Lee, A., Yeung, L.-K., Barense, M., 2012. The hippocampus and visual perception. *Front. Hum. Neurosci.* 6.
94. Lee, J., Seo, S.W., Yang, J.-J., Jang, Y.K., Lee, J.S., Kim, Y.J., Chin, J., Lee, J.M., Kim, S.T., Lee, K.-H., Lee, J.H., Kim, J.S., Kim, S., Yoo, H., Lee, A.Y., Na, D.L., Kim, H.J., 2018. Longitudinal cortical thinning and cognitive decline in patients with early- versus late-stage subcortical vascular mild cognitive impairment. *Eur. J. Neurol.* 25, 326–333. <https://doi.org/10.1111/ene.13500>
95. Lee, Juyoun, Sohn, E.H., Oh, E., Lee, A.Y., 2018. Characteristics of Cerebral Microbleeds. *Dement. Neurocognitive Disord.* 17, 73–82. <https://doi.org/10.12779/dnd.2018.17.3.73>
96. Lehmann, M., Koedam, E.L.G.E., Barnes, J., Bartlett, J.W., Ryan, N.S., Pijnenburg, Y.A.L., Barkhof, F., Wattjes, M.P., Scheltens, P., Fox, N.C., 2012. Posterior cerebral atrophy in the absence of medial temporal lobe atrophy in pathologically-confirmed Alzheimer’s disease. *Neurobiol. Aging* 33, 627.e1-627.e12. <https://doi.org/10.1016/j.neurobiolaging.2011.04.003>
97. Leiner, H.C., Leiner, A.L., Dow, R.S., 1993. Cognitive and language functions of the human cerebellum. *Trends Neurosci.* 16, 444–447. [https://doi.org/10.1016/0166-2236\(93\)90072-t](https://doi.org/10.1016/0166-2236(93)90072-t)
98. Lim, A.T., Chandra, R.V., Trost, N.M., McKelvie, P.A., Stuckey, S.L., 2015. Large anterior temporal Virchow-Robin spaces: unique MR imaging features. *Neuroradiology* 57, 491–499. <https://doi.org/10.1007/s00234-015-1491-y>
99. Lin, H.-Y., Huang, C.-C., Chou, K.-H., Yang, A.C., Lo, C.-Y.Z., Tsai, S.-J., Lin, C.-P., 2021. Differential Patterns of Gyral and Sulcal Morphological Changes During Normal Aging Process. *Front. Aging Neurosci.* 13.
100. Liu, J.-Y., Zhou, Y.-J., Zhai, F.-F., Han, F., Zhou, L.-X., Ni, J., Yao, M., Zhang, S., Jin, Z., Cui, L., Zhu, Y.-C., 2020. Cerebral Microbleeds Are Associated with Loss of White Matter Integrity. *AJNR Am. J. Neuroradiol.* 41, 1397–1404. <https://doi.org/10.3174/ajnr.A6622>

101. Livingston, G., Huntley, J., Sommerlad, A., Ames, D., Ballard, C., Banerjee, S., Brayne, C., Burns, A., Cohen-Mansfield, J., Cooper, C., Costafreda, S.G., Dias, A., Fox, N., Gitlin, L.N., Howard, R., Kales, H.C., Kivimäki, M., Larson, E.B., Ogunniyi, A., Orgeta, V., Ritchie, K., Rockwood, K., Sampson, E.L., Samus, Q., Schneider, L.S., Selbæk, G., Teri, L., Mukadam, N., 2020. Dementia prevention, intervention, and care: 2020 report of the Lancet Commission. *Lancet Lond. Engl.* 396, 413–446. [https://doi.org/10.1016/S0140-6736\(20\)30367-6](https://doi.org/10.1016/S0140-6736(20)30367-6)
102. Lombardi, G., Crescioli, G., Cavedo, E., Lucenteforte, E., Casazza, G., Bellatorre, A.-G., Lista, C., Costantino, G., Frisoni, G., Virgili, G., Filippini, G., 2020. Structural magnetic resonance imaging for the early diagnosis of dementia due to Alzheimer's disease in people with mild cognitive impairment. *Cochrane Database Syst. Rev.* <https://doi.org/10.1002/14651858.CD009628.pub2>
103. Machulda, M.M., Lundt, E.S., Albertson, S.M., Spsychalla, A.J., Schwarz, C.G., Mielke, M.M., Jack Jr., C.R., Kremers, W.K., Vemuri, P., Knopman, D.S., Jones, D.T., Bondi, M.W., Petersen, R.C., 2020. Cortical atrophy patterns of incident MCI subtypes in the Mayo Clinic Study of Aging. *Alzheimers Dement.* 16, 1013–1022. <https://doi.org/10.1002/alz.12108>
104. MacLulich, A.M.J., Wardlaw, J.M., Ferguson, K.J., Starr, J.M., Seckl, J.R., Deary, I.J., 2004. Enlarged perivascular spaces are associated with cognitive function in healthy elderly men. *J. Neurol. Neurosurg. Psychiatry* 75, 1519–1523. <https://doi.org/10.1136/jnnp.2003.030858>
105. Marek, S., Dosenbach, N.U.F., 2018. The frontoparietal network: function, electrophysiology, and importance of individual precision mapping. *Dialogues Clin. Neurosci.* 20, 133–140.
106. Mårtensson, G., Håkansson, C., Pereira, J.B., Palmqvist, S., Hansson, O., van Westen, D., Westman, E., 2020. Medial temporal atrophy in preclinical dementia: Visual and automated assessment during six year follow-up. *NeuroImage Clin.* 27, 102310. <https://doi.org/10.1016/j.nicl.2020.102310>
107. Martinez, G.V., 2018. Introduction to MRI Physics, in: García Martín, M.L., López Larrubia, P. (Eds.), *Preclinical MRI: Methods and Protocols, Methods in Molecular Biology.* Springer, New York, NY, pp. 3–19. https://doi.org/10.1007/978-1-4939-7531-0_1
108. Martinez-Ramirez, S., Greenberg, S.M., Viswanathan, A., 2014. Cerebral microbleeds: overview and implications in cognitive impairment. *Alzheimers Res. Ther.* 6, 33. <https://doi.org/10.1186/alzrt263>
109. Mavridis, I., Boviatsis, E., Anagnostopoulou, S., 2011. The human nucleus accumbens suffers parkinsonism-related shrinkage: a novel finding. *Surg. Radiol. Anat. SRA* 33, 595–599. <https://doi.org/10.1007/s00276-011-0802-1>
110. Mavridis, I.N., 2015. Is nucleus accumbens atrophy correlated with cognitive symptoms of Parkinson's disease? *Brain* 138, e319. <https://doi.org/10.1093/brain/awu197>

111. McEvoy, L.K., Brewer, J.B., 2010. Quantitative structural MRI for early detection of Alzheimer's disease. *Expert Rev. Neurother.* 10, 1675–1688. <https://doi.org/10.1586/ern.10.162>
112. McKeever, A., Paris, A.F., Cullen, J., Hayes, L., Ritchie, C.W., Ritchie, K., Waldman, A.D., Wells, K., Busza, A., Carriere, I., O'Brien, J.T., Su, L., 2020. Hippocampal Subfield Volumes in Middle-Aged Adults at Risk of Dementia. *J. Alzheimers Dis.* 75, 1211–1218. <https://doi.org/10.3233/JAD-200238>
113. McRae-McKee, K., Evans, S., Hadjichrysanthou, C., Wong, M.M., de Wolf, F., Anderson, R.M., 2019. Combining hippocampal volume metrics to better understand Alzheimer's disease progression in at-risk individuals. *Sci. Rep.* 9, 7499. <https://doi.org/10.1038/s41598-019-42632-w>
114. Mercadante, A.A., Tadi, P., 2022. Neuroanatomy, Gray Matter, in: StatPearls. StatPearls Publishing, Treasure Island (FL).
115. Miller, A.A., Spencer, S.J., 2014. Obesity and neuroinflammation: A pathway to cognitive impairment. *Brain. Behav. Immun.* 42, 10–21. <https://doi.org/10.1016/j.bbi.2014.04.001>
116. Mitoma, H., Buffo, A., Gelfo, F., Guell, X., Fucà, E., Kakei, S., Lee, J., Manto, M., Petrosini, L., Shaikh, A.G., Schmahmann, J.D., 2020. Consensus Paper. Cerebellar Reserve: From Cerebellar Physiology to Cerebellar Disorders. *Cerebellum Lond. Engl.* 19, 131–153. <https://doi.org/10.1007/s12311-019-01091-9>
117. Mortamais, M., Artero, S., Ritchie, K., 2013. Cerebral white matter hyperintensities in the prediction of cognitive decline and incident dementia. *Int. Rev. Psychiatry Abingdon Engl.* 25, 686–698. <https://doi.org/10.3109/09540261.2013.838151>
118. Murphy, M.P., LeVine, H., 2010. Alzheimer's disease and the amyloid-beta peptide. *J. Alzheimers Dis. JAD* 19, 311–323. <https://doi.org/10.3233/JAD-2010-1221>
119. Muzio, B.D., n.d. Global cortical atrophy scale | Radiology Reference Article | Radiopaedia.org [WWW Document]. Radiopaedia. <https://doi.org/10.53347/rID-37584>
120. Nasreddine, Z.S., Phillips, N.A., Bédirian, V., Charbonneau, S., Whitehead, V., Collin, I., Cummings, J.L., Chertkow, H., 2005. The Montreal Cognitive Assessment, MoCA: a brief screening tool for mild cognitive impairment. *J. Am. Geriatr. Soc.* 53, 695–699. <https://doi.org/10.1111/j.1532-5415.2005.53221.x>
121. Nasreddine, Z.S., Rossetti, H., Phillips, N., Chertkow, H., Lacroix, L., Cullum, M., Weiner, M., 2012. Normative data for the Montreal Cognitive Assessment (MoCA) in a population-based sample. *Neurology* 78, 765–766. <https://doi.org/10.1212/01.wnl.0000413072.54070.a3>

122. Nesteruk, M., Nesteruk, T., Styczyńska, M., Barczak, A., Mandecka, M., Walecki, J., Barcikowska-Kotowicz, M., 2015. Predicting the conversion of mild cognitive impairment to Alzheimer's disease based on the volumetric measurements of the selected brain structures in magnetic resonance imaging. *Neurol. Neurochir. Pol.* 49, 349–353. <https://doi.org/10.1016/j.pjnns.2015.09.003>
123. Ngandu, T., Lehtisalo, J., Solomon, A., Levälähti, E., Ahtiluoto, S., Antikainen, R., Bäckman, L., Hänninen, T., Jula, A., Laatikainen, T., Lindström, J., Mangialasche, F., Paajanen, T., Pajala, S., Peltonen, M., Rauramaa, R., Stigsdotter-Neely, A., Strandberg, T., Tuomilehto, J., Soininen, H., Kivipelto, M., 2015. A 2 year multidomain intervention of diet, exercise, cognitive training, and vascular risk monitoring versus control to prevent cognitive decline in at-risk elderly people (FINGER): a randomised controlled trial. *The Lancet* 385, 2255–2263. [https://doi.org/10.1016/S0140-6736\(15\)60461-5](https://doi.org/10.1016/S0140-6736(15)60461-5)
124. Nie, X., Sun, Y., Wan, S., Zhao, H., Liu, R., Li, X., Wu, S., Nedelska, Z., Hort, J., Qing, Z., Xu, Y., Zhang, B., 2017. Subregional Structural Alterations in Hippocampus and Nucleus Accumbens Correlate with the Clinical Impairment in Patients with Alzheimer's Disease Clinical Spectrum: Parallel Combining Volume and Vertex-Based Approach. *Front. Neurol.* 8.
125. Nobis, L., Manohar, S.G., Smith, S.M., Alfaro-Almagro, F., Jenkinson, M., Mackay, C.E., Husain, M., 2019. Hippocampal volume across age: Nomograms derived from over 19,700 people in UK Biobank. *NeuroImage Clin.* 23, 101904. <https://doi.org/10.1016/j.nicl.2019.101904>
126. Nuzum, H., Stickel, A., Corona, M., Zeller, M., Melrose, R.J., Wilkins, S.S., 2020. Potential benefits of physical activity in MCI and dementia. *Behav. Neurol.* 2020. <https://doi.org/10.1155/2020/7807856>
127. Oishi, K., Mielke, M.M., Albert, M., Lyketsos, C.G., Mori, S., 2011. DTI Analyses and Clinical Applications in Alzheimer's Disease. *J. Alzheimers Dis.* 26, 287–296. <https://doi.org/10.3233/JAD-2011-0007>
128. Paradise, M., Crawford, J.D., Lam, B.C.P., Wen, W., Kochan, N.A., Makkar, S., Dawes, L., Trollor, J., Draper, B., Brodaty, H., Sachdev, P.S., 2021. Association of Dilated Perivascular Spaces With Cognitive Decline and Incident Dementia. *Neurology* 96, e1501–e1511. <https://doi.org/10.1212/WNL.0000000000011537>
129. Paradiso, S., Andreasen, N.C., O'Leary, D.S., Arndt, S., Robinson, R.G., 1997. Cerebellar size and cognition: correlations with IQ, verbal memory and motor dexterity. *Neuropsychiatry. Neuropsychol. Behav. Neurol.* 10, 1–8.
130. Pasquier, F., Leys, D., Weerts, J.G.E., Mounier-Vehier, F., Barkhof, F., Scheltens, P., 1996a. Inter-and Intraobserver Reproducibility of Cerebral Atrophy Assessment on MRI Scans with Hemispheric Infarcts. *Eur. Neurol.* 36, 268–272. <https://doi.org/10.1159/000117270>

131. Pasquier, F., Leys, D., Weerts, J.G.E., Mounier-Vehier, F., Barkhof, F., Scheltens, P., 1996b. Inter- and Intraobserver Reproducibility of Cerebral Atrophy Assessment on MRI Scans with Hemispheric Infarcts. *Eur. Neurol.* 36, 268–272. <https://doi.org/10.1159/000117270>
132. Pemberton, H.G., Zaki, L.A.M., Goodkin, O., Das, R.K., Steketee, R.M.E., Barkhof, F., Vernooij, M.W., 2021. Technical and clinical validation of commercial automated volumetric MRI tools for dementia diagnosis—a systematic review. *Neuroradiology* 63, 1773–1789. <https://doi.org/10.1007/s00234-021-02746-3>
133. Pessoa, L., Hof, P.R., 2015. From Paul Broca’s great limbic lobe to the limbic system. *J. Comp. Neurol.* 523, 2495–2500. <https://doi.org/10.1002/cne.23840>
134. Potter, G.M., Chappell, F.M., Morris, Z., Wardlaw, J.M., 2015. Cerebral Perivascular Spaces Visible on Magnetic Resonance Imaging: Development of a Qualitative Rating Scale and its Observer Reliability. *Cerebrovasc. Dis.* 39, 224–231. <https://doi.org/10.1159/000375153>
135. Poulin, S.P., Dautoff, R., Morris, J.C., Barrett, L.F., Dickerson, B.C., 2011. Amygdala atrophy is prominent in early Alzheimer’s disease and relates to symptom severity. *Psychiatry Res.* 194, 7–13. <https://doi.org/10.1016/j.psychres.2011.06.014>
136. Prieto del Val, L., Cantero, J.L., Atienza, M., 2016. Atrophy of amygdala and abnormal memory-related alpha oscillations over posterior cingulate predict conversion to Alzheimer’s disease. *Sci. Rep.* 6, 31859. <https://doi.org/10.1038/srep31859>
137. Prins, N.D., Scheltens, P., 2015. White matter hyperintensities, cognitive impairment and dementia: an update. *Nat. Rev. Neurol.* 11, 157–165. <https://doi.org/10.1038/nrneurol.2015.10>
138. Purves, D., Augustine, G.J., Fitzpatrick, D., Katz, L.C., LaMantia, A.-S., McNamara, J.O., Williams, S.M., 2001. *The Lateral Surface of the Brain*, in: *Neuroscience*. 2nd Edition. Sinauer Associates.
139. Raghavan, S., Przybelski, S.A., Reid, R.I., Graff-Radford, J., Lesnick, T.G., Zuk, S.M., Knopman, D.S., Machulda, M.M., Mielke, M.M., Petersen, R.C., Jack, C.R., Vemuri, P., 2020. Reduced fractional anisotropy of genu of corpus callosum as a predictor of longitudinal cognition in MCI. *Neurobiol. Aging* 96, 176–183. <https://doi.org/10.1016/j.neurobiolaging.2020.09.005>
140. Ramirez, J., Berezuk, C., McNeely, A.A., Gao, F., McLaurin, J., Black, S.E., 2016. Imaging the Perivascular Space as a Potential Biomarker of Neurovascular and Neurodegenerative Diseases. *Cell. Mol. Neurobiol.* 36, 289–299. <https://doi.org/10.1007/s10571-016-0343-6>
141. Rawal, S., Croul, S.E., Willinsky, R.A., Tymianski, M., Krings, T., 2014. Subcortical Cystic Lesions within the Anterior Superior Temporal Gyrus: A Newly Recognized Characteristic Location for Dilated Perivascular Spaces. *Am. J. Neuroradiol.* 35, 317–322. <https://doi.org/10.3174/ajnr.A3669>

142. Reuter, M., Rosas, H.D., Fischl, B., 2010. Highly Accurate Inverse Consistent Registration: A Robust Approach. *NeuroImage* 53, 1181–1196. <https://doi.org/10.1016/j.neuroimage.2010.07.020>
143. Reuter, M., Schmansky, N.J., Rosas, H.D., Fischl, B., 2012. Within-Subject Template Estimation for Unbiased Longitudinal Image Analysis. *NeuroImage* 61, 1402–1418. <https://doi.org/10.1016/j.neuroimage.2012.02.084>
144. Ribeiro da Costa, C., Soares, J.M., Oliveira-Silva, P., Sampaio, A., Coutinho, J.F., 2022. Interplay Between the Salience and the Default Mode Network in a Social-Cognitive Task Toward a Close Other. *Front. Psychiatry* 12, 718400. <https://doi.org/10.3389/fpsyt.2021.718400>
145. Rudie, J.D., Rauschecker, A.M., Nabavizadeh, S.A., Mohan, S., 2018. Neuroimaging of Dilated Perivascular Spaces: From Benign and Pathologic Causes to Mimics. *J. Neuroimaging* 28, 139–149. <https://doi.org/10.1111/jon.12493>
146. Sangha, O., Ma, D., Popuri, K., Stocks, J., Wang, L., Beg, M.F., 2021. Structural volume and cortical thickness differences between males and females in cognitively normal, cognitively impaired and Alzheimer’s dementia population. *Neurobiol. Aging* 106, 1–11. <https://doi.org/10.1016/j.neurobiolaging.2021.05.018>
147. Scheltens, P., Launer, L.J., Barkhof, F., Weinstein, H.C., van Gool, W.A., 1995. Visual assessment of medial temporal lobe atrophy on magnetic resonance imaging: Interobserver reliability. *J. Neurol.* 242, 557–560. <https://doi.org/10.1007/BF00868807>
148. Scheltens, P., Leys, D., Barkhof, F., Huglo, D., Weinstein, H.C., Vermersch, P., Kuiper, M., Steinling, M., Wolters, E.C., Valk, J., 1992. Atrophy of medial temporal lobes on MRI in “probable” Alzheimer’s disease and normal ageing: diagnostic value and neuropsychological correlates. *J. Neurol. Neurosurg. Psychiatry* 55, 967–972.
149. Scheltens, P., Pasquier, F., Weerts, J.G.E., Barkhof, F., Leys, D., 1997. Qualitative Assessment of Cerebral Atrophy on MRI: Inter- and Intra-Observer Reproducibility in Dementia and Normal Aging. *Eur. Neurol.* 37, 95–99. <https://doi.org/10.1159/000117417>
150. Schmidt, R., Schmidt, H., Haybaeck, J., Loitfelder, M., Weis, S., Cavalieri, M., Seiler, S., Enzinger, C., Ropele, S., Erkinjuntti, T., Pantoni, L., Scheltens, P., Fazekas, F., Jellinger, K., 2011. Heterogeneity in age-related white matter changes. *Acta Neuropathol. (Berl.)* 122, 171–185. <https://doi.org/10.1007/s00401-011-0851-x>
151. Schwarz, C.G., Gunter, J.L., Wiste, H.J., Przybelski, S.A., Weigand, S.D., Ward, C.P., Senjem, M.L., Vemuri, P., Murray, M.E., Dickson, D.W., Parisi, J.E., Kantarci, K., Weiner, M.W., Petersen, R.C., Jack, C.R., 2016. A large-scale comparison of cortical thickness and volume methods for measuring Alzheimer’s disease severity. *NeuroImage Clin.* 11, 802–812. <https://doi.org/10.1016/j.nicl.2016.05.017>

152. Segonne, F., Dale, A.M., Busa, E., Glessner, M., Salat, D., Hahn, H.K., Fischl, B., 2004. A hybrid approach to the skull stripping problem in MRI. *NeuroImage* 22, 1060–1075. <https://doi.org/DOI: 10.1016/j.neuroimage.2004.03.032>
153. Sexton, C.E., Walhovd, K.B., Storsve, A.B., Tamnes, C.K., Westlye, L.T., Johansen-Berg, H., Fjell, A.M., 2014. Accelerated Changes in White Matter Microstructure during Aging: A Longitudinal Diffusion Tensor Imaging Study. *J. Neurosci.* 34, 15425–15436. <https://doi.org/10.1523/JNEUROSCI.0203-14.2014>
154. Silhan, D., Bartos, A., Mrzilkova, J., Pashkovska, O., Ibrahim, I., Tintera, J., 2020. The Parietal Atrophy Score on Brain Magnetic Resonance Imaging is ^{[[1]]}Reliable Visual Scale. *Curr. Alzheimer Res.* 17, 534–539. <https://doi.org/10.2174/1567205017666200807193957>
155. Silva-Spínola, A., Baldeiras, I., Arrais, J.P., Santana, I., 2022. The Road to Personalized Medicine in Alzheimer’s Disease: The Use of Artificial Intelligence. *Biomedicines* 10, 315. <https://doi.org/10.3390/biomedicines10020315>
156. Smeijer, D., Ikram, M.K., Hilal, S., 2019. Enlarged Perivascular Spaces and Dementia: A Systematic Review. *J. Alzheimers Dis. JAD* 72, 247–256. <https://doi.org/10.3233/JAD-190527>
157. Stebbins, G.T., 2010. Diffusion Tensor Imaging in Parkinson’s Disease, in: Kompoliti, K., Metman, L.V. (Eds.), *Encyclopedia of Movement Disorders*. Academic Press, Oxford, pp. 308–310. <https://doi.org/10.1016/B978-0-12-374105-9.00020-4>
158. Stephan, K.E., Friston, K.J., 2009. Functional Connectivity, in: Squire, L.R. (Ed.), *Encyclopedia of Neuroscience*. Academic Press, Oxford, pp. 391–397. <https://doi.org/10.1016/B978-008045046-9.00308-9>
159. Tax, C.M.W., Bastiani, M., Veraart, J., Garyfallidis, E., Okan Irfanoglu, M., 2022. What’s new and what’s next in diffusion MRI preprocessing. *NeuroImage* 249, 118830. <https://doi.org/10.1016/j.neuroimage.2021.118830>
160. Thomann, A.E., Berres, M., Goettel, N., Steiner, L.A., Monsch, A.U., 2020. Enhanced diagnostic accuracy for neurocognitive disorders: a revised cut-off approach for the Montreal Cognitive Assessment. *Alzheimers Res. Ther.* 12, 39. <https://doi.org/10.1186/s13195-020-00603-8>
161. Timmermans, C., Smeets, D., Verheyden, J., Terzopoulos, V., Anania, V., Parizel, P.M., Maas, A., 2019. Potential of a statistical approach for the standardization of multicenter diffusion tensor data: A phantom study. *J. Magn. Reson. Imaging* 49, 955–965. <https://doi.org/10.1002/jmri.26333>
162. Torrico, T.J., Abdijadid, S., 2023. Neuroanatomy, Limbic System, in: *StatPearls*. StatPearls Publishing, Treasure Island (FL).
163. van Strien, N.M., Cappaert, N.L.M., Witter, M.P., 2009. The anatomy of memory: an interactive overview of the parahippocampal–hippocampal network. *Nat. Rev. Neurosci.* 10, 272–282. <https://doi.org/10.1038/nrn2614>

164. Velayudhan, L., Proitsi, P., Westman, E., Muehlboeck, J.-S., Mecocci, P., Vellas, B., Tsolaki, M., Kloszewska, I., Soininen, H., Spenger, C., Hodges, A., Powell, J., Lovestone, S., Simmons, A., dNeuroMed Consortium, 2013. Entorhinal cortex thickness predicts cognitive decline in Alzheimer's disease. *J. Alzheimers Dis. JAD* 33, 755–766. <https://doi.org/10.3233/JAD-2012-121408>
165. Veldsman, M., Kindalova, P., Husain, M., Kosmidis, I., Nichols, T.E., 2020. Spatial distribution and cognitive impact of cerebrovascular risk-related white matter hyperintensities. *NeuroImage Clin.* 28, 102405. <https://doi.org/10.1016/j.nicl.2020.102405>
166. Velickaite, V., Ferreira, D., Cavallin, L., Lind, L., Ahlström, H., Kilander, L., Westman, E., Larsson, E.-M., 2018. Medial temporal lobe atrophy ratings in a large 75-year-old population-based cohort: gender-corrected and education-corrected normative data. *Eur. Radiol.* 28, 1739–1747. <https://doi.org/10.1007/s00330-017-5103-6>
167. Vemuri, P., Jack, C.R., 2010. Role of structural MRI in Alzheimer's disease. *Alzheimers Res. Ther.* 2, 23. <https://doi.org/10.1186/alzrt47>
168. Verfaillie, S.C.J., Tijms, B., Versteeg, A., Benedictus, M.R., Bouwman, F.H., Scheltens, P., Barkhof, F., Vrenken, H., van der Flier, W.M., 2016. Thinner temporal and parietal cortex is related to incident clinical progression to dementia in patients with subjective cognitive decline. *Alzheimers Dement. Diagn. Assess. Dis. Monit.* 5, 43–52. <https://doi.org/10.1016/j.dadm.2016.10.007>
169. Vernooij, M.W., Pizzini, F.B., Schmidt, R., Smits, M., Yousry, T.A., Bargallo, N., Frisoni, G.B., Haller, S., Barkhof, F., 2019. Dementia imaging in clinical practice: a European-wide survey of 193 centres and conclusions by the ESNR working group. *Neuroradiology* 61, 633–642. <https://doi.org/10.1007/s00234-019-02188-y>
170. Vossel, S., Geng, J.J., Fink, G.R., 2014. Dorsal and Ventral Attention Systems. *The Neuroscientist* 20, 150–159. <https://doi.org/10.1177/1073858413494269>
171. Wahlund, L.-O., Westman, E., van Westen, D., Wallin, A., Shams, S., Cavallin, L., Larsson, E.-M., 2016. Imaging biomarkers of dementia: recommended visual rating scales with teaching cases. *Insights Imaging* 8, 79–90. <https://doi.org/10.1007/s13244-016-0521-6>
172. Wardlaw, J.M., Smith, E.E., Biessels, G.J., Cordonnier, C., Fazekas, F., Frayne, R., Lindley, R.I., O'Brien, J.T., Barkhof, F., Benavente, O.R., Black, S.E., Brayne, C., Breteler, M., Chabriat, H., DeCarli, C., de Leeuw, F.-E., Doubal, F., Duering, M., Fox, N.C., Greenberg, S., Hachinski, V., Kilimann, I., Mok, V., Oostenbrugge, R. van, Pantoni, L., Speck, O., Stephan, B.C.M., Teipel, S., Viswanathan, A., Werring, D., Chen, C., Smith, C., van Buchem, M., Norrving, B., Gorelick, P.B., Dichgans, M., 2013. Neuroimaging standards for research into small vessel disease and its contribution to ageing and neurodegeneration. *Lancet Neurol.* 12, 822–838. [https://doi.org/10.1016/S1474-4422\(13\)70124-8](https://doi.org/10.1016/S1474-4422(13)70124-8)

173. Wardlaw, J.M., Valdés Hernández, M.C., Muñoz-Maniega, S., 2015. What are White Matter Hyperintensities Made of? *J. Am. Heart Assoc.* 4, e001140. <https://doi.org/10.1161/JAHA.114.001140>
174. Wasserthal, J., Neher, P., Maier-Hein, K.H., 2018. TractSeg – Fast and accurate white matter tract segmentation. *NeuroImage* 183, 239–253. <https://doi.org/10.1016/j.neuroimage.2018.07.070>
175. Weiner, M.W., Veitch, D.P., Aisen, P.S., Beckett, L.A., Cairns, N.J., Green, R.C., Harvey, D., Jack, C.R., Jagust, W., Morris, J.C., Petersen, R.C., Salazar, J., Saykin, A.J., Shaw, L.M., Toga, A.W., Trojanowski, J.Q., Alzheimer’s Disease Neuroimaging Initiative, 2017. The Alzheimer’s Disease Neuroimaging Initiative 3: Continued innovation for clinical trial improvement. *Alzheimers Dement. J. Alzheimers Assoc.* 13, 561–571. <https://doi.org/10.1016/j.jalz.2016.10.006>
176. Weller, R.O., Boche, D., Nicoll, J.A.R., 2009. Microvasculature changes and cerebral amyloid angiopathy in Alzheimer’s disease and their potential impact on therapy. *Acta Neuropathol. (Berl.)* 118, 87–102. <https://doi.org/10.1007/s00401-009-0498-z>
177. Xiao, D., Wang, K., Theriault, L., Charbel, E., Alzheimer’s Disease Neuroimaging Initiative, 2022. White matter integrity and key structures affected in Alzheimer’s disease characterized by diffusion tensor imaging. *Eur. J. Neurosci.* 56, 5319–5331. <https://doi.org/10.1111/ejn.15815>
178. Xing, Y., Yang, J., Zhou, A., Wang, F., Wei, C., Tang, Y., Jia, J., 2021. White Matter Fractional Anisotropy Is a Superior Predictor for Cognitive Impairment Than Brain Volumes in Older Adults With Confluent White Matter Hyperintensities. *Front. Psychiatry* 12.
179. Yew, B., Nation, D.A., for the Alzheimer’s Disease Neuroimaging Initiative, 2017. Cerebrovascular resistance: effects on cognitive decline, cortical atrophy, and progression to dementia. *Brain* 140, 1987–2001. <https://doi.org/10.1093/brain/awx112>
180. Yuan, Z., Pan, C., Xiao, T., Liu, M., Zhang, W., Jiao, B., Yan, X., Tang, B., Shen, L., 2019. Multiple Visual Rating Scales Based on Structural MRI and a Novel Prediction Model Combining Visual Rating Scales and Age Stratification in the Diagnosis of Alzheimer’s Disease in the Chinese Population. *Front. Neurol.* 10.
181. Zahodne, L.B., Stern, Y., Manly, J.J., 2015. Differing effects of education on cognitive decline in diverse elders with low versus high educational attainment. *Neuropsychology* 29, 649–657. <https://doi.org/10.1037/neu0000141>
182. Zanon Zotin, M.C., Sveikata, L., Viswanathan, A., Yilmaz, P., 2021. Cerebral small vessel disease and vascular cognitive impairment: from diagnosis to management. *Curr. Opin. Neurol.* 34, 246–257. <https://doi.org/10.1097/WCO.0000000000000913>

183. Zarei, M., Ibarretxe-Bilbao, N., Compta, Y., Hough, M., Junque, C., Bargallo, N., Tolosa, E., Martí, M.J., 2013. Cortical thinning is associated with disease stages and dementia in Parkinson's disease. *J. Neurol. Neurosurg. Psychiatry* 84, 875–882. <https://doi.org/10.1136/jnnp-2012-304126>
184. Zdanovskis, N., Platkājis, A., Kostiks, A., Grigorjeva, O., Karelis, G., 2021. Cerebellar Cortex and Cerebellar White Matter Volume in Normal Cognition, Mild Cognitive Impairment, and Dementia. *Brain Sci.* 11, 1134. <https://doi.org/10.3390/brainsci11091134>
185. Zhang, F., Daducci, A., He, Y., Schiavi, S., Seguin, C., Smith, R.E., Yeh, C.-H., Zhao, T., O'Donnell, L.J., 2022. Quantitative mapping of the brain's structural connectivity using diffusion MRI tractography: A review. *NeuroImage* 249, 118870. <https://doi.org/10.1016/j.neuroimage.2021.118870>

Annexes

Quantitative data of cerebral cortex in both hemispheres

				95% Confidence Interval Mean								
		Valid	Median	Mean	Std. Error of Mean	Upper	Lower	Std. Deviation	Range	Maximum		
Denipu daiva	lh_enthorinal_thickness	Normāla KT	24	2,888	2,845	0,049	2,941	2,75	0,239	0,824	3,124	
		Vieglī KT	37	2,825	2,761	0,057	2,873	2,649	0,347	1,472	3,323	
		Mēreni KT	10	2,186	2,202	0,097	2,392	2,012	0,307	0,944	2,711	
		Smagi KT	9	2,298	2,097	0,291	2,667	1,526	0,873	2,801	2,801	
	rh_enthorinal_thickness	Normāla KT	24	2,905	2,904	0,069	3,04	2,768	0,339	1,646	3,797	
		Vieglī KT	37	2,875	2,914	0,059	3,029	2,798	0,359	1,516	3,53	
		Mēreni KT	10	2,516	2,43	0,173	2,868	2,191	0,547	1,534	3,268	
		Smagi KT	9	2,436	2,167	0,305	2,766	1,569	0,916	3,112	3,112	
	lh_parahal_thickness	Normāla KT	24	2,633	2,665	0,055	2,773	2,557	0,27	0,927	3,205	
		Vieglī KT	37	2,776	2,775	0,05	2,873	2,676	0,305	1,259	3,459	
		Mēreni KT	10	2,383	2,375	0,102	2,575	2,175	0,323	0,933	2,803	
		Smagi KT	9	2,339	2,038	0,271	2,63	1,567	0,813	2,747	2,747	
	rh_parahal_thickness	Normāla KT	24	2,607	2,625	0,028	2,68	2,57	0,137	0,534	2,95	
		Vieglī KT	37	2,616	2,651	0,038	2,725	2,576	0,231	0,906	3,117	
		Mēreni KT	10	2,405	2,363	0,091	2,541	2,185	0,287	0,927	2,871	
		Smagi KT	9	2,222	2,046	0,269	2,573	1,52	0,806	2,69	2,69	
	lh_middletemporal_thickness	Normāla KT	24	2,512	2,535	0,025	2,564	2,466	0,123	0,474	2,762	
		Vieglī KT	37	2,518	2,517	0,018	2,552	2,482	0,108	0,377	2,703	
		Mēreni KT	10	2,321	2,323	0,062	2,446	2,201	0,197	0,626	2,586	
		Smagi KT	9	2,273	2,409	0,116	2,635	2,182	0,347	1,094	3,2	
	rh_midtemporal_thickness	Normāla KT	24	2,572	2,56	0,019	2,598	2,522	0,095	0,329	2,709	
		Vieglī KT	37	2,58	2,587	0,024	2,633	2,54	0,145	0,536	2,849	
		Mēreni KT	10	2,436	2,415	0,047	2,506	2,323	0,147	0,408	2,631	
		Smagi KT	9	2,451	2,488	0,087	2,658	2,318	0,26	0,809	3	
	lh_fusiform_thickness	Normāla KT	24	2,5	2,482	0,023	2,537	2,447	0,112	0,466	2,692	
		Vieglī KT	37	2,512	2,502	0,022	2,546	2,458	0,137	0,605	2,768	
		Mēreni KT	10	2,356	2,379	0,055	2,486	2,272	0,172	0,583	2,766	
		Smagi KT	9	2,308	2,329	0,049	2,425	2,232	0,147	0,457	2,566	
	rh_fusiform_thickness	Normāla KT	24	2,548	2,534	0,02	2,572	2,495	0,097	0,363	2,71	
		Vieglī KT	37	2,574	2,585	0,027	2,619	2,511	0,167	0,654	2,914	
		Mēreni KT	10	2,485	2,465	0,055	2,573	2,357	0,175	0,584	2,755	
		Smagi KT	9	2,449	2,398	0,056	2,508	2,289	0,168	0,47	2,64	
	lh_superior temporal_thickness	Normāla KT	24	2,537	2,535	0,022	2,561	2,475	0,107	0,505	2,753	
		Vieglī KT	37	2,535	2,534	0,022	2,576	2,491	0,132	0,496	2,76	
		Mēreni KT	10	2,397	2,333	0,07	2,471	2,195	0,222	0,619	2,558	
		Smagi KT	9	2,266	2,319	0,063	2,443	2,195	0,19	0,519	2,552	
	rh_superior temporal_thickness	Normāla KT	24	2,542	2,539	0,029	2,63	2,517	0,141	0,56	2,91	
		Vieglī KT	37	2,64	2,627	0,027	2,68	2,575	0,164	0,684	2,897	
		Mēreni KT	10	2,485	2,394	0,072	2,535	2,254	0,227	0,722	2,683	
		Smagi KT	9	2,505	2,379	0,077	2,53	2,229	0,23	0,586	2,628	
	rh_transverse temporal_thickness	Normāla KT	24	2,378	2,314	0,042	2,396	2,232	0,205	0,782	2,656	
		Vieglī KT	37	2,37	2,41	0,034	2,476	2,344	0,204	0,828	2,784	
		Mēreni KT	10	2,179	2,222	0,068	2,354	2,089	0,213	0,627	2,495	
		Smagi KT	9	2,298	2,126	0,092	2,307	1,945	0,277	0,769	2,45	
	Paura daiva	lh_supramarginal_thickness	Normāla KT	24	2,317	2,328	0,022	2,372	2,284	0,109	0,414	2,586
			Vieglī KT	37	2,292	2,308	0,019	2,344	2,272	0,113	0,469	2,502
			Mēreni KT	10	2,224	2,201	0,048	2,296	2,107	0,153	0,508	2,466
			Smagi KT	9	2,004	2,095	0,068	2,229	1,962	0,204	0,577	2,403
rh_supramarginal_thickness		Normāla KT	24	2,302	2,319	0,017	2,352	2,287	0,082	0,351	2,538	
		Vieglī KT	37	2,388	2,347	0,019	2,385	2,309	0,118	0,474	2,584	
		Mēreni KT	10	2,204	2,242	0,039	2,318	2,166	0,123	0,316	2,406	
		Smagi KT	9	2,133	2,188	0,075	2,336	2,04	0,226	0,683	2,561	
lh_isthmuscingulate_thickness		Normāla KT	24	2,204	2,234	0,03	2,293	2,175	0,147	0,533	2,512	
		Vieglī KT	37	2,249	2,23	0,025	2,279	2,182	0,151	0,645	2,525	
		Mēreni KT	10	2,109	2,153	0,068	2,285	2,02	0,214	0,74	2,585	
		Smagi KT	9	2,106	2,082	0,045	2,17	1,995	0,134	0,371	2,252	
lh_inferoparietal_thickness	Normāla KT	24	2,269	2,272	0,021	2,312	2,231	0,101	0,409	2,464		
	Vieglī KT	37	2,261	2,273	0,018	2,308	2,239	0,107	0,366	2,446		
	Mēreni KT	10	2,195	2,179	0,033	2,245	2,114	0,106	0,329	2,348		
	Smagi KT	9	2,101	2,092	0,084	2,256	1,927	0,251	0,741	2,526		
Pakausa daiva	rh_pericalcarine_thickness	Normāla KT	24	1,656	1,644	0,023	1,69	1,598	0,114	0,438	1,834	
		Vieglī KT	37	1,738	1,752	0,026	1,803	1,701	0,158	0,681	2,067	
		Mēreni KT	10	1,648	1,704	0,048	1,798	1,61	0,152	0,463	1,96	
		Smagi KT	9	1,557	1,685	0,12	1,921	1,45	0,36	1,156	2,602	

Spearman correlations between visual rating scales

Spirmena korelācijas															
Variable		MDA labajā pusē	MDA kreisajā pusē	Fazekas skala PVBV	Fazekas skala DzBV	Fazekas kopējā	Paura daivas atrofija labajā pusē	Paura daivas atrofijas skala kreisajā pusē	ERICA labajā pusē	ERICA kreisajā pusē	Microbleeds	PVS BG	PVS CS	PVS MidB	GCA
1. MDA labajā pusē	Spearman's rho	—													
	p-value	—													
2. MDA kreisajā pusē	Spearman's rho	0.912	—												
	p-value	<.001	—												
3. Fazekas skala PVBV	Spearman's rho	0.423	0.378	—											
	p-value	<.001	<.001	—											
4. Fazekas skala DzBV	Spearman's rho	0.285	0.221	0.742	—										
	p-value	0.010	0.048	<.001	—										
5. Fazekas kopējā	Spearman's rho	0.397	0.321	0.908	0.857	—									
	p-value	<.001	0.003	<.001	<.001	—									
6. Paura daivas atrofija labajā pusē	Spearman's rho	0.263	0.301	0.233	0.131	0.110	—								
	p-value	0.018	0.006	0.036	0.245	0.326	—								
7. Paura daivas atrofijas skala kreisajā pusē	Spearman's rho	0.257	0.294	0.152	0.087	0.057	0.938	—							
	p-value	0.020	0.008	0.174	0.440	0.614	<.001	—							
8. ERICA labajā pusē	Spearman's rho	0.668	0.731	0.340	0.185	0.295	0.403	0.432	—						
	p-value	<.001	<.001	0.002	0.098	0.008	<.001	<.001	—						
9. ERICA kreisajā pusē	Spearman's rho	0.717	0.729	0.301	0.168	0.272	0.405	0.432	0.917	—					
	p-value	<.001	<.001	0.006	0.133	0.014	<.001	<.001	<.001	—					
10. Microbleeds	Spearman's rho	0.234	0.183	-0.066	0.020	0.057	-0.271	-0.176	0.107	0.147	—				
	p-value	0.035	0.101	0.556	0.857	0.615	0.015	0.115	0.342	0.192	—				
11. PVS BG	Spearman's rho	0.101	0.099	0.397	0.329	0.381	0.065	0.043	0.033	0.071	-0.032	—			
	p-value	0.369	0.380	<.001	0.003	<.001	0.567	0.705	0.767	0.530	0.776	—			
12. PVS CS	Spearman's rho	0.250	0.211	0.359	0.329	0.402	0.079	0.091	0.078	0.123	0.041	0.515	—		
	p-value	0.025	0.059	<.001	0.003	<.001	0.483	0.417	0.490	0.273	0.719	<.001	—		
13. PVS MidB	Spearman's rho	-0.050	0.002	-0.011	-0.072	-0.027	-0.025	-0.007	-0.095	0.005	-0.060	0.396	0.323	—	
	p-value	0.659	0.984	0.924	0.522	0.809	0.827	0.953	0.998	0.964	0.592	<.001	0.003	—	
14. GCA	Spearman's rho	0.692	0.713	0.674	0.543	0.641	0.510	0.503	0.687	0.707	0.156	0.467	0.540	0.179	—
	p-value	<.001	<.001	<.001	<.001	<.001	<.001	<.001	<.001	<.001	<.001	0.164	<.001	<.001	0.110

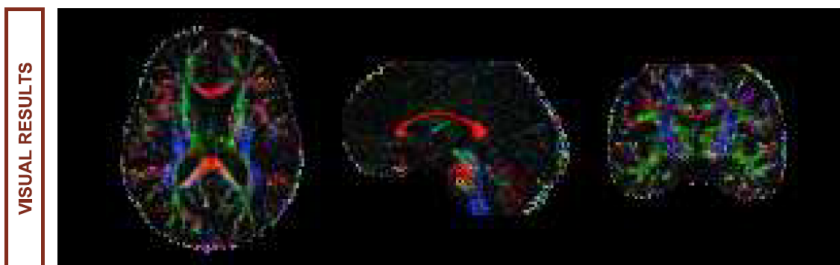
Icometrix output data for study participants for the total brain fractional anisotropy and corpus callosum fractional anisotropy values

icobrain tbi

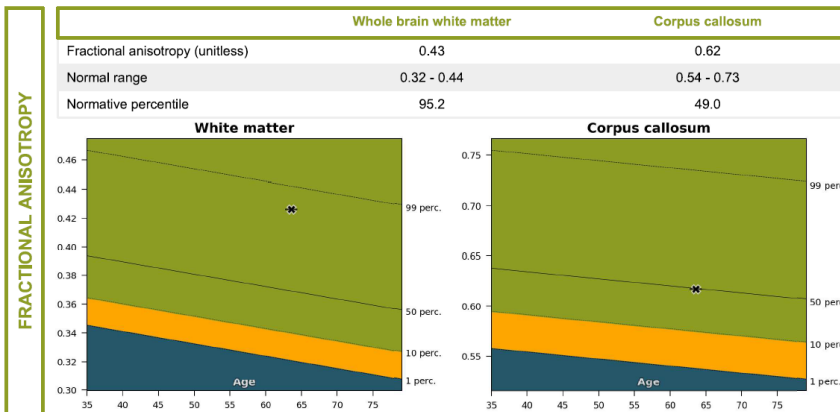


INFO	NAME	ID	YEAR OF BIRTH	STUDY DATE
	5936c95588	fb26aba4e1		

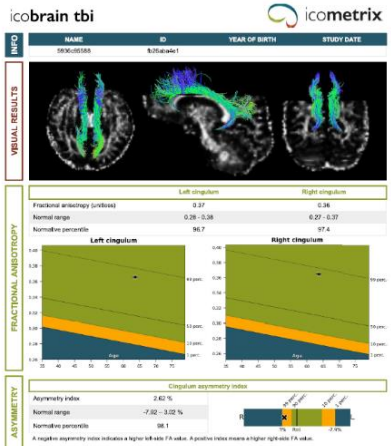
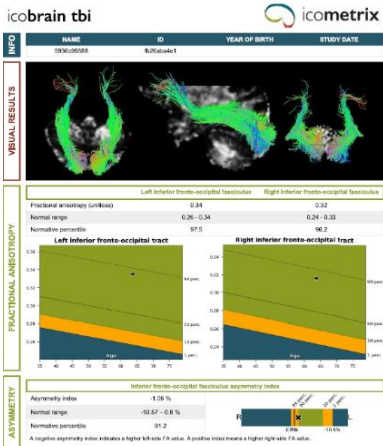
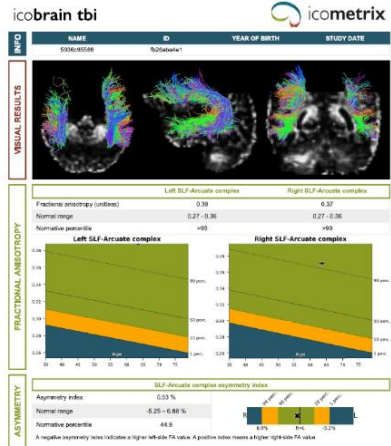
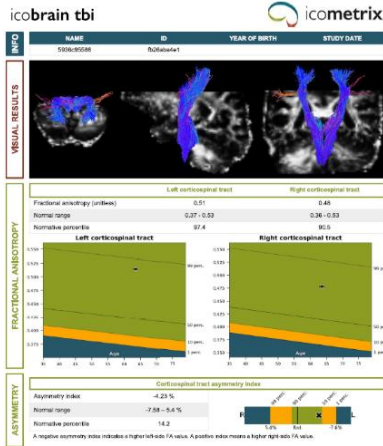
QC	STATUS	REMARKS
	Approved with remarks	No remarks.




	Whole brain white matter	Corpus callosum
Fractional anisotropy (unitless)	0.43	0.62
Normal range	0.32 - 0.44	0.54 - 0.73
Normative percentile	95.2	49.0



Icometrix output data for study participants for corticospinal tract FA, superior long ligament - arcuate ligament FA, inferior fronto-occipital FA, and cingulum FA



Permission of the scientific department to conduct academic research



aslimnica
RĪGAS AUSTRUMU KLINISKĀ UNIVERSITĀTES SLIMNĪCA

SIA Rīgas Austrumu klīniskā universitātes slimnīca
Reģistrācijas Nr.: 40003951628
Hipokrāta iela 2, Rīga, LV-1038, Latvija
Tālrunis: 67 042 460, fakss: 67 042 786
E-pasts: aslimnica@aslimnica.lv, www.aslimnica.lv

ZINĀTNES DAĻA
Hipokrāta iela 2, Rīga, LV-1038, Latvija
Tālrunis: 67 303 180
E-pasts: zinatne@aslimnica.lv

APSTIPRINĀTS
ar SIA „Rīgas Austrumu klīniskā universitātes
slimnīca” valdes 2019. gada 22. janvāra lēmumu
Nr. V1/01-01/19/31

Rīgā

RSU studentam
Naurim Zdanovskim

2019.gada 21. oktobrī
Nr. ZD/08-06/01-19/144

ATĻAUJA AKADEMISKĀ PĒTĪUMA VEIKŠANAI

Zinātnes daļa ir izskatījusi Jūsu iesniegto akadēmiskā pētījuma „Galvas smadzeņu kvantitatīvu un kvantitatīvu radioloģisko biomarkieru (volumetrisko un virsmas raksturlielumu biomarkieru) izmaiņu korelācija ar kognitīvo funkciju traucējumiem un demences attīstību” dokumentāciju, kas reģistrēta Zinātnes daļā ar numuru AP-144/19, kas apstiprina akadēmiskā pētījuma veikšanu SIA „Rīgas Austrumu klīniskā universitātes slimnīca” (turpmāk – Iestāde) stacionārā “Gaiļezers” Neiroķirurģijas un neiroloģijas klīnikā, vadītājs Guntis Karelis un Diagnostiskās radioloģijas centrā, vadītāja Māra Epermane.

Atbildīgais par pētniecības norisi Iestādē ir Ardis Platkājis.


Zinātnes daļā iesniegti un izskatīti:

1. Pieteikums par akadēmiskā pētījuma AP-144/19 veikšanu.
2. Pētījuma protokols ar pielikumu.
3. Naura Zdanovska konfidencialitātes apliecinājums.
4. Ētikas komitejas atzinums, izsniegts 2019.gada 3.oktobrī.

Prospektīvā pētījumā, iegūstot pacientu rakstisku piekrišanu, plānots analizēt 100 ambulatoro un 100 stacionāra “Gaiļezers” 2019.-2024. gada pacientu ar kognitīvo funkciju traucējumiem un demences attīstību datus.

Atļauja derīga līdz 2024.gada 1.septembrim.

Dr.med. Daiga Šantare


 (paraksts)

Speciāliste akadēmisko pētījumu jautājumos
Zinātnes daļa
Šantare, 67303179

Approval of the medical and biomedical research ethics committee

fonds *etika*
 MEDICĪNISKO UN BIOMEDICĪNISKO PĒTĪJUMU ĒTIKAS KOMITEJA

Darbojas saskaņā ar SHK LKP noteikumiem

Nr. 08-A/19
 03.10.2019.
 Rīgā

Rīgas Austrumu klīniskās universitātes slimnīcas atbalsta fonda
 Medicīnisko un biomedicīnisko pētījumu ētikas komitejas

ATZINUMS

Pētījuma nosaukums: Galvas smadzeņu kvalitatīvu un kvantitatīvu radioloģisko biomarkieru (volumetrisko un virsmas raksturlielumu biomarkieru) izmaiņu korelācija ar kognitīvo funkciju traucējumiem un demences attīstību

Pētījuma pieteikuma iesniedzējs: Nauris Zdanovskis

Pētījuma pieteikuma iesniedzēja darba vieta: RAKUS

SIA "Rīgas Austrumu klīniskās universitātes slimnīcas" atbalsta fonda Medicīnisko un biomedicīnisko pētījumu ētikas komiteja (sēdes prot. 09/19., 03.10.2019.) ir izvērtējusi plānotā zinātniskā pētījuma nozīmi un mērķi, iesniedzēja sniegto paredzamā ieguvuma un riska novērtējumu un tā pamatotību. Balstoties uz iesniegto dokumentu izvērtējumu, komiteja nolēma izteikt:

- pozitīvu atzinumu
- negatīvu atzinumu, ar iespēju veikt izmaiņas un iesniegt pieteikumu atkārtoti
- negatīvu atzinumu

par pieteikuma atbilstību zinātnisko pētījumu ētikas prasībām.

Rīgas Austrumu klīniskās universitātes slimnīcas atbalsta fonda
 Medicīnisko un biomedicīnisko pētījumu
 ētikas komitejas priekšsēdētājs Roberts Stašinskis

Rīgas Ārlietu centra 2./11.038
 1.202811.1

**Evaluation of fractional anisotropy (FA) values
of diffusion tensor examination by dividing patients into 2 groups**

Structure	W	p value
Whole brain FA	175,000	0,660
Normative percentile of the entire brain	89,000	0,007
<i>Corpus Callosum</i> FA	199,500	0,853
<i>Corpus Callosum</i> normative percentile	173,500	0,635
Left-sided corticospinal tract FA	133,500	0,125
Left cortico-spinal tract normative percentile	103,000	0,020
Right cortico-spinal tract FA	146,500	0,233
Normative percentile of the right-sided corticospinal tract	112,000	0,036
Asymmetry of the cortical tract	203,500	0,772
Corticospinal tract asymmetry normative percentile	183,000	0,823
Deviation of asymmetry of the corticospinal tract from the 50 normative percentile	190,000	0,968
Left SLF-Arcuate FA	199,500	0,853
Left SLF-Arcuate normative percentile	156,500	0,356
Right SLF-Arcuate FA	206,500	0,710
Right SLF-Arcuate normative percentile	142,500	0,197
Asymmetry of the SLF-Arcuate bundle	189,000	0,947
Asymmetries of the SLF-Arcuate bundle normative percentile	192,000	1,000
Asymmetry deviation of the upper long bundle – arcuate bundle from the 50 normative percentile	194,500	0,957
Left-sided lower fronto-occipital tract FA	203,000	0,781
Left-sided lower fronto-occipital tract normative percentile	173,500	0,634
Right-sided lower fronto-occipital tract FA	210,500	0,633
Right-sided lower fronto-occipital tract normative percentile	169,500	0,562
Asymmetry of the lower fronto-occipital tract	217,000	0,516
Inferior fronto-occipital tract asymmetry normative percentile	205,500	0,727
Deviation of asymmetry of the lower fronto-occipital tract from 50 percentile	210,500	0,628
Left <i>cingulum</i> FA	181,000	0,780
Left <i>cingulum</i> normative percentile	123,000	0,071
Right <i>cingulum</i> FA	197,000	0,905
Right <i>cingulum</i> normative percentile	134,500	0,133
<i>Cingulum</i> asymmetry	213,000	0,586
<i>Cingulum</i> asymmetry deviation from 50 percentile	188,000	0,926
<i>Cingulum</i> asymmetry normative percentile	200,000	0,842

**Statistically significant correlation between volume
and MoCA results with correlation coefficients and p-values**

Structure	Spearman rho and p-value	Correlation with MoCA
Left <i>putamen</i>	Spearman rho	0,310**
	p-value	0,005
Left hippocampus	Spearman rho	0,473***
	p-value	< 0,001
Left amygdala	Spearman rho	0,532***
	p-value	< 0,001
Left <i>accumbens</i>	Spearman rho	0,302**
	p-value	0,006
Right hippocampus	Spearman rho	0,372***
	p-value	< 0,001
Right amygdala	Spearman rho	0,467***
	p-value	< 0,001
<i>Corpus callosum</i> middle part	Spearman rho	0,264*
	p-value	0,018
Left cortical volume	Spearman rho	0,267*
	p-value	0,016
Right cortical volume	Spearman rho	0,241*
	p-value	0,031
Total cortical volume	Spearman rho	0,263*
	p-value	0,019
Subcortical gray matter	Spearman rho	0,262*
	p-value	0,019
Total gray matter volume	Spearman rho	0,240*
	p-value	0,032

* p < 0,05; ** p < 0,01; *** p < 0,001.

**Statistically significant correlation between volume
and MoCA scores with correlation coefficients and p-values**

Structure	Spearman rho and p-value	Correlation with MoCA
Left entorhinal	Spearman rho	0,515***
	p-value	< 0,001
Left fusiform cortex	Spearman rho	0,323**
	p-value	0,003
Left inferior parietal cortex	Spearman rho	0,326**
	p-value	0,003
Left inferior temporal cortex	Spearman rho	0,245*
	p-value	0,029
Left middle temporal cortex	Spearman rho	0,328**
	p-value	0,003
Left parahippocampal cortex	Spearman rho	0,291**
	p-value	0,009
Left <i>praecuneus</i> cortex	Spearman rho	0,235*
	p-value	0,036
Left superior parietal cortex	Spearman rho	0,222*
	p-value	0,048
Left superior temporal cortex	Spearman rho	0,364***
	p-value	< 0,001
Left supramarginal cortex	Spearman rho	0,348**
	p-value	0,002
Right entorhinal	Spearman rho	0,345**
	p-value	0,002
Right fusiform cortex	Spearman rho	0,252*
	p-value	0,024
Right inferior parietal cortex	Spearman rho	0,230*
	p-value	0,040
Right middle temporal cortex	Spearman rho	0,240*
	p-value	0,032
Right parahippocampal cortex	Spearman rho	0,382***
	p-value	< 0,001
Right <i>praecuneus</i> cortex	Spearman rho	0,310**
	p-value	0,005
Right superior temporal cortex	Spearman rho	0,261*
	p-value	0,020

* p < 0,05, ** p < 0,01, *** p < 0,001.